Design and Detailing Requirements for Columns under Collision

Final Report
March 2021

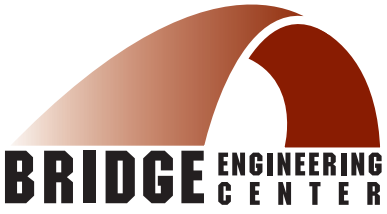

IOWA STATE UNIVERSITY
Institute for Transportation

Sponsored by
Iowa Highway Research Board
(IHRB Project TR-768)
Iowa Department of Transportation
(InTrans Project 19-680)

About the Bridge Engineering Center

The mission of the Bridge Engineering Center (BEC) is to conduct research on bridge technologies to help bridge designers/owners design, build, and maintain long-lasting bridges.

About the Institute for Transportation

The mission of the Institute for Transportation (InTrans) at Iowa State University is to develop and implement innovative methods, materials, and technologies for improving transportation efficiency, safety, reliability, and sustainability while improving the learning environment of students, faculty, and staff in transportation-related fields.

Iowa State University Nondiscrimination Statement

Iowa State University does not discriminate on the basis of race, color, age, ethnicity, religion, national origin, pregnancy, sexual orientation, gender identity, genetic information, sex, marital status, disability, or status as a US veteran. Inquiries regarding nondiscrimination policies may be directed to the Office of Equal Opportunity, 3410 Beardshear Hall, 515 Morrill Road, Ames, Iowa 50011, telephone: 515-294-7612, hotline: 515-294-1222, email: eooffice@iastate.edu.

Disclaimer Notice

The contents of this report reflect the views of the authors, who are responsible for the facts and the accuracy of the information presented herein. The opinions, findings and conclusions expressed in this publication are those of the authors and not necessarily those of the sponsors.

The sponsors assume no liability for the contents or use of the information contained in this document. This report does not constitute a standard, specification, or regulation.

The sponsors do not endorse products or manufacturers. Trademarks or manufacturers' names appear in this report only because they are considered essential to the objective of the document.

Iowa DOT Statements

Federal and state laws prohibit employment and/or public accommodation discrimination on the basis of age, color, creed, disability, gender identity, national origin, pregnancy, race, religion, sex, sexual orientation or veteran's status. If you believe you have been discriminated against, please contact the Iowa Civil Rights Commission at 800-457-4416 or Iowa Department of Transportation's affirmative action officer. If you need accommodations because of a disability to access the Iowa Department of Transportation's services, contact the agency's affirmative action officer at 800-262-0003.

The preparation of this report was financed in part through funds provided by the Iowa Department of Transportation through its "Second Revised Agreement for the Management of Research Conducted by Iowa State University for the Iowa Department of Transportation" and its amendments.

The opinions, findings, and conclusions expressed in this publication are those of the authors and not necessarily those of the Iowa Department of Transportation.

2Technical Report Documentation Page

1. Report No.	2. Government Accession No.	3. Recipient's Catalog No.
IHRB Project TR-768		

4. Title and Subtitle	5. Report Date
Design and Detailing Requirements for Columns under Collision	March 2021
	6. Performing Organization Code

7. Author(s)	8. Performing Organization Report No.
Alice Alipour (orcid.org/0000-0001-6893-9602), Behrouz Shafei (orcid.org/0000-0001-5677-6324), Aleksander Nelson (orcid.org/0000-0003-2059-7564), and Kofi Oppong (orcid.org/0000-0003-1506-1474)	InTrans Project 19-680

9. Performing Organization Name and Address	10. Work Unit No. (TRAIS)
Bridge Engineering Center Iowa State University 2711 South Loop Drive, Suite 4700 Ames, IA 50010-8664	11. Contract or Grant No.

12. Sponsoring Organization Name and Address	13. Type of Report and Period Covered
Iowa Highway Research Board Iowa Department of Transportation 800 Lincoln Way Ames, IA 50010	Final Report
	14. Sponsoring Agency Code IHRB Project TR-768

15. Supplementary Notes

Visit https://intrans.iastate.edu/ for color pdfs of this and other research reports.

16. Abstract

This study investigated the differences between the American Railway Engineering and Maintenance-of-Way Association (AREMA), American Association of State Highway and Transportation Officials (AASHTO), and Iowa Department of Transportation (DOT) concerning vehicular collisions. The researchers evaluated the performance of common Iowa bridges and their components when an 80 kip tractor-semitrailer collides into them. The researchers also performed a parametric study on a frame pier and T-pier that experience vehicular collision.

The frame pier with two 3.5 ft column diameters with a spiral of #5 rebar and 4 in. pitch experiences minor damage when impacted by a tractor-semitrailer at an impact velocity of 50 mph. There is, however, severe damage and failure for the impact velocity of 70 mph and 90 mph, respectively. The T-pier commonly used in Iowa does not collapse under any of the three impact velocities. The minimum requirements for a crash wall specified by the Iowa DOT were able to keep the frame pier from failure when it was struck by a tractor-semitrailer traveling at each of the three impact velocities. The Iowa DOT's 54 in. tall concrete barrier successfully redirects a tractor-semitrailer and therefore prevents it from hitting the frame pier it is set up to protect.

The frame pier with two column diameters of 4 ft with at least 1.0% longitudinal reinforcement, #5 spiral rebar at a 4 in. pitch, and Grade 60 steel, did not collapse under any of the three impact velocities. The T-pier with no ties experiences minor damage when impacted at the 50 mph impact velocity. However, ties spaced at 24 in. and 12 in. are required for minor damage at a 70 mph and 90 mph impact velocity, respectively.

The damage ratio index (DRI) values and damage description for the frame pier accurately predicted the damage observed in the frame pier due to vehicular collision. The DRI damage state description for the frame pier did not accurately describe the damage for the T-pier. Therefore, a DRI damage state description table was developed for the T-pier.

17. Key Words	18. Distribution Statement
bridge frame piers—bridge T-piers—finite element modeling—vehicular collisions—vulnerability assessment	No restrictions.

19. Security Classification (of this report)	20. Security Classification (of this page)	21. No. of Pages	22. Price
Unclassified.	Unclassified.	82	NA

DESIGN AND DETAILING REQUIREMENTS FOR COLUMNS UNDER COLLISION

Final Report
March 2021

Principal Investigator
Alice Alipour, Associate Professor
Department of Civil, Construction, and Environmental Engineering
Bridge Engineering Center, Iowa State University

Co-Principal Investigators
Behrouz Shafei, Associate Professor
Department of Civil, Construction, and Environmental Engineering
Bridge Engineering Center, Iowa State University

Aleksander Nelson, Senior Bridge Engineer/Senior Professional Associate
HDR

Research Assistant
Kofi Oppong

Authors
Alice Alipour, Behrouz Shafei, Aleksander Nelson, and Kofi Oppong

Sponsored by
Iowa Department of Transportation and
Iowa Highway Research Board
(IHRB Project TR-768)

Preparation of this report was financed in part
through funds provided by the Iowa Department of Transportation
through its Research Management Agreement with the
Institute for Transportation
(InTrans Project 19-680)

A report from
Bridge Engineering Center
Institute for Transportation
Iowa State University
2711 South Loop Drive, Suite 4700
Ames, IA 50010-8664
Phone: 515-294-8103 / Fax: 515-294-0467
https://intrans.iastate.edu/

TABLE OF CONTENTS

ACKNOWLEDGMENTS xi

EXECUTIVE SUMMARY xiii

1. INTRODUCTION AND LITERATURE REVIEW 1

1.1 AREMA Provision for the Protection of a Pier 1
1.2 AASHTO Provision for the Protection of a Pier 2
1.3 Iowa DOT Bridge Design Manual Provision for the Protection of a Pier 3
1.4 Differences between the Iowa DOT BDM and the Other Two Manuals on Pier Protection 5

2. FINITE ELEMENT MODELING OF REPRESENTATIVE BRIDGES 8

2.1 Introduction 8
2.2 Tractor-Semitrailer Model 8
2.3 Modeling of Frame Pier 9
2.4 Modeling of T-Pier 15
2.5 Modeling of Frame Pier with Barrier 20
2.6 Modeling of Frame Pier with Crash Wall 23
2.7 Reinforced Concrete Modeling and Model Validation 24
2.8 Simulation Setup 27
2.9 Analysis of Frame Pier and T-Pier Damage from Impact Simulations 28
2.10 Analysis of Frame Pier and T-Pier Impact Forces from Impact Simulations 34
2.11 Analysis of Frame Pier and T-Pier Shear Forces from Impact Simulations 36
2.12 Analysis of Frame Pier and T-Pier Bending Moments from Impact Simulations 36
2.13 Analysis of Frame Pier and T-Pier Displacements from Impact Simulations 37
2.14 Analysis of the Performance of a Crash Wall Integrated into a Frame Pier 38
2.15 Analysis of the Performance of a Crash Barrier Placed Around a Frame Pier 39

3. PARAMETRIC STUDY 42

3.1 Introduction 42
3.2 Effect of Different Frame Pier Column Diameters 42
3.3 Effect of Extension of Frame Pier Spiral Reinforcement into Pier Cap and Pile Cap 46
3.4 Effect of Different Impact Angles on T-Pier 48
3.5 Effect of Different Spacing of Tie Reinforcement in T-Pier 53

4. COST IMPLICATIONS 57

5. DESIGN RECEOMMNDATIONS 58

5.1 Spiral or Tied Determination – AASHTO LRFD 5.7.4.6 (7th Edition) 58
5.2 Minimum Longitudinal Reinforcement – AASHTO LRFD Article 5.7.4.2 (7th Edition) 59
5.3 Minimum Transverse Reinforcement – AASHTO LRFD Article 5.8.2.5 (7th Edition) 60

5.4 Transverse Reinforcement for Compression Members – AASHTO LRFD Article 5.10.6 (7th Edition) 60
5.5 Provisions for Seismic Design – AASHTO LRFD Article 5.10.11 (7th Edition) 61
6. SUMMARY AND CONCLUSIONS 63
REFERENCES 65

LIST OF FIGURES

Figure 1.1. Frame pier with crash wall requirements in AREMA (2014) 2
Figure 1.2. Frame pier with a crash wall requirement in Iowa DOT BDM (2020) 5
Figure 2.1. Tractor-semitrailer FE model for collision simulations 8
Figure 2.2. Frame pier model 10
Figure 2.3. Details of the frame pier's bent cap: (a) concrete and (b) steel reinforcement 12
Figure 2.4. Details of the frame pier's columns: (a) side view, (b) close-up of steel reinforcement in the column, and (c) column cross-section 12
Figure 2.5. Steel reinforcement details of frame pier's pile cap: (a) side view and (b) top view 13
Figure 2.6. Details of the frame pier's deep foundation: (a) view in pier's longitudinal direction and (b) side view from road 13
Figure 2.7. T-pier model 16
Figure 2.8. Details of the T-pier's bent cap: (a) concrete and (b) steel reinforcement 18
Figure 2.9. Details of the T-pier's column: (a) concrete, (b) column steel reinforcement, and (c) column cross-section 18
Figure 2.10. Steel reinforcement details of T-pier's pile cap: (a) side view from road, (b) view in column's longitudinal axis, and (c) top veiw 19
Figure 2.11. Details of the T-pier's deep foundation: (a) side view from the road and (b) view in column's longitudinal axis 20
Figure 2.12. Frame pier model with barrier 20
Figure 2.13. Frame pier model with barrier: (a) view of barrier's longitudinal axis, and (b) cross-sections of barrier 21
Figure 2.14. Frame pier model with barrier: (a) side view with concrete, (b) side view with reinforcing steel bar, and (c) top view 22
Figure 2.15. Frame pier model with crash wall 23
Figure 2.16. Frame pier model with crash wall showing: (a) side view from road, (b)view in crash wall's longitudinal axis, and (c) crash wall concrete 24
Figure 2.17. Details of the beam models for validating the reinforced concrete material model: (a) beam and hammer and (b) beam cross-section 25
Figure 2.18. Comparison of simulation and experimental resuslts: (a), (b) 5.91 in. drop height, and (c), (d) 47.2 m drop height 26
Figure 2.19. Frame pier model with crash wall 27
Figure 2.20. Collision simulation of tractor-semitrailer into frame pier: (a) 50 mph, (b) 70 mph, and (c) 90 mph 28
Figure 2.21. Simulation of damage from vehicle collision into the frame pier: (a) 50 mph, (b) 70 mph, and (c) 90 mph 29
Figure 2.22. Pier column showing two shear failure planes 31
Figure 2.23. Collision simulation of tractor-semitrailer into T-pier: (a) 50 mph, (b) 70 mph, and (c) 90 mph 33
Figure 2.24. Simulation of damage from vehicle collision into the T-pier: (a) 50 mph, (b) 70 mph, and (c) 90 mph 34
Figure 2.25. Impact force time history of tractor-semitrailer colliding into: (a) frame pier and (b) T-pier 35
Figure 2.26. Shear profile along (a) frame pier and (b) T-pier 36

Figure 2.27. Bending moment profile along: (a) frame pier and (b) T-pier 37
Figure 2.28. Displacement profile along (a) frame pier and (b) T-pier 37
Figure 2.29. Collision simulation of tractor-semitrailer into frame pier with barrier: (a) 50 mph, (b) 70 mph, and (c) 90 mph 38
Figure 2.30. Simulation of damage from vehicle collision into the frame pier with a crash wall: (a) 50 mph, (b) 70 mph, and (c) 90 mph 38
Figure 2.31. Response measures for frame pier with crash wall: (a) impact force, (b) shear force, (c) bending moment, and (d) displacement.....39
Figure 2.32. Simulation of tractor-semtrailer running into a frame pier with a crash barrier: (a) starting point, (b) 50 mph, (c) 70 mph, and (d) 90 mph 40
Figure 2.33. Simulation of damage from vehicle collision into the crash barriers around the frame pier (side and top views): (a) 50 mph, (b) 70 mph, and (c) 90 mph 41
Figure 3.1. Frame pier with different diameters: (a) 3 ft, (b) 3.5 ft, and (c) 4 ft. 42
Figure 3.2. Damage in frame pier with different diameters.....43
Figure 3.3. Response measures for frame pier with different diameters: (a) impact force time history, (b) shear force, (c) bending moment, and (d) displacement 45
Figure 3.4. Frame pier with and without extended spiral rebar 46
Figure 3.5. Damage in frame pier with extended spiral rebar 47
Figure 3.6. Tractor-semitrailer approaching the T-pier at: (a) 0°, (b) 45°, and (c) 90° from the pier's longitudinal axis 49
Figure 3.7. Damage in frame pier with different diameters.....50
Figure 3.8. Effect of placing the reinforcement in the tension region of the pile cap lower 52
Figure 3.9. Impact force along longitudinal axis of T-pier.....53
Figure 3.10. Longitudinal reinforcing steel bar and ties in T-pier: (a) no ties, (b) 24-in. tie spacing, and (c) 12-in. tie spacing.....53
Figure 3.11. Damage in frame pier with different diameters.....54

LIST OF TABLES

Table 1.1. Differences in pier column detail requirements....6
Table 2.1. Geometric and material properties of real and model superstructure of frame pier....11
Table 2.2. Stiff clay soil parameters....14
Table 2.3. Load-displacement (*p*-*y*) curves....15
Table 2.4. Geometric and material properties of real and model superstructure of T-pier....17
Table 2.5. Comparison of estimated and observed initial kinetic energy for 80,000 lb load....28
Table 2.6. Determination of DRI values for frame pier....30
Table 2.7. Description of damage state for DRI values....30
Table 2.8. Determination of DRI values of frame pier special design case....32
Table 2.9. Determination of DRI values of T-pier....34
Table 3.1. Determination of DRI values for frame pier....44
Table 3.2. Internal energy of various components of the frame pier....48
Table 3.3. Determination of DRI values for T-pier impacted at different angles....51
Table 3.4. Internal energies in bridge pier components....52
Table 3.5. Determination of DRI values for T-pier with different tie spacings....54
Table 3.6. Description of damage state for the DRI values determined for T-piers....55
Table 3.7. Internal energies in bridge components due to different tie spacings....56

ACKNOWLEDGMENTS

The authors would like to thank the Iowa Highway Research Board and the Iowa Department of Transportation for sponsoring this research. The authors also would like to thank the technical advisory committee for their time and effort working on this project.

EXECUTIVE SUMMARY

Objectives

The objectives of this project were to investigate how the vehicular collision section of the Iowa Department of Transportation's (DOT's) Bridge Design Manual could be improved by comparing it to the current American Railway Engineering and Maintenance-of-Way Association (AREMA) and American Association of State Highway and Transportation Officials (AASHTO) manuals, performing finite element simulations of vehicle collisions on representative bridge piers, and conducting a parametric study.

Research Description

This study investigated the differences between AREMA, AASHTO, and Iowa DOT manuals concerning vehicular collisions to bridge piers. The researchers evaluated the performance of common Iowa bridges and their components when an 80,000 lb (36,287 kg) tractor-semitrailer collides into them. The researchers also performed a parametric study on a frame pier and T-pier that experience vehicular collision.

To investigate the structural resistance of typical Iowa bridges to vehicular collision using the finite element method (FEM), two bridge pier types were modeled: a frame pier and a T-pier. Two other bridge pier models were developed to involve the typical pier protection strategies used by the Iowa DOT in cases where vehicular collision into a frame pier is likely.

One of the strategies used by the Iowa DOT for frame pier protection in urban areas is to construct a 54-in.-high median barrier that is routed around and directly adjacent to the frame pier. In such cases, each column of the frame pier is also supposed to be designed for the AASHTO-required 600-kip vehicular collision design force. The other main design strategy for frame pier protection against vehicular collision is to integrate a crash wall (or strut) into the frame pier.

Finite element modeling was conducted using the LS-DYNA software package. This software package is capable of performing nonlinear impact simulations, capturing various vehicle collision scenarios. The FEM process involved modeling the truck striking the bridge given the bridge frame or T-pier, foundation, and superstructure.

The parametric study that the researchers performed on the frame pier and T-pier investigated and evaluated the effect of different frame pier column diameters, the effect of the extension of frame pier spiral reinforcement into the pier cap and pile cap, the effect of different impact angles on the T-pier, and the effect of different tie reinforcement spacing in the T-pier. Various response measures were analyzed, and these included damage pattern (plastic strains), impact force time history, shear force, bending moment, displacement, and internal energy.

One of the unique aspects of the project was to develop a damage ratio index (DRI) to allow for potential implementation of performance-based design philosophy for design of columns under collision. As part of this effort the DRI was determined for the various scenarios considered.

Key Findings

The researchers found a few differences between the three design manuals investigated in this study concerning pier protection for vehicular collisions and pier column detail requirements. However, for the most part, the requirements in all three are similar.

- The DRI values and damage description for the frame pier accurately predicted the damage observed in the frame pier due to vehicular collision.

- The T-pier commonly used in Iowa did not collapse under any of the three impact velocities considered when it was impacted along its longitudinal axis.

- The minimum requirements for a crash wall specified in the Iowa DOT BDM (2020) were able to keep the frame pier from failure when it was struck by a tractor-semitrailer traveling at the three impact velocities considered.

- The 54 in. (1.37 m) tall concrete barrier for the Iowa DOT successfully redirects a tractor-semitrailer and therefore prevents it from hitting the frame pier it is set up to protect.

- The 1. 4 ft (1.22 m) column pier with at least 1.0% longitudinal reinforcement, #5 (#16) spiral rebar at a 4 in. (101.6 mm) pitch made of Grade 60 steel, does not collapse for any of the three impact velocities considered.

- Extending the spiral reinforcement in the column of the frame pier to the pier cap and pile cap only slightly increases the stiffness of the pier and does not significantly increase the pier's resistance to vehicular collision loads.

- Greater impact angles on a pier from its longitudinal axis causes the pier to experience greater damage. It is important that there is no vertical region in the pile cap without steel reinforcement when considering vehicular collision design for impact velocities of 70 mph (112.7 km/h) and greater.

- The T-pier commonly used in Iowa, and with no ties, experiences minor damage when impacted at the 50 mph (80.5 km/h) impact velocity. However, ties spaced at 24 in. (0.61 m) and 12 in. (0.30 m) are required to maintain a minor damage at a 70 mph (112.7 km/h) and 90 mph (144.8 km/h) impact velocity, respectively.

Recommendations for Future Research

Additional vehicular collision simulations can be conducted using finite element modeling to further refine the Iowa DOT's Bridge Design Manual.

Implementation Readiness and Benefits

The findings from this study will aid the Iowa DOT in making revisions and additions to its Bridge Design Manual.

Based on the modeling results and the parametric data, few modifications are recommended to bridge piers designed per the Iowa DOT Bridge Design Manual (2020). The one item of potential change would be lowering the bottom mat of reinforcing within frame pier footings to provide connection to the piles for better performance when vehicular impact occurs perpendicular to the long axis of the frame pier.

Other variances were present when the column or reinforcing was less than that recommended in the Iowa DOT Bridge Design Manual. Therefore, the results of this study have no direct impacts on the cost of bridge piers designed per the Iowa DOT Bridge Design Manual. Further recommendations include the following:

- Upon adoption of the AASHTO Load and Resistance Factor Design (LRFD) Bridge Design Specifications 9th edition, additional attention to the changes to Article 5.10.4.3 regarding tie reinforcing in a column

- Clarification of Iowa DOT guidance on the AASTHO LRFD detailing requirements plastic hinging when the seismic design zone 1 (SD1 in AASHTO terms) is greater than or equal to 0.1

1. INTRODUCTION AND LITERATURE REVIEW

The research team investigated the differences in vehicle collision design requirements of bridge piers from three design codes: the American Railway Engineering and Maintenance-of-Way Association (AREMA) Bridge Inspection Handbook (2014), American Association of State Highway and Transportation Officials (AASHTO) Load and Resistance Factor Design (LRFD) Bridge Design Specifications (2017), and Iowa Department of Transportation (DOT) LRFD Bridge Design Manual (BDM) (2020).

The pier protection strategy for each design code is explained first. The differences are briefly discussed after that.

1.1 AREMA Provision for the Protection of a Pier

The AREMA provisions for the protection of a pier that is adjacent to railroad tracks are not intended to create a structure that will resist the full impact of a direct collision by a loaded train at high speed. Rather, the intent is to reduce the damage caused by shifted loads or derailed equipment.

The reduction of damage in the bridge pier is accomplished by either deflecting the force from the pier or distributing the forces over several columns if the pier is struck by a train. A pier clear distance of 25 ft (7.6 m) from the centerline of the railway track is advised. Piers within 25 ft (7.6 m) of the centerline of a railway track are to be designed in accordance with AREMA's heavy construction requirements or protected by a reinforced concrete crash wall.

The bridge piers are considered to be of heavy construction if they have a cross-sectional area equal to or greater than 30 ft^2 (2.79 m^2), which represents the minimum area required for a crash wall with minimum dimensions of 2.5 ft (0.76 m) thick by 12 ft (3.6 m) long, with the larger of its dimensions parallel to the track. Piers that are located 12 ft (3.6 m) to 25 ft (7.6 m) from the centerline of the railway track are to have a minimum crash wall height of 6 ft (1.8 m) above the top of the rail. Piers that are located less than 12 ft (3.6 mm) from the centerline of the railway track are to have a minimum crash wall height of 12 ft (3.6 m) above the top of the rail.

When two or more columns compose a pier, the crash wall shall connect the columns and extend at least 1 ft (0.30 m) beyond the outermost columns parallel to the track. The crash wall shall be anchored to the footings and columns, if applicable, with adequate reinforcing steel, and shall extend to at least 4 ft (1.2 m) below the lowest surrounding grade. The crash wall, integrated into frame piers, is shown in Figure 1.1.

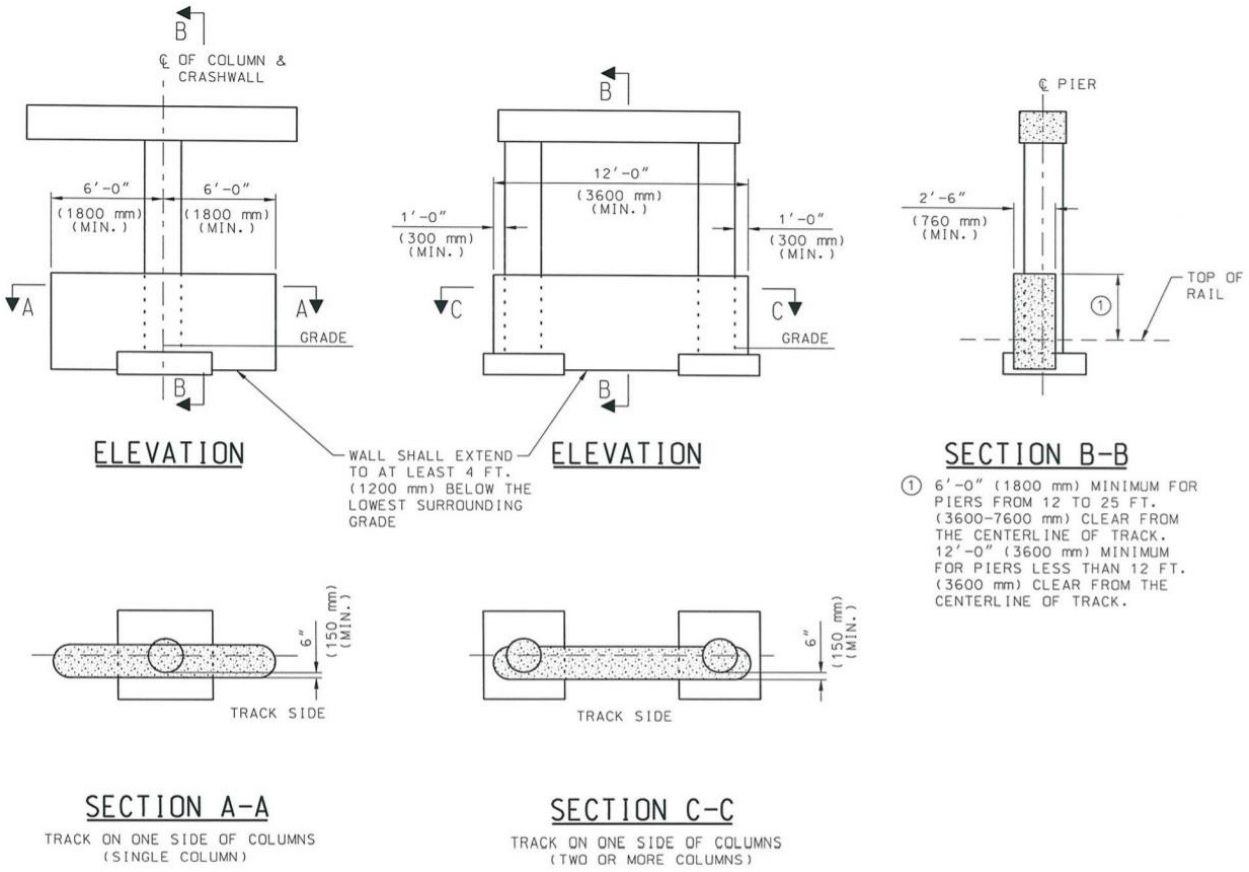

Figure 1.1. Frame pier with crash wall requirements in AREMA (2014)

Consideration may be given to providing protection for bridge piers more than 25 ft (7.6 m) from the centerline of the railway track as conditions warrant. In making this determination, account shall be taken of such factors as horizontal and vertical alignment of the track and embankment height, along with an assessment of the consequences of serious damage if a collision occurs.

1.2 AASHTO Provision for the Protection of a Pier

On vehicular collisions from AASHTO (2017), unless the owner determines that site conditions indicate otherwise, abutments and piers located within 30 ft (9.14 m) from the edge of the roadway have to be investigated for collisions. If the pier needs to be located within 30 ft (9.14 m) of the roadway, an exemption from vehicle collision protection is investigated. This involves evaluating the annual frequency of heavy vehicle impacts. The design for vehicular collision force is not required if the annual frequency of impact from heavy vehicles is less than 0.0001 for critical or essential bridges or 0.001 for typical bridges.

Vehicle collision into a pier is addressed by either providing structural resistance to the pier or by redirecting or absorbing the collision load. When the design choice is to provide structural resistance to the pier, it is required to be designed for an equivalent static force of 600 kips (2,669 kN), which is assumed to act in a direction of 0° to 15° with the edge of the pavement in a

horizontal plane 5 ft (1.52 m) above the ground. The equivalent static force of 600 kips (2,669 kN) is based on the information from full-scale crash tests of rigid columns impacted by 80,000 lb (36,287 kg) tractor trailers at 50 mph (80.5 km/h).

For columns of a frame pier, the 600 kip (2,669 kN) load is to be considered a point load. AASHTO field observations indicated shear failures were the primary mode of failure for frame pier columns and the most vulnerable column diameters were 2.5 ft (0.76 m) and smaller. For T-piers or wall piers, the load may be considered to be a point load or may be distributed over an area deemed suitable for the size of the structure and the anticipated impacting vehicle, but not greater than 5 ft (1.52 m) wide by 2 ft (0.62 m) high. These dimensions were determined by considering the size of a truck frame.

When the design choice is to redirect or absorb the collision load, protection shall consist of one of the following: an embankment; a structurally independent, crashworthy, ground-mounted, 54-in. (1.37 m) high barrier located within 10 ft (3.05 m) of the component being protected; or a 42-in. (1.07 m) high barrier located more than 10 ft (3.05 m) from the component being protected. The barrier shall be structurally and geometrically capable of surviving the crash test for what AASHTO (2017) defines as Test Level 5. A barrier may be considered structurally independent if it does not transmit loads to the bridge.

Full-scale crash tests have shown that some vehicles have a greater tendency to lean over or partially cross over a 42-in. (1.07 m) high barrier than a 54-in. (1.37 m) high barrier. This behavior would allow a significant collision of the vehicle with the component being protected if the component is located within a few feet of the barrier.

The requirements for a train collision load found in previous editions of AASHTO (2017) have been removed from this more recent version, and designers are encouraged to consult the AREMA Manual for Railway Engineering or local railroad company guidelines for train collision requirements.

1.3 Iowa DOT Bridge Design Manual Provision for the Protection of a Pier

The Iowa DOT LRFD BDM (2020) requires that bridge piers be located outside 30 ft (9.14 m) of a roadway and 25 ft (7.62 m) of a railway when there is space. Pier design for collisions is not required for bridge piers located outside these limits. If a pier needs to be located within 25 ft (7.62 m) of a railway, the use of heavy construction as defined in the AREMA manual (2014) is required. If the bridge pier needs to be located within 30 ft (9.14 m) of a roadway, an exemption from vehicle collision design is investigated. This involves evaluating the annual frequency of heavy vehicle impacts. The design for vehicular collision force is not required if the annual frequency of impact from heavy vehicles is less than 0.0001 for critical or essential bridges or 0.001 for typical bridges. In addition, an exemption may be granted on a case-by-case basis in urban areas having low traffic speeds with consideration given to the traffic control devices present along the route.

A pier within 30 ft (9.14 m) of a roadway that does not have an exemption either shall be designed for the 600-kip (2,669 kN) vehicular collision force from AASHTO (2017) or shall be provided with an embankment; a structurally independent, crashworthy, ground-mounted, 54-in. (1.37 m) high barrier located within 10 ft (3.05 m) of the component being protected; or a 42-in. (1.07 m) high barrier located more than 10 ft (3.05 m) from the component being protected.

Iowa DOT investigations have indicated that providing structural resistance in the pier usually will be a better and more economical option than providing an embankment or barrier, except when a median barrier meeting the above requirements will be provided as part of the highway design. In urban areas when a median barrier is necessary, the Iowa DOT prefers using a 54-in. (1.37 m) high barrier routed around and directly adjacent to the pier. In such cases, the pier is to be designed for the 600-kip (2,669 kN) collision force.

In some cases, the Iowa DOT may plan for safety cables or rails to prevent vehicles from impacting a bridge pier. However, the cables or rails do not satisfy the AASHTO (2017) pier protection requirement given that their function is primarily passenger safety. When piers must be designed for the vehicular collision force, the Iowa DOT prefers the following pier types, in the order in which they are listed: (1) T-pier or wall pier, (2) frame pier without a crash wall, or (3) frame pier with a crash wall.

T-piers and wall piers within 30 ft (9.14 m) of a roadway that meet the heavy construction requirements as defined by AREMA (2014) are deemed to meet the 600-kip (2,669 kN) collision force requirements in AASHTO (2017), and no further design of the pier is required with respect to collisions. The heavy construction requirements for these pier types are as follows: cross-sectional area equal to or greater than 30 ft^2 (2.79 m^2) and minimum pier thickness of 2.5 ft (0.76 m), with the larger pier dimension parallel to the roadway. Frame piers without a crash wall are deemed to meet the 600-kip (2,669 kN) collision force requirements, and no further design of the pier is required with respect to collisions when the following stipulations are met: three or more columns connected by a continuous pier cap; minimum column diameters of 4 ft (1.22 m); column vertical reinforcement greater than what is required by design by AASHTO (2017) and 1.0% of the gross concrete section; and Grade 60 shear reinforcement consisting of a minimum #5 (#16) tie bar that is continuously wound (or spiral) with a maximum vertical pitch of 4 in. (101.2 mm). Individual ties shall not be substituted. When frame piers with a crash wall are to be considered for the 600-kip (2,669 kN) design force, they are typically detailed as shown in Figure 1.2.

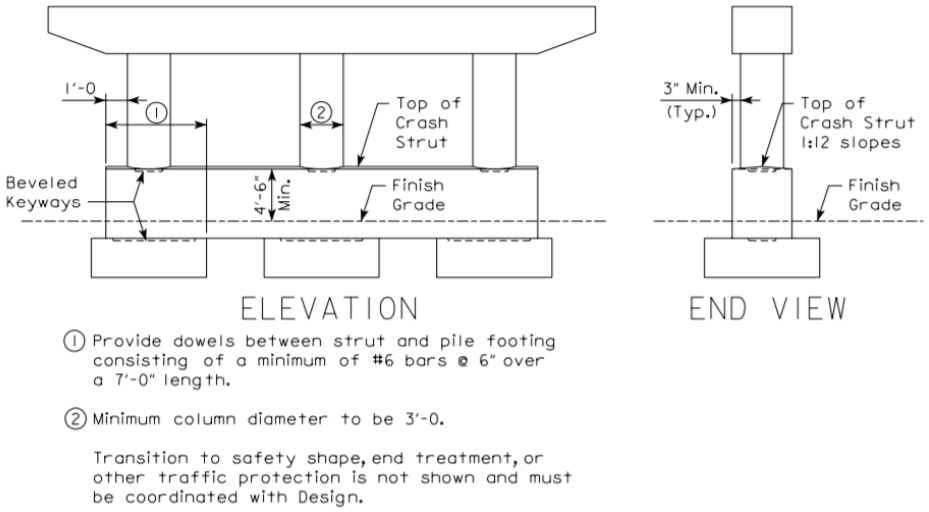

Figure 1.2. Frame pier with a crash wall requirement in Iowa DOT BDM (2020)

1.4 Differences between the Iowa DOT BDM and the Other Two Manuals on Pier Protection

The points given in this section do not insinuate that the Iowa DOT BDM violates the other design codes or is deficient in any way. They only provide factual differences between the various design manuals compared.

1. In the Iowa DOT BDM (2020), the Iowa DOT prefers using a 54-in. (1.37 m) high barrier routed around and directly adjacent to the pier in urban areas when a median barrier is necessary, and, in those cases, the pier is also supposed to be designed for the 600-kip (2,669 kN) collision force. AASHTO (2017) does not require design for the 600-kip (2,669 kN) collision force when the required barriers are provided and are directly adjacent to the pier.

2. In the Iowa DOT BDM (2020), the Iowa DOT may plan to set up safety cables or rails to prevent vehicles from impacting a bridge pier. However, the cables or rails do not satisfy the AASHTO (2017) pier protection requirement of using barriers that satisfy the crash test for what they define as Test Level 5. The Iowa DOT BDM acknowledges this.

3. In the Iowa DOT BDM (2020), frame piers without a crash wall are deemed to meet the 600-kip (2,669 kN) collision force requirements, and no further design of the pier is required with respect to collisions when some stipulations are met. Even though this provision in the Iowa DOT BDM (2020) satisfies the structural resistance requirement from AASHTO (2017), it does not satisfy the heavy construction requirement from AREMA (2014).

4. In the Iowa DOT BDM (2020), frame piers with crash walls are considered as a third option when a bridge pier must be designed for the vehicular collision force of 600 kips (2,669 kN). A frame pier with a crash wall requirement in the Iowa DOT BDM (2020) satisfies the heavy construction requirement from AREMA (2014), even if only two columns are considered

(Figure 1.2). There is however no clear indication in the Iowa DOT BDM (2020) that it requires at least 3 columns, even though the figure provided suggests that. The minimum column spacing in the Iowa DOT BDM (2020) is 16 ft (4.88 m). The frame pier with a crash wall in Figure 1.2 does not satisfy the crash wall requirement from AREMA (2014) due to differences in the required crash wall height. (Compare the wall heights in Figures 1.1 and 1.2.)

5. In the Iowa DOT BDM (2020), the crash wall is required to be a minimum of 3 in. (76.2 mm) wider than the column on one side, and, from AREMA (2014), the crash wall is required to be a minimum of 6 in. (152.4 mm) wider than the column on one side. (Compare Figures 1.1 and 1.2.)

For pier column detailing requirements, AREMA (2014) states that, unless otherwise specified by the highway authority, all highway bridges shall be designed in accordance with the latest Standard Specifications for Highway Bridges adopted by AASHTO (2017). Therefore, in Table 1.1, any differences in AREMA (2014) and AASHTO (2017) are due to specific statements in AREMA (2014). Table 1.1 shows the differences in pier column detailing requirements between the three manuals.

Table 1.1. Differences in pier column detail requirements

Detail	**AREMA (2014)**	**AASHTO (2017)**	**Iowa DOT BDM (2020)**
Minimum bars for spirals	Minimum spiral reinforcement is #3 (#10).	Same as AREMA (2014).	Minimum spiral reinforcement is #4 (#13).
Minimum bars for ties	Minimum tie reinforcement is #3 (#10) for longitudinal bars #10 (#32) or smaller, and #4 (#13) for #11, #14, #18 (#36, #43, #57), and bundled longitudinal bars.	Same as AREMA (2014).	Minimum tie reinforcement is #4 (#13).
Spacing of spiral reinforcement	The clear spacing between spirals shall not exceed 3 in. (76.2 mm), nor be less than 1.5 in. (38.1 mm) or 2 times the maximum size of the coarse aggregate used.	The clear spacing between spirals shall not be less than the greater of 1 in. (25.4 mm) or 1.33 times the maximum size of the aggregate. The center-to-center spacing of the spiral is not to exceed 6 times the diameter of the longitudinal bars or 6 in. (152.4 mm)	No information is given on the spacing of spirals and therefore the provisions from AASHTO (2017) are to be assumed. For the special case of "no design required' however, #5 (#16) spiral with a maximum pitch of 4 in (101.2 mm) is required.

Detail	AREMA (2014)	AASHTO (2017)	Iowa DOT BDM (2020)
Spacing of tie reinforcement	Vertical spacing of ties shall not exceed the least dimension of the compression member or 12 in. (300 mm). When bars larger than #10 (#32) are bundled more than 2 in any one bundle, tie spacing shall be 1/2 that specified.	The spacing of ties along single bars or bundles of #9 (#29) bars or smaller shall not exceed the lesser of the least dimension of the member or 12 in. (300 mm). When 2 or more bars larger than #10 (#32) are bundled together, the spacing shall not exceed the lesser of half the least dimension of the member or 6 in. (152.4 mm)	No information on the spacing of ties is given and therefore the provisions from AASHTO (2017) are to be assumed.
Minimum pier column diameter	No requirements; however, for heavy construction, the area of the column is required to not be less than the area of a crash wall that has minimum cross-section dimensions of 2.5 ft (0.76 m) by 12 ft (3.66 m).	No requirements.	For frame piers, the preferred round column diameters are 2.5 ft (0.76 m), 3 ft (0.91 m), 3.5 ft (1.07 m), and 4 ft (1.22 m). Columns for T-piers shall be at least 2.5 ft (0.76 m) thick. T-pier columns with rounded ends should have thicknesses the same as typical round column diameters.
Minimum column spacing	The minimum column spacing is not specified. However, note that a column spacing less than 10 ft (3.05 m) is used in the 2-column frame pier in Figure 1.1.	The minimum column spacing is not specified.	Column spacing is be a minimum of 16 ft (4.88 m).

The next step was to investigate how a sample of current bridge piers in Iowa respond to vehicle collisions, which is the focus of Chapter 2. The simulations conducted involve a tractor-semitrailer traveling at 50 mph and colliding into bridge piers. The vehicle and speed selected are similar to that considered by AASHTO (2017) in establishing the vehicular collision design force of 600 kips.

2. FINITE ELEMENT MODELING OF REPRESENTATIVE BRIDGES

2.1 Introduction

This chapter investigates the structural resistance of typical Iowa bridges to vehicular collision using the finite element method (FEM). Two bridge pier types were modeled: a frame pier and a T-pier. Two other bridge pier models were developed to involve the typical pier protection strategies used by the Iowa DOT in cases where vehicular collision into a frame pier is likely.

One of the strategies used by the Iowa DOT for frame pier protection in urban areas is to construct a 54-in. (1.37 m) high median barrier that is routed around and directly adjacent to the frame pier. In such cases, each column of the frame pier is also supposed to be designed for the AASHTO-required 600-kip (2,669 kN) vehicular collision design force. The other main design strategy for frame pier protection against vehicular collision is to integrate a crash wall (or strut) into the frame pier.

Details of the finite element modeling of these four typical Iowa DOT piers and mitigation strategies are discussed in this chapter. Finite element modeling was conducted using the LS-DYNA software package (LSTC 2016). This software package is capable of performing nonlinear impact simulations, capturing various vehicle collision scenarios. The FEM process involved modeling the truck striking the bridge given the bridge frame pier or T-pier, foundation, and superstructure.

2.2 Tractor-Semitrailer Model

The isometric front and back views of the tractor-semitrailer model are shown in Figure 2.1.

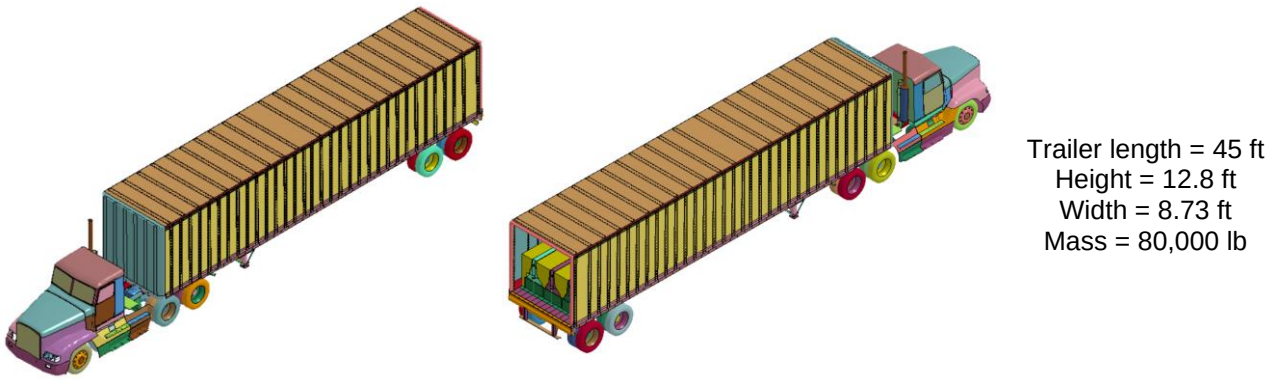

Figure 2.1. Tractor-semitrailer FE model for collision simulations

The vehicle consisted of a tractor with a semitrailer that was 45 ft (13.7 m) long. The height of the trailer was 12.8 ft (3.90 m) and the width was 8.73 ft (2.66 m). The total mass of the tractor-semitrailer was 80,000 lb (36,287 kg).

This mass is achieved in the FEM model by comparing the initial kinetic energy from simulations to calculated values using $0.5mv^2$, and adjusting the density of the concrete portion of the ballast accordingly. This mass was used because it represents the maximum allowable mass of a vehicle on interstate highways in Iowa (Iowa DOT 2020). The mass was also the basis for the determination of the 600-kip (2,669 kN) design collision force from AASHTO (2017). With the back door of the semitrailer removed, the back view of the tractor-semitrailer in Figure 2.1 reveals the ballast.

The ballast is made of concrete barriers and foam. This tractor-semitrailer model was developed by the Battelle Memorial Institute, Oak Ridge National Laboratory, and the University of Tennessee for the Federal Highway Administration (FHWA) (NTRC 2018). This model is the most advanced model available for this vehicle class with respect to the accuracy of material properties, geometric details, and physical functions.

2.3 Modeling of Frame Pier

The modeled frame pier bridge was the bridge on Iowa County Road (CR) E-57 over I-35. Its superstructure is made of pretensioned, prestressed, concrete beams (PPCBs), which rest on elastomeric neoprene bearings at the piers. The bridge has four piers, each consisting of a pier/bent cap, two columns, two pile caps, and a deep foundation. The modeled frame pier was Pier 3 in the bridge plans, as shown in Figure 2.2(a).

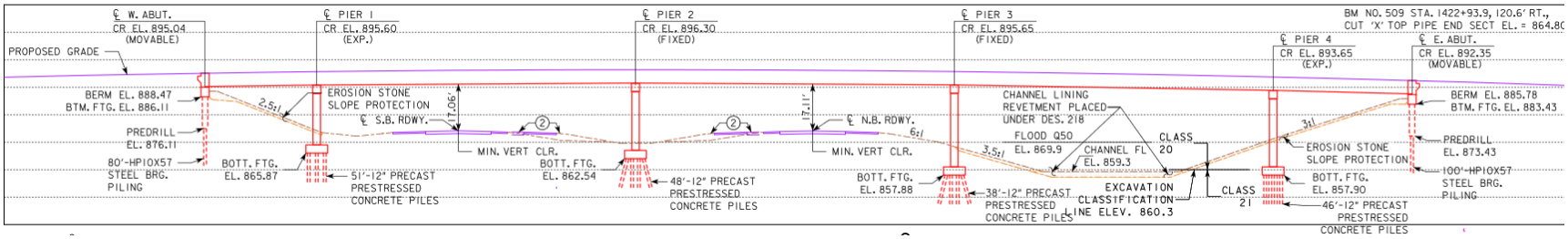

(a)

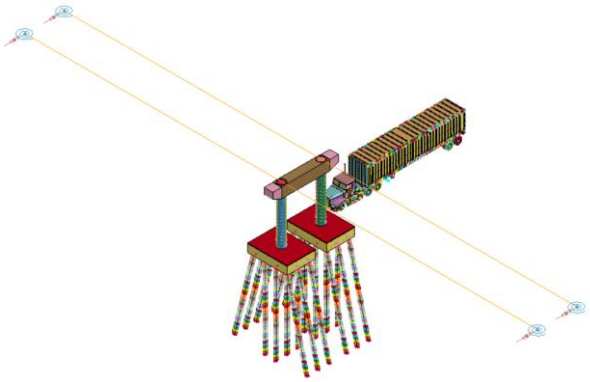

(b)

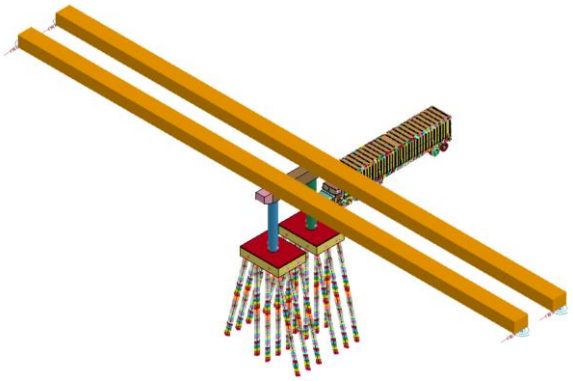

(c)

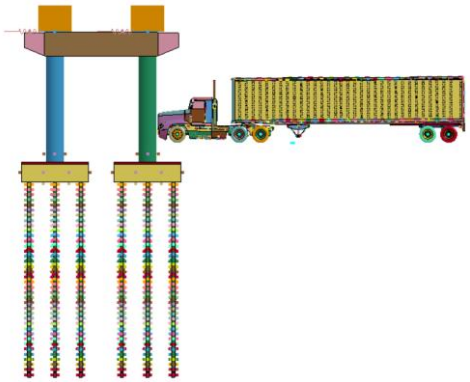

(d)

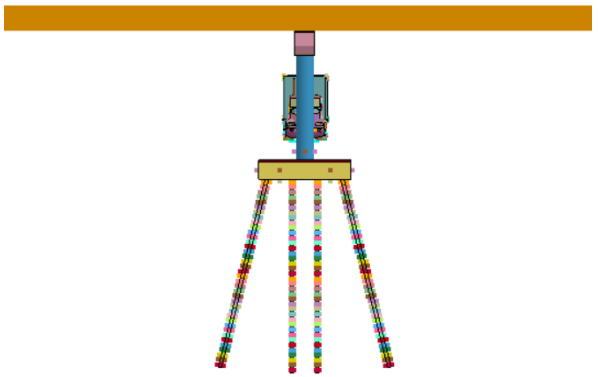

(e)

Figure 2.2. Frame pier model

Pier 3 was the third pier from the west end of the bridge and was similar to the second pier (Pier 2) but had shallower piles. The finite element (FE) model of the frame pier is shown in Figures 2.2(b) through (e). The superstructure was in two parallel parts, and it was modeled using beam elements and elastic material. The dimensions and properties of the beam elements were determined from the cross-section and material properties of the real superstructure. The components of the superstructure considered in developing the model were the prestressed beams, concrete deck, and barriers. Each of the two superstructure parts had a cross-section width and height of 6.2572 ft (1.9072 m) and 5.0843 ft (1.5497 m), respectively, and spaced 18.1667 ft (5.5372 m) apart. Table 2.1 shows the comparison of the dimensions and material properties of the real and model superstructure.

Table 2.1. Geometric and material properties of real and model superstructure of frame pier

	Cross-section area (ft^2)	**I_{xx} (ft^4)**	**I_{yy} (ft^4)**	**Span length (ft)**	**Span mass (lb)**	**Density (pcf)**	**E (ksi)**	**Poisson's ratio**
Real	48.48	137.0	5456.9	117.0	849,776	150.0	3,626	0.2
Model	63.63	137.1	5456.9	117.0	849,776	114.2	3,626	0.2

The moment of inertia was determined about the centroid of the real and model superstructure. The longitudinal ends of the superstructure model corresponded to the locations of the adjacent piers. The adjacent piers were modeled with translational and rotational springs. The springs were modeled using discrete elements. The translational and rotational stiffness of the frame pier were 3.448×10^4 kN/m and 4.689×10^5 kN.m/rad, respectively. The reported stiffness values were determined by applying a lateral load and couple to the bent cap of the frame pier model without the superstructure and measuring the corresponding deflection and rotation. The superstructure transmits its weight to the piers through elastomeric bearing pads.

Eight plain 70-durometer neoprene bearing pads were used at Pier 3. The bearing pads were modeled using two beam elements, one under each of the two superstructure parts, and were connected to the superstructure by merged nodes. The geometric and material properties for each of the two model bearings were as follows: 48.15 in. × 15.2 in. × 1.0 in. mm (1,223 mm × 386 mm × 25.4 mm), density of 490 pcf (7,850 kg/m^3), Poisson's ratio of 0.3, and modulus of elasticity of 29,000 ksi (200 GPa). The model bearings were connected to the pier cap at the two locations corresponding to the center of the column cross-section by merged nodes.

The cantilever of the pier cap was tapered at the bottom. The dimensions of the pier cap, including the cantilever, were 30 ft × 4 ft × 4.5 ft (9.19 m × 1.22 m × 1.37 m).

Concrete material for the frame pier had a compressive strength of 4 ksi (28 MPa) and was modeled with solid elements. The reinforcement was Grade 60 steel and was modeled using beam elements. Details of the concrete material and steel reinforcement, in addition to the reinforced concrete model validation, are presented later in the report.

The top-most horizontal steel reinforcement in the pier cap was made up of #9 (#29) bars and the bottom-most was made up of #8 (#25) bars. The horizontal steel reinforcement between these two bars were #5 (#16) bars. The vertical reinforcement was made up of #5 (#16) bars. The pier cap model is shown in Figure 2.3 along with its steel reinforcement detailing.

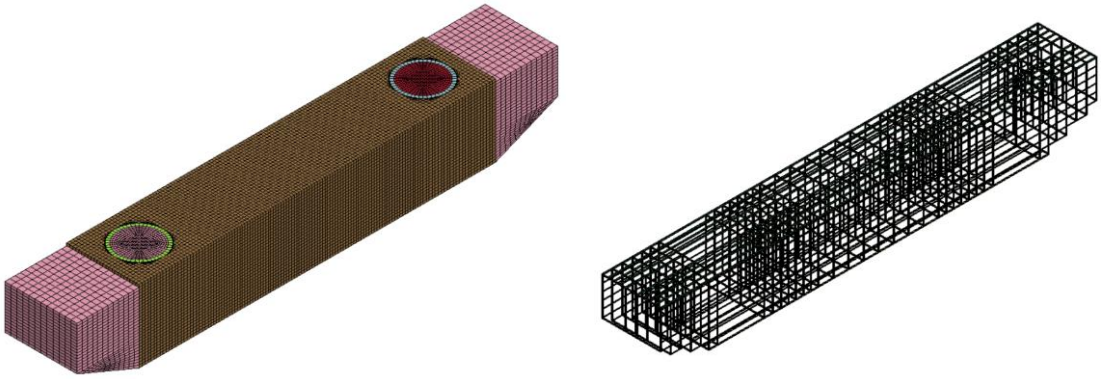

(a) (b)

Figure 2.3. Details of the frame pier's bent cap: (a) concrete and (b) steel reinforcement

The bridge columns were 21 ft (6.4 m) tall and 3.5 ft (1.07 m) in diameter. The longitudinal reinforcement of each column was made up of 16 #8 (#25) bars, and the nodes in the model were merged with those of the pier cap, column, and pile cap. The transverse reinforcement was made up of #5 (#16) spirals at a 4 in. (101.6 mm) pitch and were constrained in the columns using beam-in-solid constraints. The clear cover was 2 in. (50.8 mm). The dimensions of the pile cap were 18 ft × 13 ft × 3.5 ft (5.49 m × 3.96 m × 1.07 m). The details of the modeled piers are shown in Figure 2.4.

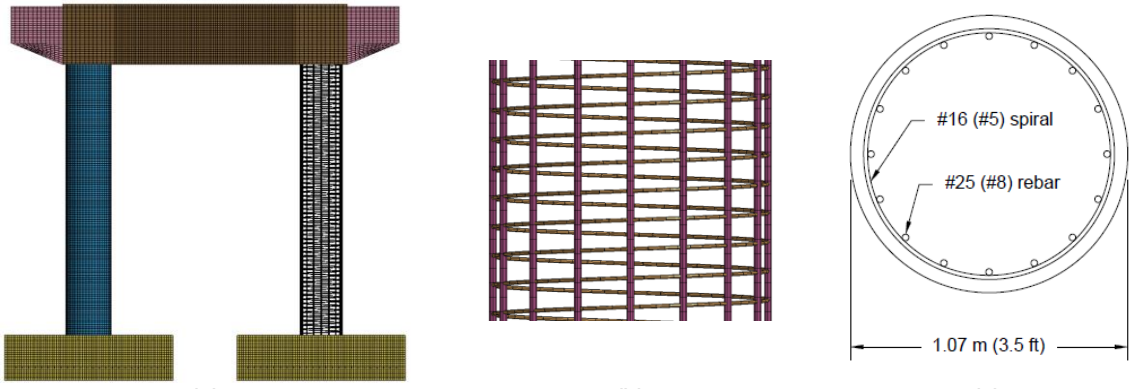

(a) (b) (c)

Figure 2.4. Details of the frame pier's columns: (a) side view, (b) close-up of steel reinforcement in the column, and (c) column cross-section

In the pile cap, both the tension and compression regions were reinforced with horizontal bars placed longitudinally and transversely. The rebar in the bottom of the pile cap consisted of #9 (#29) bars spaced at 6 in. (152.4 mm) in both the longitudinal and transverse directions. The reinforcing steel bar in the top of the pile cap consisted of #5 (#16) bars spaced at 10 in. (254

mm) in both the longitudinal and transverse directions. The steel reinforcement in the pile cap are shown in Figure 2.5.

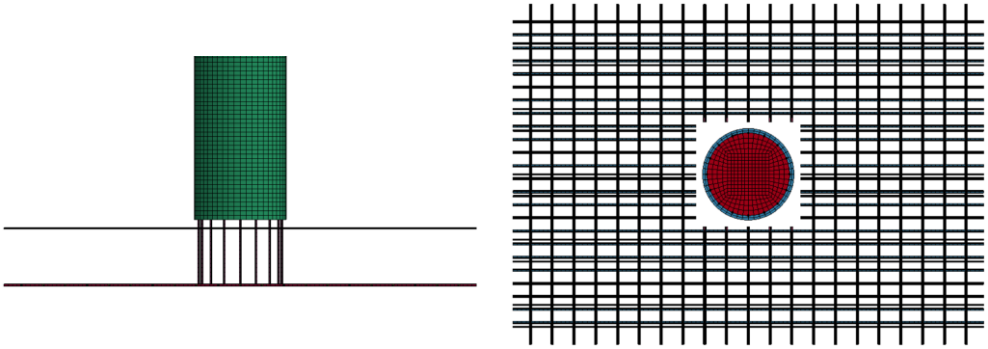

Figure 2.5. Steel reinforcement details of frame pier's pile cap: (a) side view and (b) top view

The deep foundation of the frame pier in the bridge plans was made up of precast prestressed concrete piles. However, steel H-piles (HP 10×57) were used in the bridge modeling to reduce computation time during simulations. The length of the piles was 38 ft (11.58 m) long. Figure 2.6 shows the details of the deep foundation and soil.

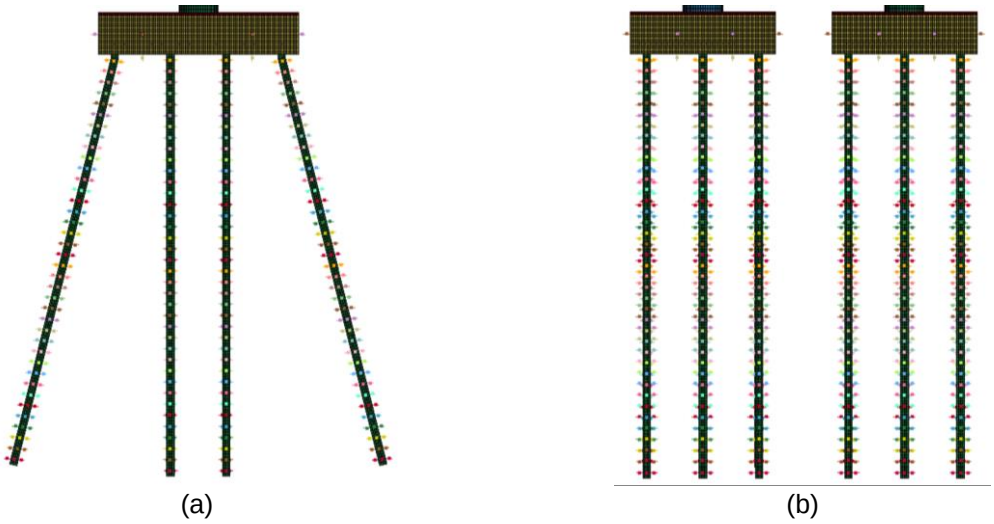

Figure 2.6. Details of the frame pier's deep foundation: (a) view in pier's longitudinal direction and (b) side view from road

Soil was modeled as stiff clay using springs in two horizontally perpendicular directions. The springs were modeled with discrete elements. Table 2.2 shows the properties of the stiff clay that were used to develop the soil model.

Table 2.2. Stiff clay soil parameters

Parameter	Value Implemented	Literature
c (kpa)	150	100–200*, 96–192**
$\boldsymbol{\gamma_{sat}}$ (kN/m^3)	19.6	18.9–22.0*, 19.6***
$\boldsymbol{\varepsilon_c}$ (mm/mm)	0.007	0.007****
J	0.5	0.5****

*Bowles 1988, **NAVFAC 1986, ***Lindeburg 2018, ****Klinga and Alipour 2015

The spring properties were obtained following the procedure outlined by the American Petroleum Institute (API 2002). The API provides lateral soil resistance-deflection (*p-y*) curves to model the lateral load bearing capacity of piles. The springs were placed at 1.0 ft (0.3 m) intervals along the pile length. The bottom nodes of the piles were fixed in all directions of translation and rotation. The API method for stiff clay was developed from Reese et al. (1975). The ultimate resistance, P_u, of the stiff clay soil at 1.0 ft (0.3 m) intervals was determined from Equations 2.1 and 2.2.

$$P_u = 3c + \gamma X + J\frac{cX}{D} \text{ for } X < X_R \quad (2.1)$$

$$P_u = 9c \text{ for } X \geq X_R \quad (2.2)$$

where c is the undrained shear strength for undisturbed clay soil samples, γ is the effective unit weight of the soil, X is the depth below soil surface, J is a dimensionless empirical constant with values ranging from 0.25 to 0.5 having been determined by field testing (J = 0.5 assumed following Matlock [1970]), D is the pile diameter, and X_R is the depth below soil surface to bottom of reduced resistance zone.

The bottom of the reduced resistance zone is where P_u does not go past 9c, and this occurs at a soil depth where Equations 2.1 and 2.2 are equal. Combining Equations 2.1 and 2.2 gives Equation 2.3.

$$X_R = \frac{6D}{\frac{\gamma D}{c} + J} \quad (2.3)$$

Minimum values of X_R should be about 2.5 times the pile diameters (API 2002). For the case when equilibrium is reached under cyclic loading, the *p-y* curves may be generated from Table 2.3.

Table 2.3. Load-displacement (*p-y*) curves

$X > X_R$		$X < X_R$	
P/P_u	y/y_c	P/P_u	y/y_c
0	0	0	0
0.5	1.0	0.5	1.0
0.72	3.0	0.72	3.0
0.72	∞	0.72 X/X_R	15.0
		0.72 X/X_R	∞

Cyclic loading was assumed in this study and, therefore, Table 2.3 was used to develop the *p-y* curves for stiff clay.

2.4 Modeling of T-Pier

The bridge on IA 152 over I-35 was used to model the T-pier bridge. Its superstructure is made of PPCBs, which rest on elastomeric neoprene bearing pads at the piers. The bridge had three piers, each consisting of a pier cap, column, pile cap, and deep foundation. The T-pier was modeled as the middle pier in the bridge plans as shown in Figure 2.7(a).

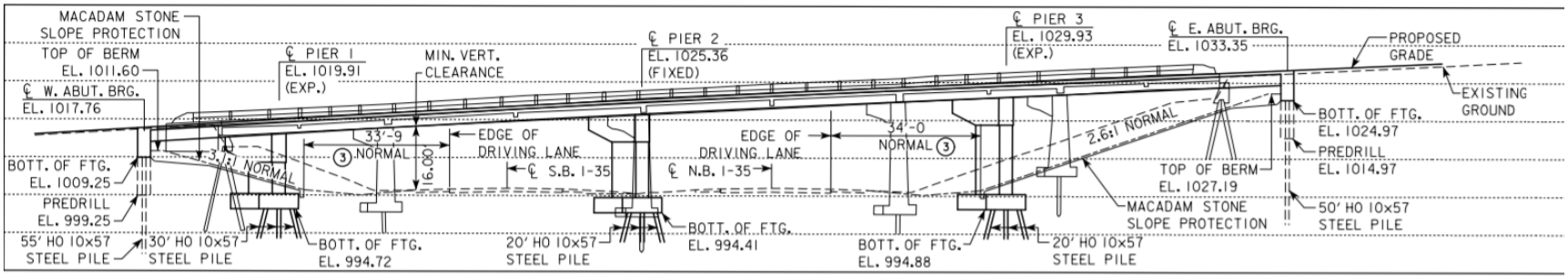

(a)

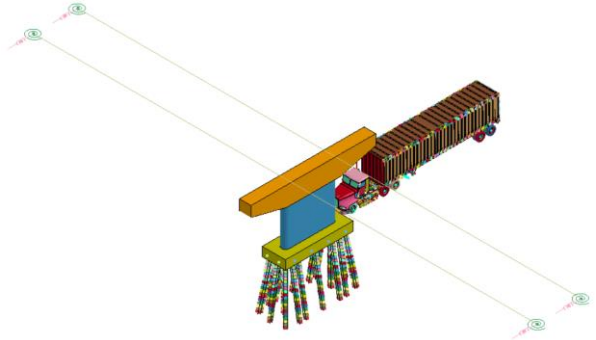

(b)

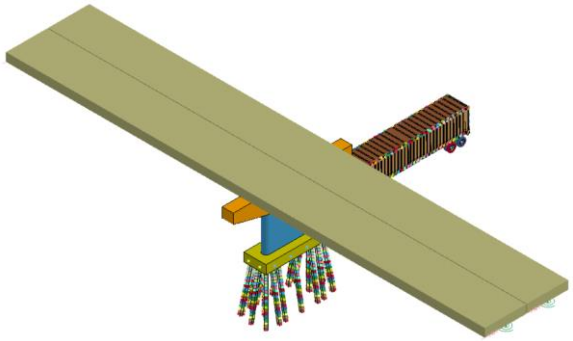

(c)

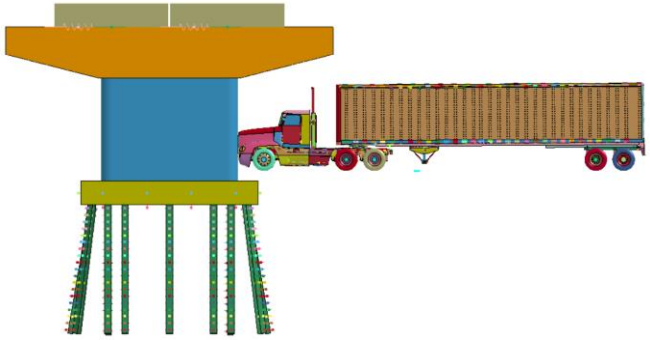

(d)

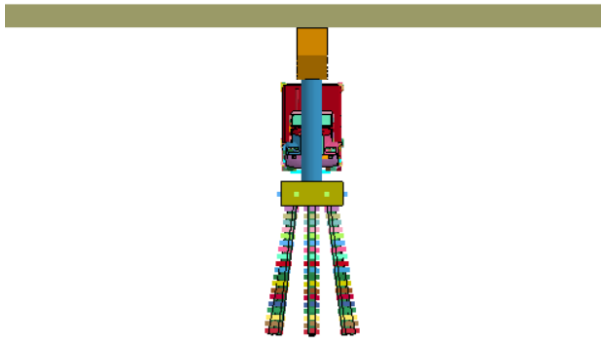

(e)

Figure 2.7. T-pier model

The FE model of the T-pier is shown in Figures 2.7(b) through (e). Like the frame pier, the superstructure of the T-pier was modeled as two parallel parts using beam elements and elastic material. The dimensions and properties of the beam elements were determined from the cross-section and material properties of the actual superstructure, and the components considered were the prestressed beams, concrete deck, and barriers. Each of the two parallel superstructure parts had a cross-section width and height of 200.5 in. (5,092.9 mm) and 40.9 in. (1,039.5 mm), respectively, spaced 204.0 in. (5,181.6 mm) apart. Table 2.4 shows the comparison of the dimensions and material properties of the actual and model superstructure.

Table 2.4. Geometric and material properties of real and model superstructure of T-pier

	Cross-section area (ft^2)	**I_{xx} (ft^4)**	**I_{yy} (ft^4)**	**Span length (ft)**	**Span mass (lb)**	**Density (pcf)**	**E (ksi)**	**Poisson's ratio**
Actual	58.32	110.42	10,884.7	96.85	846,295	150.0	3,626	0.2
Model	113.97	110.42	10,884.7	96.85	846,295	76.7	3,626	0.2

The moment of inertia was determined about the centroid of the actual and model superstructure. The ends of the superstructure model corresponded to the locations of the adjacent piers. The adjacent piers were modeled with translational and rotational springs, and the springs were modeled using discrete elements.

The translational and rotational stiffness of the T-pier were 1.667×10^5 kN/m and 1.034×10^6 kN.m/rad, respectively. The reported stiffness values were determined by applying a lateral load and couple to the bent cap of the frame pier model without the superstructure and measuring the corresponding deflection and rotation.

The superstructure transmits its weight to the piers through elastomeric bearing pads. Ten plain neoprene bearing pads were used at Pier 2. The bearing pads were modeled using two beam elements, one under each of the two superstructure parts, connected to the superstructure by merged nodes. The geometric and material properties for each of the two model bearings were 87.13 in × 6757 in. × 0.13 in. (1,984.4 mm × 1,716.3 mm × 3.2 mm), with a density of 490 pcf (7,850 kg/m^3), Poisson's ratio of 0.3, and modulus of elasticity of 29,000 ksi (200 GPa). The model bearings were connected to the pier cap by merged nodes.

The pier cap model is shown in Figure 2.8 along with its steel reinforcement.

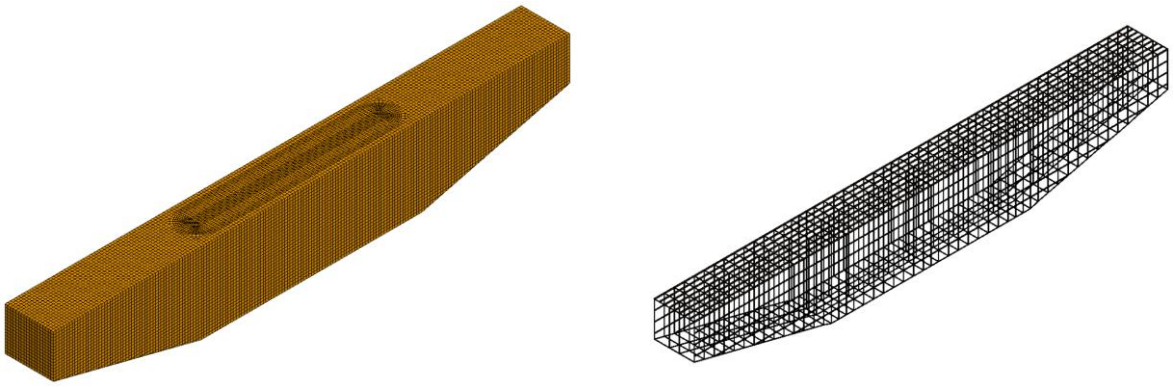

(a) (b)

Figure 2.8. Details of the T-pier's bent cap: (a) concrete and (b) steel reinforcement

The cantilever of the pier cap was tapered. The dimensions of the pier cap were 48 ft × 4.5 ft × 7.5 ft (14.63 m × 1.37 m × 2.29 m).

Concrete material for the T-pier had a compressive strength of 4 ksi (28 MPa) and was modeled with solid elements. The reinforcement was Grade 60 steel and was modeled using beam elements. The modeling details of the concrete and steel materials are presented later in this report. The top-most horizontal steel reinforcement in the pier cap were #11 (#35) bars, and the ones below were #8 (#25) bars spaced at 1.0 ft (0.30 m) intervals. The vertical reinforcement consisted of #6 (#19) bars, also spaced at 1.0 ft (0.30 m) intervals. The details of the column are shown in Figure 2.9.

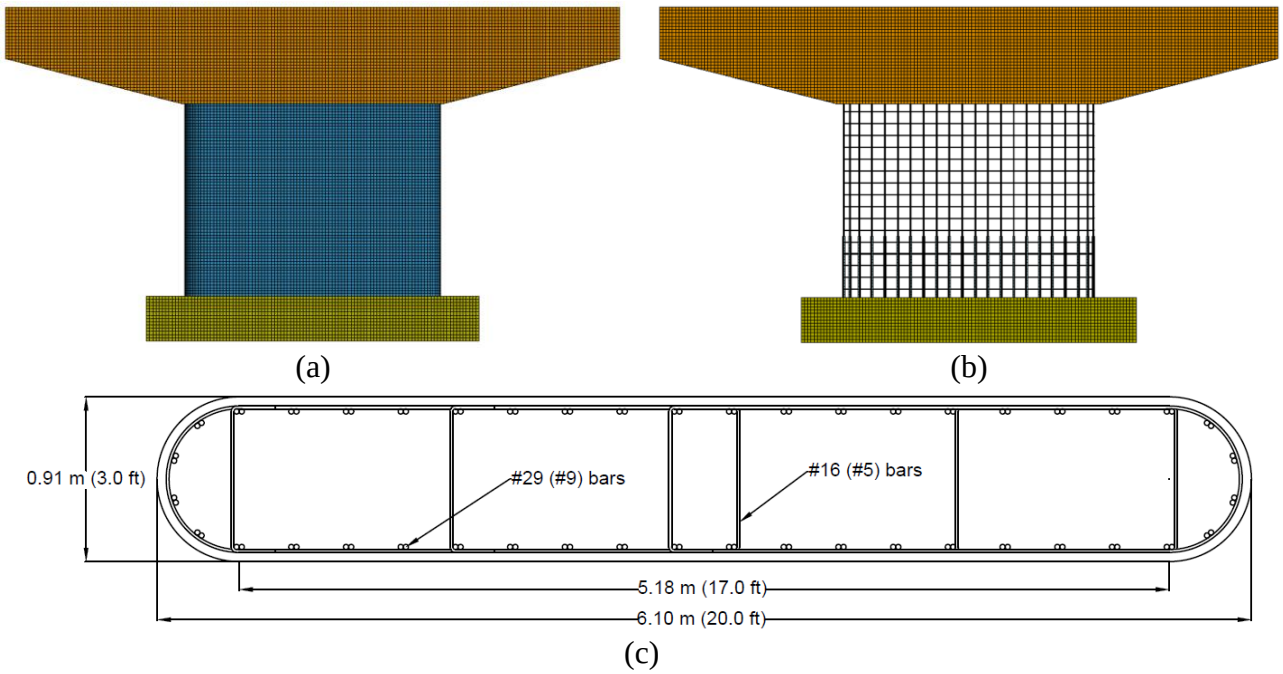

(a) (b)

(c)

Figure 2.9. Details of the T-pier's column: (a) concrete, (b) column steel reinforcement, and (c) column cross-section

The column was 15 ft (4.57 m) tall, 20 ft (6.10 m) long, and 3 ft (0.91 m) wide. It had rounded edges, as shown in Figure 2.9(c). The longitudinal reinforcement of the column was made up of 44 #9 (#29) bars. The spacing of the longitudinal reinforcing steel bar was 1 ft (0.30 m) apart.

The transverse reinforcement consisted of #5 (#16) ties at spaced 11 in. (279 mm) apart. The clear cover was 2 in. (50.8 mm). The dimensions of the pile cap were 26 ft × 9 ft × 3.5 ft (7.92 m × 2.74 m × 1.07 m). The steel reinforcement details in the pile cap are shown in Figure 2.10.

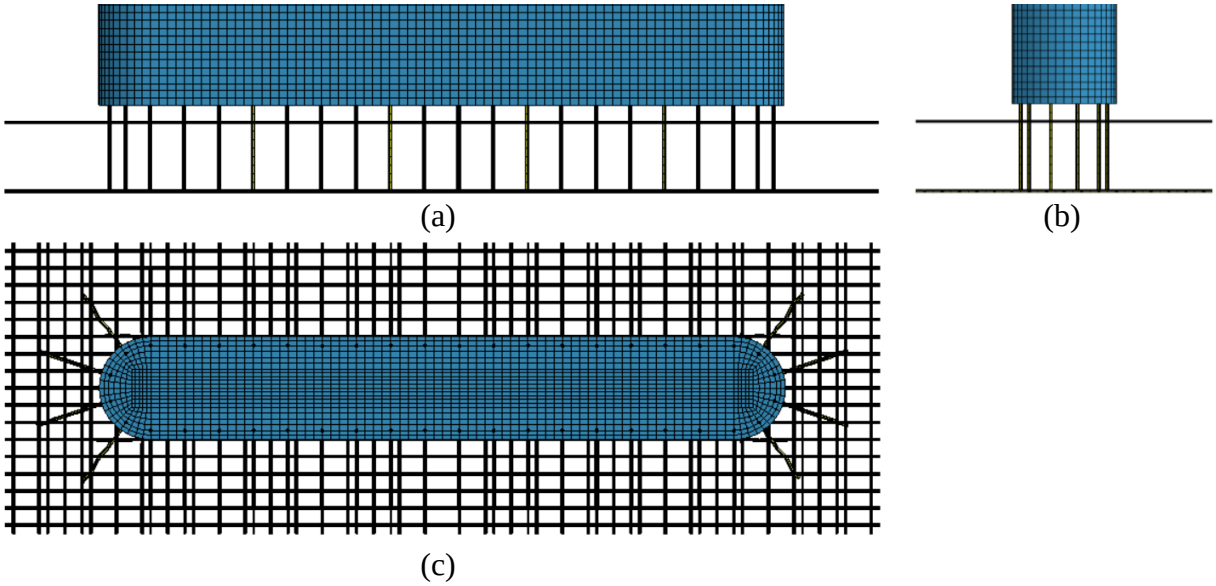

Figure 2.10. Steel reinforcement details of T-pier's pile cap: (a) side view from road, (b) view in column's longitudinal axis, and (c) top veiw

Both the bottom and top of the pile cap were reinforced with horizontal bars placed longitudinally and transversely. The reinforcing steel bars in the bottom consisted of #8 (#25) bars spaced at 8 in. (203.2 mm) in both the longitudinal and transverse directions. The reinforcing steel bars in the top consisted of #5 (#16) bars spaced at 12 in. (304.8 mm) in both the longitudinal and transverse directions. Figure 2.11 shows the details of the deep foundation and soil.

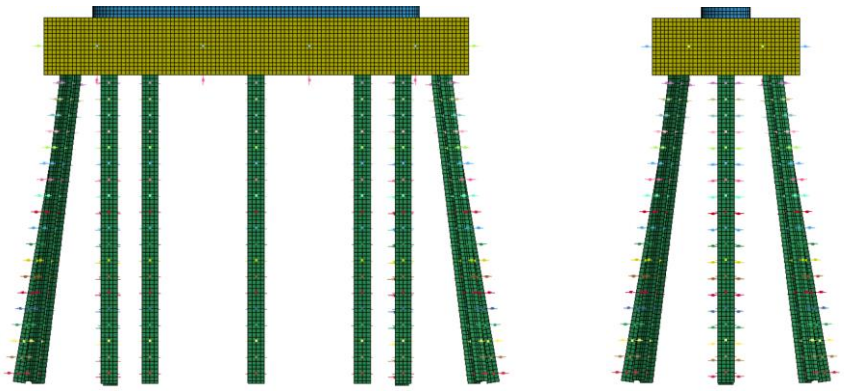

(a) (b)

Figure 2.11. Details of the T-pier's deep foundation: (a) side view from the road and (b) view in column's longitudinal axis

The deep foundation was made up of steel H-piles (HP 10×57) 20 ft (6.10 m) long. The soil was modeled as stiff clay using discrete spring elements in two horizontally perpendicular directions. The mechanical properties of the soil used to develop the soil springs were similar to that used for the frame pier, and the procedure outlined by the American Petroleum Institute (API 2002) was followed to develop the spring stiffness. The springs were placed at 1.0 ft (0.30 m) intervals along the pile length. The bottom nodes of the piles were fixed in all directions of translation and rotation.

2.5 Modeling of Frame Pier with Barrier

Part of the Iowa DOT's provisions for vehicular collisions is setting up concrete barriers around the piers to be protected (Iowa DOT 2020 BDM Section 6.6.2.6). These barriers are supposed to absorb the impact forces from vehicles and are anchored to the pavement within a region of 10 ft (3.05 m) from the bridge pier columns. A concrete barrier similar to what the Iowa DOT uses in bridge pier protection was modeled and placed around the frame pier as shown in Figure 2.12.

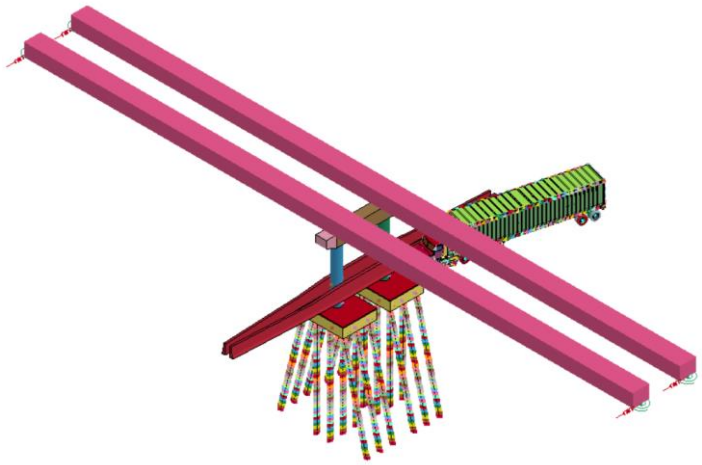

Figure 2.12. Frame pier model with barrier

Figure 2.13(a) shows the side view of the concrete barrier in the direction of vehicle travel, and Figure 2.13(b) shows the geometry and dimensions of the concrete barrier.

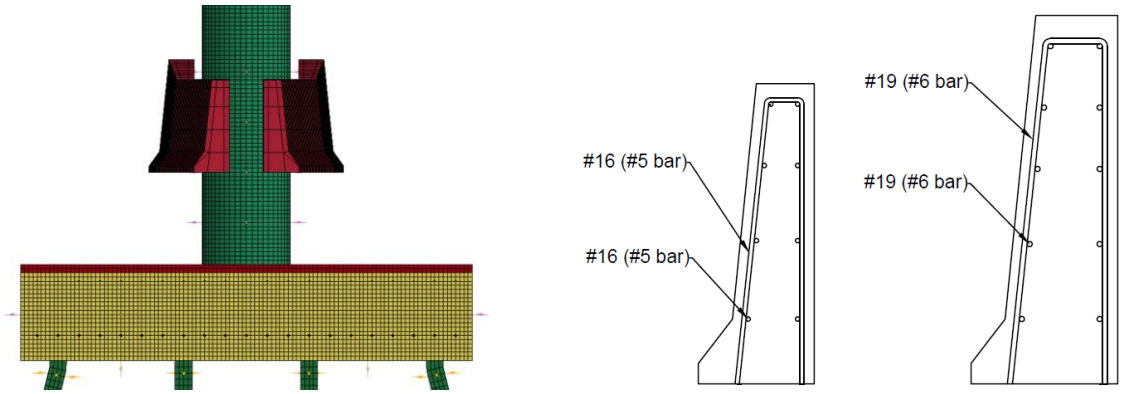

Figure 2.13. Frame pier model with barrier: (a) view of barrier's longitudinal axis, and (b) cross-sections of barrier

The smaller barrier represents the section of the barrier farther away from the pier columns, and the larger barrier represents the section in the vicinity of the pier columns. A reinforced concrete barrier taper connected the two sections together. The concrete barrier was obtained from Iowa DOT bridge plans. The side view perpendicular to the length of the barrier is shown in Figure 2.14.

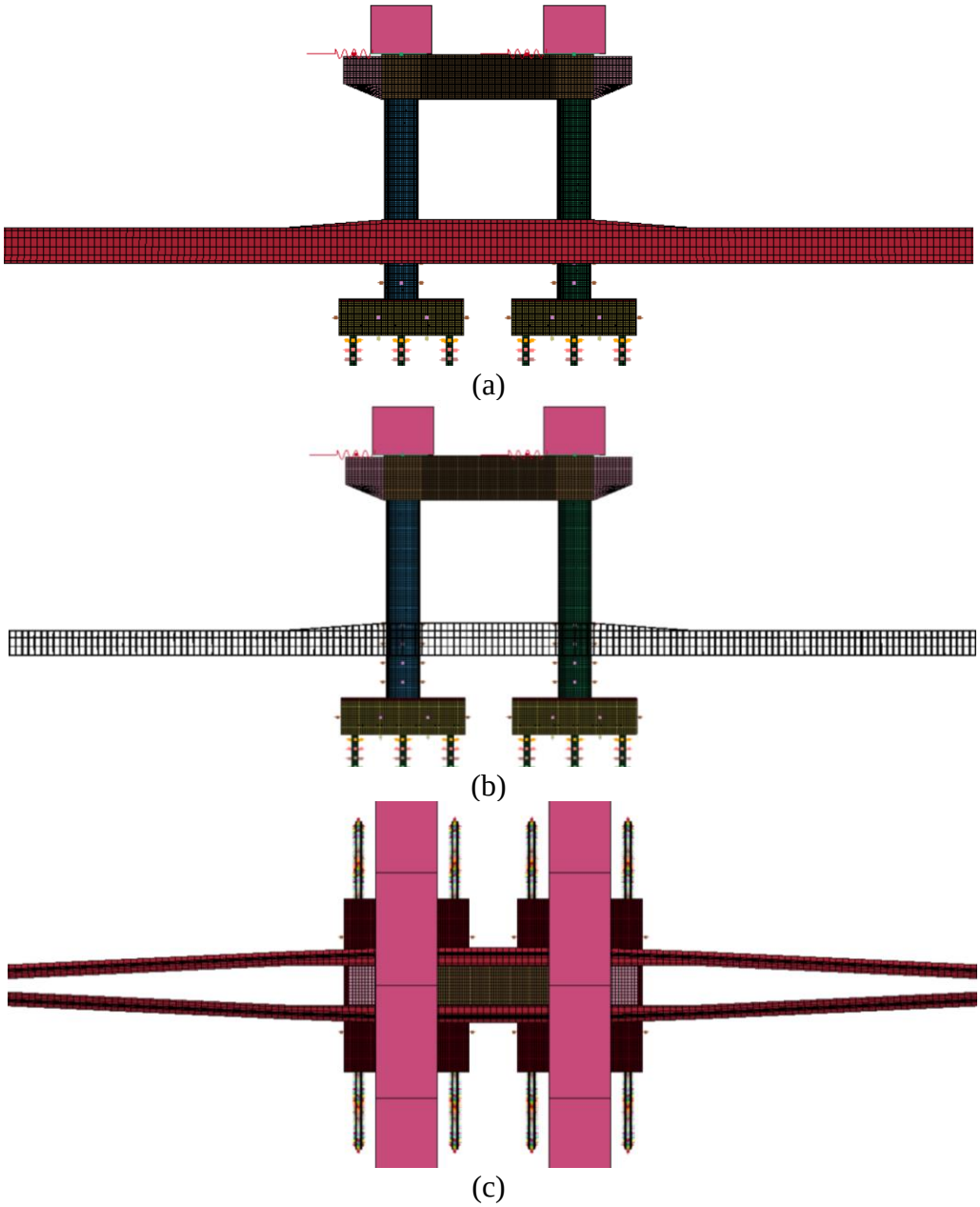

Figure 2.14. Frame pier model with barrier: (a) side view with concrete, (b) side view with reinforcing steel bar, and (c) top view

Figure 2.14(a) shows the concrete, while Figure 2.14(b) shows the reinforcement. As previously explained, a taller concrete barrier was present at the location of the bridge columns. The concrete barrier, however, tapered to a shorter height immediately after the bridge columns. Figure 2.14(c) shows the top view of the bridge frame pier with the barrier. From the top, it can be observed that the two concrete barriers that were wrapped around the pier columns were eventually joined together farther up or down the roadway.

2.6 Modeling of Frame Pier with Crash Wall

Part of the Iowa DOT's provisions for vehicular collisions is a crash wall that is integrated into a frame pier (Iowa DOT 2020 BDM Section 6.6.4.1). A schematic of the crash wall is shown in Chapter 1 (Figure 1.2). Following the schematic, a model was developed for a crash wall that barely satisfies the minimum requirements, integrated into the frame pier. The frame pier with the crash wall is shown in Figure 2.15.

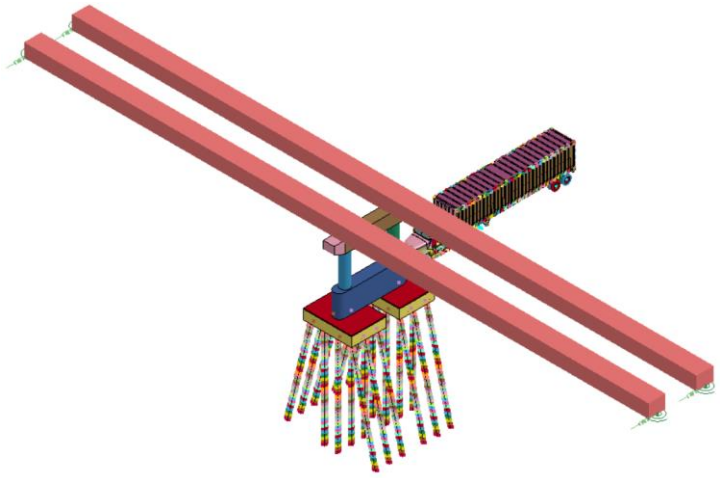

Figure 2.15. Frame pier model with crash wall

The wall extended 4 ft (1.22 m) into the ground, and the wall rested on the pile cap. Different views of the crash beam and reinforcement details are shown in Figure 2.16.

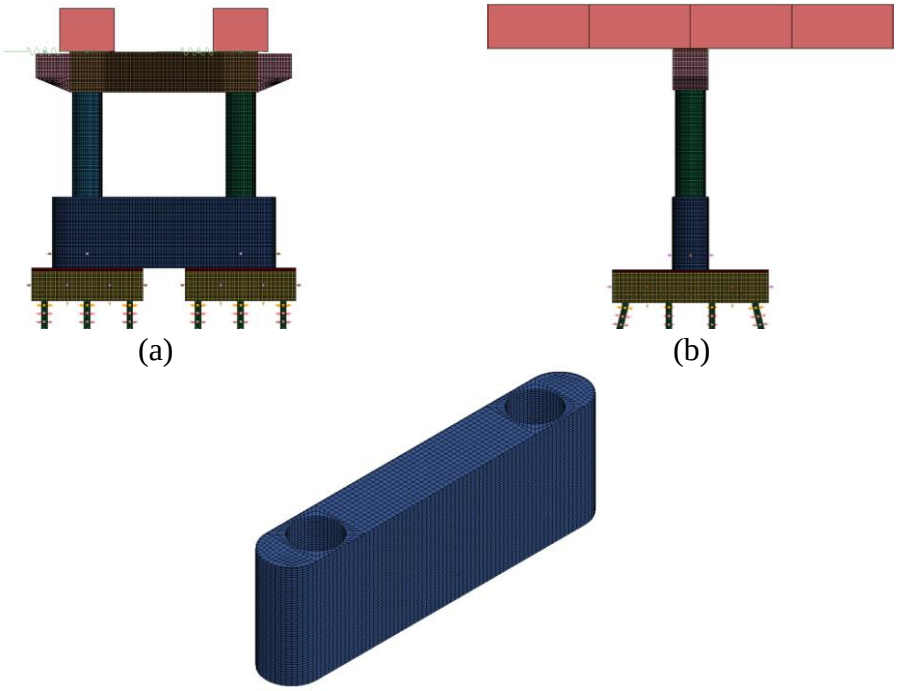

Figure 2.16. Frame pier model with crash wall showing: (a) side view from road, (b)view in crash wall's longitudinal axis, and (c) crash wall concrete.

Both the longitudinal and transverse reinforcement of the crash beam were made up of #5 (#16) reinforced steel bars spaced at 12 in. (304.8 mm).

2.7 Reinforced Concrete Modeling and Model Validation

In this study, concrete was modeled using the continuous surface cap model (CSCM). The CSCM accounts for the concrete's strength, stiffness, hardening/softening, damage, and strain rate effect. The formulation for the CSCM includes three surfaces: triaxial compression, triaxial extension, and torsional shear. The model also includes a hardening cap surface that defines the pressure under which the material begins to exhibit inelastic strains. The CSCM damage formulation includes strain softening in both compression and tension, in addition to modulus reduction. The strain rate effect captures the increase in the concrete's strength when increasing the strain rate.

In this study, normal-weight concrete was used for the bridge piers with a density of 150 pcf (2,400 kg/m^3). The unconfined compressive strength of the concrete was assumed as 4 ksi (28 MPa) based on Iowa DOT bridge plans, and the maximum aggregate size was considered to be 0.79 in. (20 mm).

The concrete was modeled using eight-node solid elements. The steel reinforcement was modeled using the piece-wise linear plasticity model. This material model allows defining the steel reinforcement density, modulus of elasticity, yield strength, Poisson's ratio, effective stress-

plastic strain relationship, and strain rate effect. The steel reinforcement density was assumed as 490 pcf (7,850 kg/m^3). The modulus of elasticity and yield strength of steel were considered to be 29,000 ksi (200 GPa) and 60 ksi (420 MPa), respectively. The Poisson's ratio was 0.3. The effective stress-plastic strain relationship for the steel material was obtained from the experimental tensile tests performed on No. 6 (#19) Grade 60 ksi (420 MPa) rebar, as reported in El-Hacha et al. (2004). The strain rate effect in the rebar followed the equations proposed by Malvar and Crawford (1988). The Hughes-Liu elements (with cross-section integration) were used to model the steel reinforcement. The steel H-piles were modeled with the piece-wise linear model, and the steel material properties remained similar to those defined for the steel reinforcement.

Prior to the main vehicle collision simulations, the reinforced concrete material model, consisting of the concrete and steel material models, was validated. Detailed setups were established to replicate the experimental tests performed by Fujikake et al. (2009). In that study, a drop hammer impact test was performed on reinforced concrete beams. Details of the drop hammer and beam model used for validating the reinforced concrete material are shown in Figure 2.17.

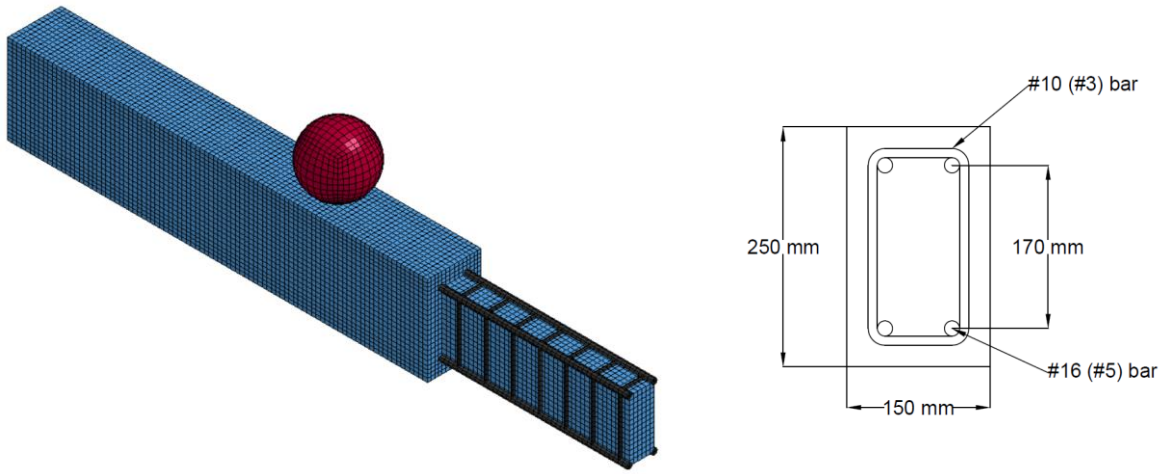

Figure 2.17. Details of the beam models for validating the reinforced concrete material model: (a) beam and hammer and (b) beam cross-section

After conducting a sensitivity analysis, a mesh size of 0.5 in. (12.5 mm) was used for the validation. The compressive strength of the reinforced concrete was 6.1 ksi (42 MPa), The dimensions of the reinforced concrete beam specimen were 66.9 in. × 9.84 in. × 5.91 in. (1,700 mm × 250 mm × 150 mm), and the clear span between supports was 55.1 in. (1,400 mm).

The spherical drop hammer had a radius of 3.54 in. (90 mm) and a mass of 882 lb (400 kg). The drop hammer was modeled using the same material model used for the rebar. Fujikake et al. (2009) considered different scenarios involving various longitudinal reinforcements and drop heights. The longitudinal rebar considered in the model validation in this study was the #5 (#16) reinforcing steel bar used as both tension and compression reinforcement.

The shear reinforcement consisted of #3 (#10) bar ties spaced at 3.0 in. (75 mm). Two drop heights were considered in this study from Fujikake et al. (2009): 6.0 in. (150 mm) and 47.2 in. (1,200 mm). These heights corresponded to the lowest and highest drop heights considered by Fujikake et al (2009) for the longitudinal reinforcement combination considered.

The nodes of the steel reinforcement were shared with those of the concrete elements. This provided a perfect bond between the reinforcing steel bars and concrete, replicating how the reinforced concrete structures respond to impact loads. To save computational time, instead of dropping the weight from the actual height, an initial velocity was applied to the drop hammer at the point of impact.

The gravity effect was also included in the model. The interaction between the drop hammer and reinforced concrete beam was considered using the automatic surface-to-surface contact algorithm. The static and dynamic coefficients of friction in the contact algorithm were set to 0.3, following El-Tawil et al. (2005). The segment-based pinball constraint was selected in the automatic surface-to-surface contact algorithm. The Belytschko-Bindeman equation with a coefficient of 0.1 was used as the hourglass. Figure 2.18 shows the comparison of the simulation results to the experimental results from Fujikake et al. (2009).

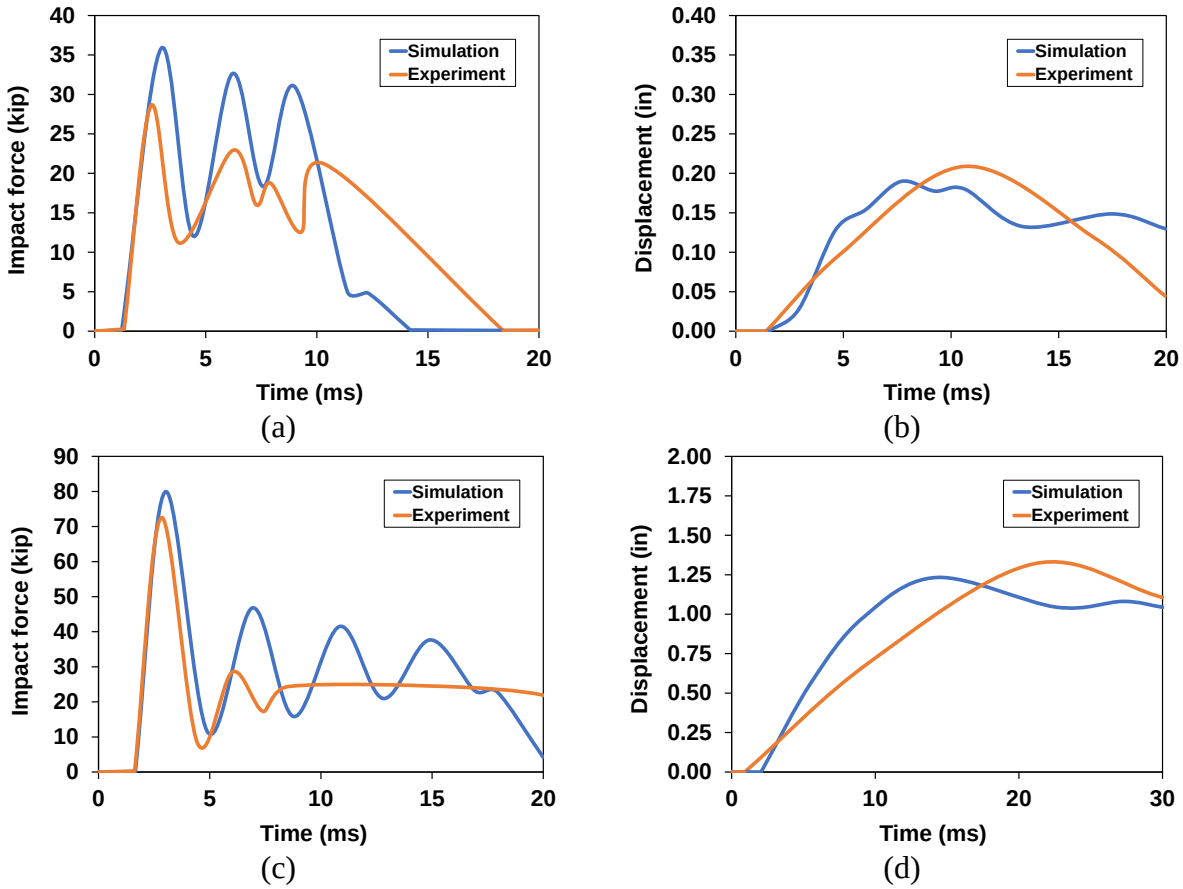

Figure 2.18. Comparison of simulation and experimental resuslts: (a), (b) 5.91 in. drop height, and (c), (d) 47.2 m drop height

The impact force time histories obtained from the simulations were in agreement with those recorded from the Fujikake et al. (2009) experiment. Similarly, the mid-span deflection time histories provided peak values that agreed to those recorded during those experiments. The comparison of damage obtained in the simulations and experimental test results are shown in Figure 2.19.

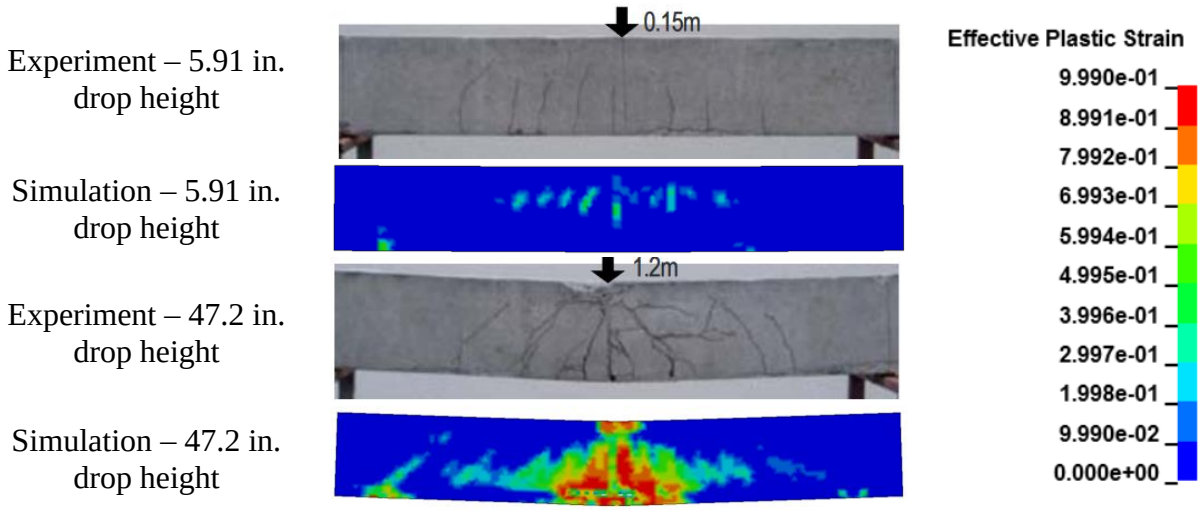

Figure 2.19. Frame pier model with crash wall

The figure shows that the damage patterns were similar for the simulation and experimental results, and, therefore, the reinforced concrete model can adequately show damage patterns compared to experimental results. This confirmed the validity of the reinforced concrete material model for this study.

2.8 Simulation Setup

The research team conducted a mesh convergence study to determine the appropriate mesh sizes for the bridge piers. After the bridge piers were modeled with approriate mesh sizes, they were allowed to undergo gravity loads and dynamic relaxation before the tractor-semitrailer was introduced into the model.

The tractor-semitrailer was allowed to collide into each bridge pier at impact velocities of 50 mph (80.5 km/h), 70 mph (112.7 km/h), and 90 mph (144.8 km/h). The various response measures discussed from the collision simulations included damage, impact force, shear force, bending moment, and displacement. To ensure that the tractor-semitrailer was loaded to 80,000 lb (36,287 kg), the initial kinetic energy (KE) estimated from 0.5 × mass × velocity^2 and the observed KE in the collision simulations were compared, as shown in Table 2.5.

Table 2.5. Comparison of estimated and observed initial kinetic energy for 80,000 lb load

Velocity (mph)	Estimated KE (ft-kip)	Observed KE (ft-kip)
50	6,685	6,684
70	13,102	13,103
90	21,658	21,651

2.9 Analysis of Frame Pier and T-Pier Damage from Impact Simulations

The collision simulations involving the tractor-semitrailer and frame pier for the various impact velocities considered are shown in Figure 2.20.

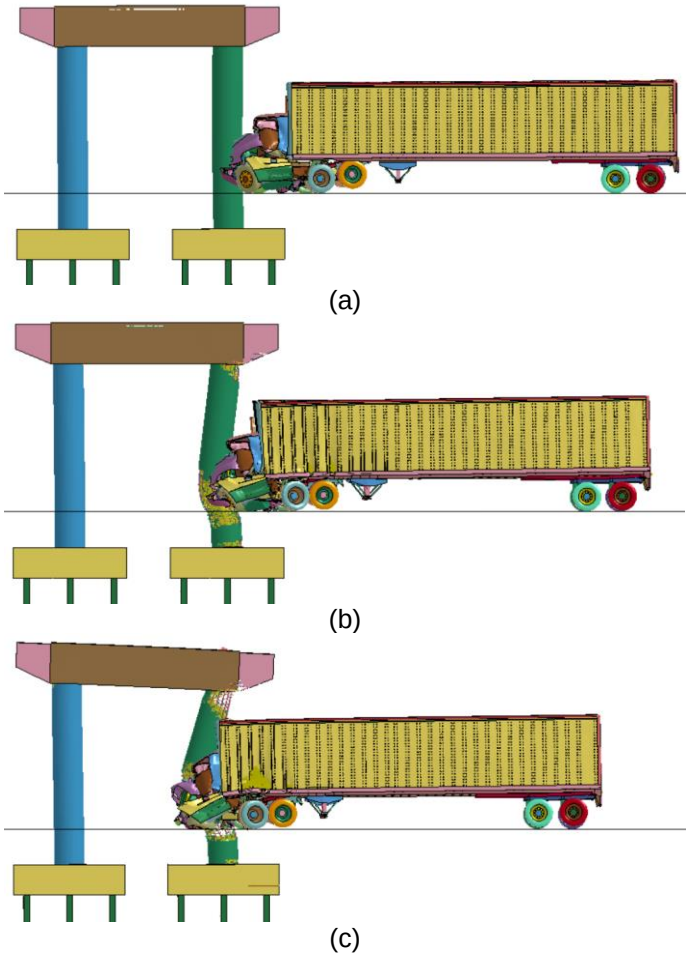

Figure 2.20. Collision simulation of tractor-semitrailer into frame pier: (a) 50 mph, (b) 70 mph, and (c) 90 mph

As expected, greater pier deterioration was observed at greater impact velocities. The effective plastic strains in the frame pier are shown in Figure 2.21.

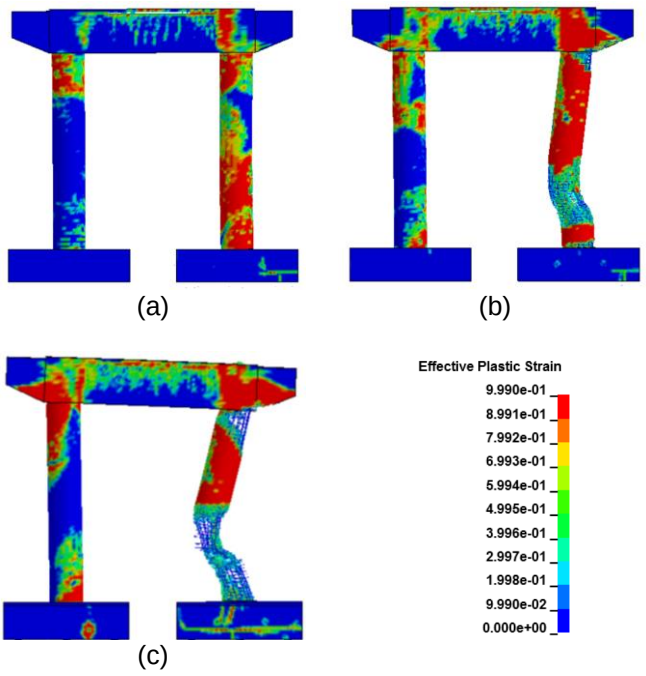

Figure 2.21. Simulation of damage from vehicle collision into the frame pier: (a) 50 mph, (b) 70 mph, and (c) 90 mph

With the tractor-semitrailer out of the way, the results showed that the frame pier column was able to withstand the vehicle collision at the impact velocity of 50 mph (80.5 km/h), and there was yielding of the reinforcing steel bar and deterioration of the concrete core for the impact velocity of 70 mph (112.7 km/h), but the pier did not collapse. There was yielding of the reinforcing steel bar and deterioration of the concrete core for the impact velocity of 90 mph (144.8 km/h), while the pier collapsed as well. These were visual evaluations of the level of bridge pier damage after most of the collision had occurred. However, to quantify the level of damage, a damage index ratio (DRI), which was developed by Auyeung et al. (2019) to define the expected damage on frame piers from vehicle collisions, was implemented.

The DRI can be used for both design and analysis. It was used in this study to analyze and validate the conditions of the frame pier columns after they experienced vehicle collisions (see Equation 2.4).

$$DRI = \frac{Kinetic\ Energy\ (ft{-}kip)}{\phi V_n\ (kip) \times Pier\ Diameter\ (ft)} \tag{2.4}$$

where
DRI = the damage ratio index
ϕV_n = the design shear capacity

The DRI for the three collision simulations considered was determined as shown in Table 2.6, and the descriptions of the DRI states for the values are shown in Table 2.7 (Auyeung et al. 2019).

Table 2.6. Determination of DRI values for frame pier

Velocity (mph)	Tractor Weight (lb)	KE (ft-kip)	ϕV_n (kip)	Pier Dia. (ft)	DRI
50	16,982	1,419	530	3.5	0.76
70	16,982	2,782	530	3.5	1.50
90	16,982	4,599	530	3.5	2.48

Table 2.7. Description of damage state for DRI values

Damage State	Description	DRI range
Minor	Localized spalling of concrete cover, Tensile cracking of concrete	0.0–1.0
Moderate	Yielding of reinforcement, Shear cracking	1.0–1.5
Severe	Deterioration of concrete core, Plastic hinge formation	1.5–2.0
Collapse	Plastic hinge formation at top, bottom, and impact location of column, Collapse	> 2.0

Even though the tractor-semitrailer possesses the kinetic energy of both the tractor and semitrailer as one whole, during collision, the kinetic energy of the tractor and semitrailer act separately on the pier, and this is proved by the presence of two peaks in the impact force-time history if the simulation is allowed to run until the semitrailer and its contents are fully-involved in the collision. The kinetic energy used in the DRI calculation was therefore that of the tractor only. The pier column's shear capacity was defined by two shear failure planes as shown in Figure 2.22.

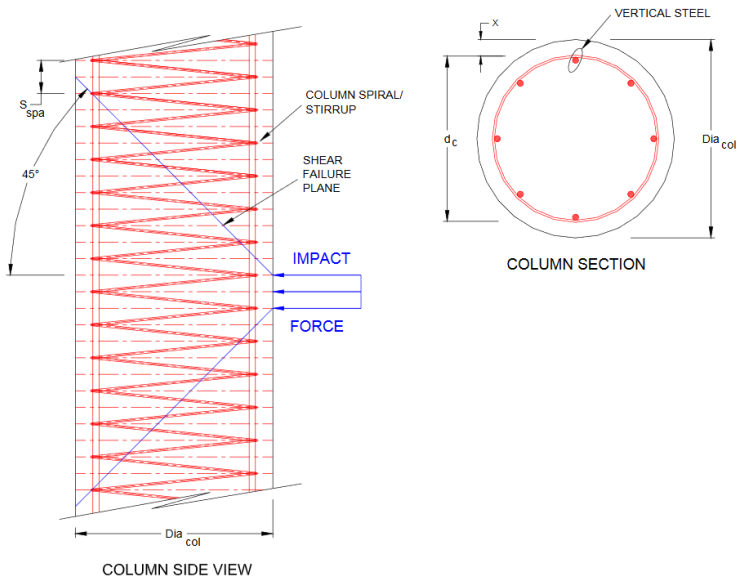

Buth et al. 2010, Texas Transportation Institute

Figure 2.22. Pier column showing two shear failure planes

Therefore, in determining the shear capacity of a pier's column, the shear capacity was determined for one shear failure plane and then multiplied by 2 to obtain the actual shear capacity of the pier.

As shown previously in Table 2.7, the DRI value of 0.76 for the pier column struck by the tractor-semitrailer traveling at 50 mph (80.5 km/h) suffers minor damage, which involves the localized spalling of the column concrete cover and the tensile cracking of column concrete. This description is exactly what is shown in the previous Figure 2.21(a), where the struck column still performs its function and there are no obvious signs that the column needs to be replaced.

According to Table 2.7, the DRI value of 1.50 is the boundary between moderate and severe damage in the column, and this DRI value is obtained for the pier column struck by the tractor-semitrailer with the impact velocity of 70 mph (112.7 km/h). The description for these damage states are yielding of column rebar, shear cracking in the column, deterioration of the column concrete core, and formation of plastic hinges in the column. This description is exactly what is shown in the previous Figure 2.21(b), where the section of the column at the impact location underwent deterioration of the concrete core due to the reinforcing steel bar yielding and forming a plastic hinge at the impact location. The pier would not collapse; however, it would be considered unstable.

According to Table 2.7, the DRI value of 2.48 for the pier column struck by the tractor-semitrailer with the impact velocity of 90 mph (144.8 km/h) falls within the category of collapse that is defined as plastic hinge formation at the top, bottom, and impact location of the column. This description is shown in the previous Figure 2.21(c), where the section of the column at the top, bottom, and impact location experience plastic hinge formation, and the bridge pier collapses.

Collision simulation results are not discussed here. However, theoretical DRI values and their physical descriptions for a special Iowa DOT BDM frame pier design against vehicular collision are discussed. The Iowa DOT BDM (2020) has a "no further design" guideline for frame piers without crash walls that meet the 600-kip collision force requirements if certain stipulations are met. The minimum design shear capacity of that guideline is 630 kips (2,803 kN), and the minimum pier diameter is 4.0 ft (1.22 m). Using these values and the kinetic energies from the three vehicle-impact velocities considered in this study, the DRI values were determined as shown in Table 2.8.

Table 2.8. Determination of DRI values of frame pier special design case

Velocity (mph)	Tractor Weight (lb)	KE (ft-kip)	ϕV_n (kip)	Pier Dia. (ft)	DRI
50	16,982	1,419	630	4.0	0.56
70	16,982	2,782	630	4.0	1.10
90	16,982	4,599	630	4.0	1.83

Comparing the DRI values in Table 2.8 to the descriptions in Table 2.7, it was observed that the 50 mph (80.5 km/h) impact velocity, which is the basis for the design guideline of 600 kips (2,669 kN) from AASHTO (2017) and the Iowa DOT BDM (2020), leads to minor damage. This reveals that the Iowa DOT BDM's guideline of "no further design" for frame piers without crash walls works well, because only minor damage is expected to be observed in the pier if it is involved in a vehicle collision with a fully-loaded tractor-semitrailer travelling at 50 mph (80.5 km/h). Investigating higher impact velocities, the 70 mph (112.7 km/h) impact velocity leads to moderate damage, and the 90 mph (144.8 km/h) impact velocity leads to severe damage. Note that failure does not occur in the pier for any of the three impact velocities considered. This goes back to the statement in the Iowa DOT BDM that the "no further design" guideline works well.

The collision simulations involving the tractor-semitrailer and the T-pier are shown in Figure 2.23.

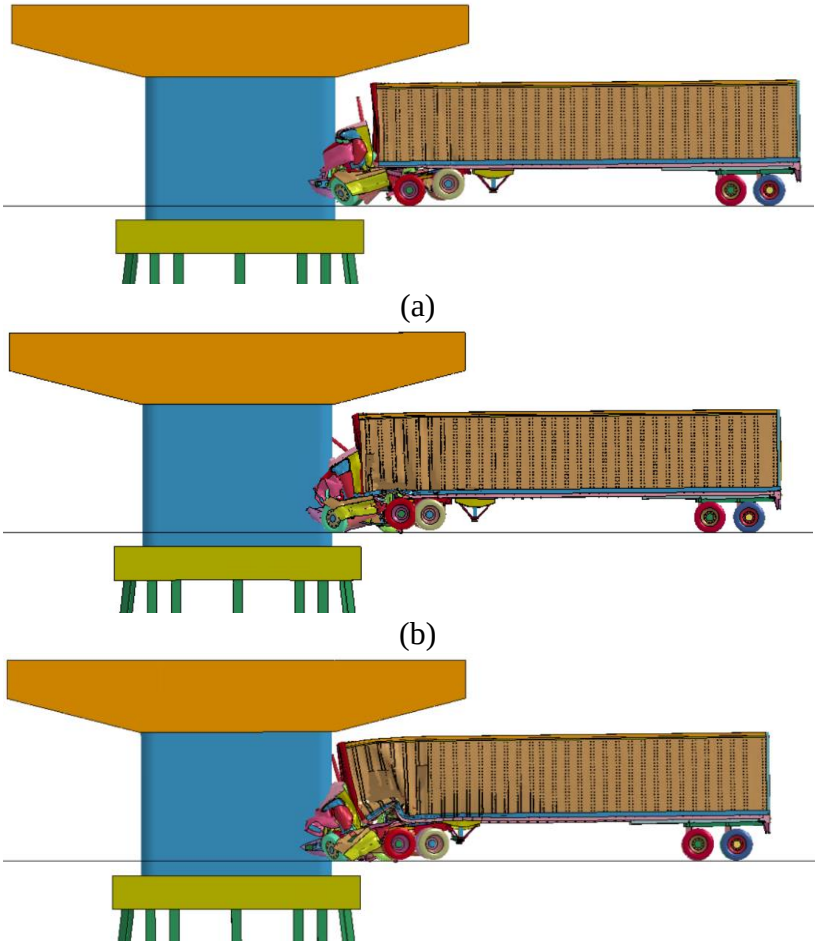

Figure 2.23. Collision simulation of tractor-semitrailer into T-pier: (a) 50 mph, (b) 70 mph, and (c) 90 mph

This figure is shown to reveal the state of vehicle collision at the time collision simulations terminated at 0.2 s. The damage in the T-pier after vehicle collision is shown in Figure 2.24.

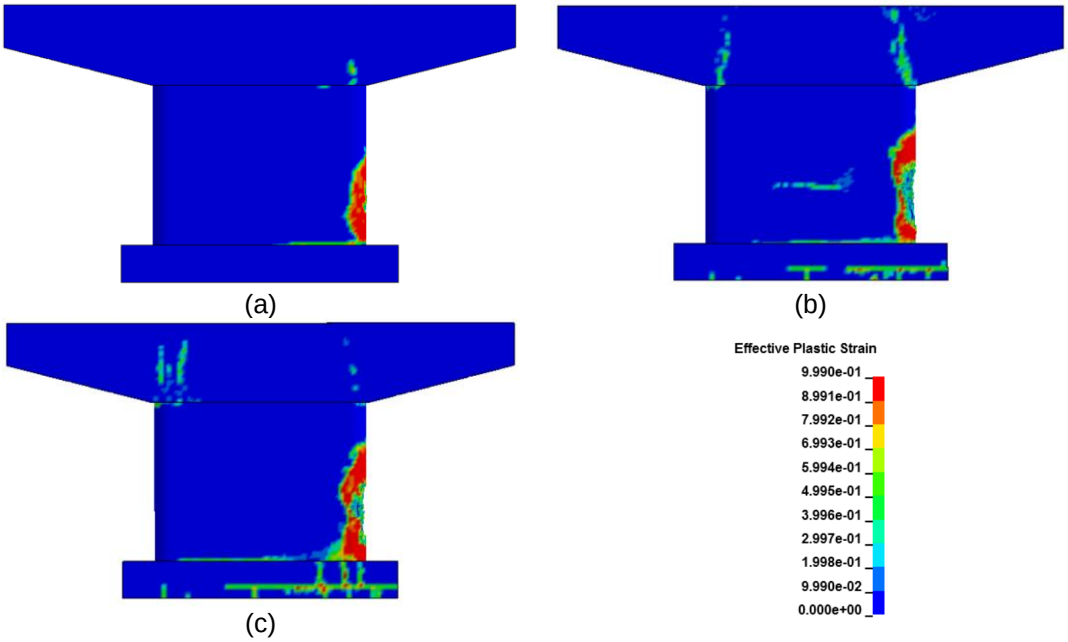

Figure 2.24. Simulation of damage from vehicle collision into the T-pier: (a) 50 mph, (b) 70 mph, and (c) 90 mph

While the T-pier suffers an increase in damage as the impact velocity increases, it remains stable even for the highest impact velocity considered. The red contour reveals the cracks observed in the concrete due to shear or spalling. Table 2.9 shows the DRI values for the T-pier impacted by the tractor-semitrailer traveling at different impact velocities.

Table 2.9. Determination of DRI values of T-pier

Velocity (mph)	Tractor Weight (lb)	KE (ft-kip)	ϕV_n (kip)	Pier Width (ft)	DRI
50	16,982	1,419	1,500	20	0.05
70	16,982	2,782	1,500	20	0.09
90	16,982	4,599	1,500	20	0.15

The results show that minor damage is expected in the bridge column due to localized concrete spalling and tensile cracking of concrete. This is an accurate description of the piers in the previous Figure 2.24. One issue, however, is that, while the column may not collapse, significant plastic strains are observed in the pile cap as the impact velocity increases.

2.10 Analysis of Frame Pier and T-Pier Impact Forces from Impact Simulations

The impact force time history of the frame pier and T-pier are shown in Figure 2.25.

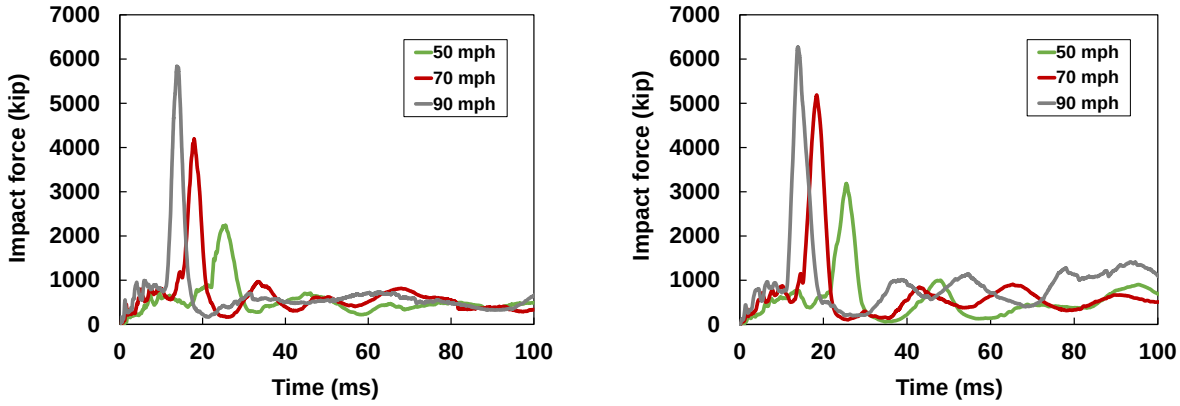

Figure 2.25. Impact force time history of tractor-semitrailer colliding into: (a) frame pier and (b) T-pier

As expected, lower impact forces are observed for the frame pier compared to the T-pier for the same impact velocity. This is attributed to the lower stiffness of the frame pier column compared to the T-pier column. The trend of the stiffer pier causing larger impact forces is in agreement with Gomez et al. (2015), Saini and Shafei (2017), and Oppong et al. (2020).

This study estimated the mean impact force and assumed it was the equivalent static force. This method was used in Tachibana et al. (2010) and Xu et al. (2013). Tachibana et al. (2010) estimated mean impact forces by dividing the collision impulse by the collision duration. On the other hand, Xu et al. (2013) averaged the impact forces over 0.1 s.

For this study, the mean impact force was estimated over 100 ms. This time period covers the duration from just after impact to right before the semitrailer and its contents are fully involved in the collision.

For the frame pier, the mean impact forces were determined as 537 kips (2,390 kN), 643 kips (2,862 kN), and 792 kips (3,523 kN) for the lowest to highest impact velocities, respectively. These values are in agreement with estimates from Auyeung and Alipour (2016). For the T-pier, the mean impact forces were determined as 564 kips (2,508 kN), 687 kips (3,054 kN), and 856 kips (3,808 kN) for the lowest to highest impact velocities, respectively.

To show that these mean impact forces are accurate estimates, the values determined for the frame pier were compared to the nominal shear capacity of the frame pier's column. From Table 2.6, the design shear capacity of the 3.5 ft (1.07 m) diameter column is 530 kip (2,358 kN) with a strength reduction factor of 0.9, which leads to a nominal shear capacity of 589 kip (2,620 kN).

Comparing this value to the mean impact forces estimated from the vehicle collision involving the frame pier, the frame pier column is expected to show no significant damage under the 50 mph (80.5 km/h) impact velocity but expected to show significant damage under the 70 mph

(112.7 km/h) and 90 mph (144.8 km/h) impact velocities. The damages reported in the frame pier in Figure 2.21 confirms this.

2.11 Analysis of Frame Pier and T-Pier Shear Forces from Impact Simulations

The shear forces along the frame pier and T-pier are shown in Figure 2.26.

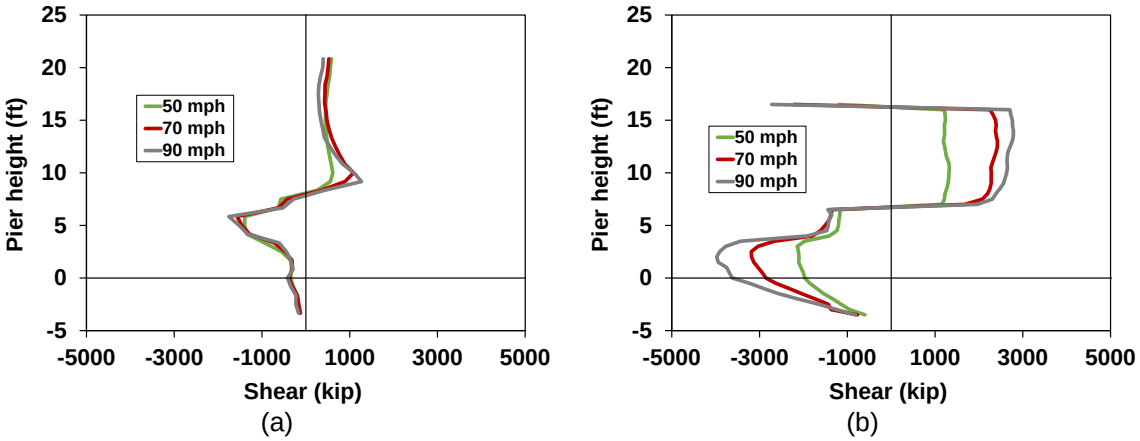

Figure 2.26. Shear profile along (a) frame pier and (b) T-pier

These shear profiles consist of the maximum shear values along the pier over the entire impact duration. The base of the column (at the top of the pile cap) is indicated by the 0 ft (0 m) mark along the pier height in the figure. The impact location is where the shear force is 0 kip (0 kN) between 5.0 ft (1.52 m) and 10 ft (3.05 m) along the pier height for the frame pier and T-pier. For both the frame pier and T-pier, the greater of the peak shear forces in each shear profile is in the negative region of the plot, which is right below the impact location but above the top of the pile cap. The location of the maximum shear force is consistent with the location of maximum column damage in the previous Figures 2.21 and 2.24.

The shear force profiles show that those in the frame pier are less than those in the T-pier. This is mainly because the frame pier is less stiff. The shear forces shown are dynamic values, and that is why the maximum value for the 50 mph (80.5 km/h) impact velocity observed for the frame pier are high compared to the calculated design capacity of 530 kips (2,358 kN) for the frame pier's column. In a dynamic situation, the material strength of the pier increases and so does its shear capacity. Therefore, it is only reasonable to compare static force demands to static strength capacities and dynamic force demands to dynamic strength capacities.

2.12 Analysis of Frame Pier and T-Pier Bending Moments from Impact Simulations

The bending moment diagrams for the frame pier and T-pier over the length of the pile cap and column are shown in Figure 2.27.

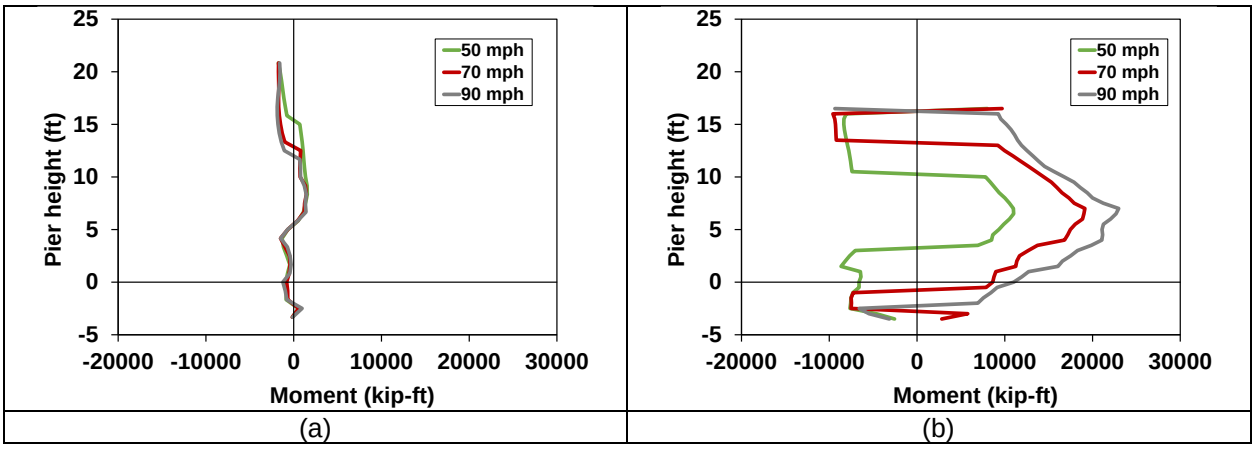

Figure 2.27. Bending moment profile along: (a) frame pier and (b) T-pier

These bending moment profiles consist of the maximum bending moment values along the pier over the entire impact duration. As expected, the maximum positive bending moment occured at the location of impact, and the negative bending moments were close to the top and bottom of the column. For the frame pier, the maximum bending moment at the location of impact did not significantly change with an increase in impact velocity. However, for the T-pier, the maximum moment increased with an increase in impact velocity. Also, the maximum bending moments observed in the frame pier were less than those observed in the T-pier.

2.13 Analysis of Frame Pier and T-Pier Displacements from Impact Simulations

The lateral displacements of the columns are shown in Figure 2.28 for the frame pier and T-pier.

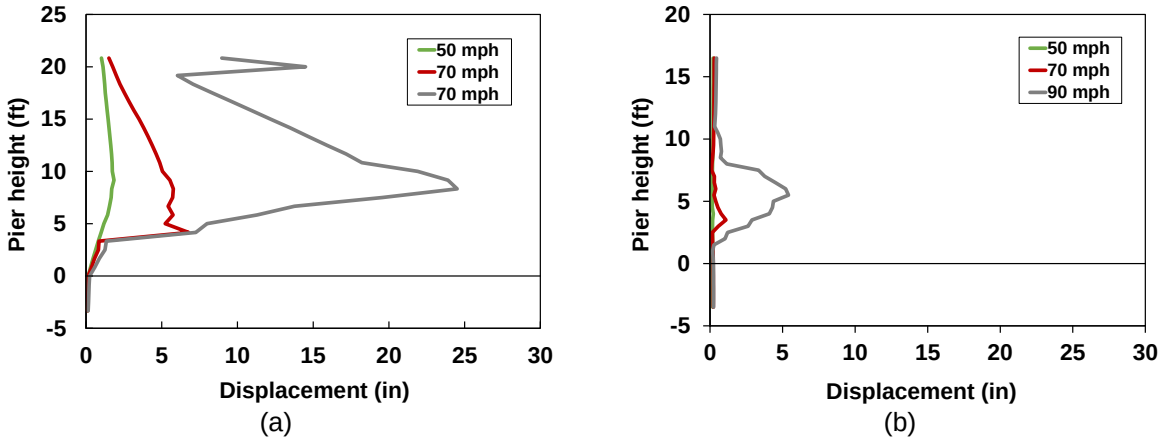

Figure 2.28. Displacement profile along (a) frame pier and (b) T-pier

These displacements were captured at 0.1 s during the collision. The displacements were slightly influenced by element erosion because entire cross-sections along the pier were selected to provide displacement data. However, as expected, the frame pier underwent greater displacements than the T-pier.

2.14 Analysis of the Performance of a Crash Wall Integrated into a Frame Pier

The collision simulations are shown in Figure 2.29, and the damage in the pier is shown in Figure 2.30.

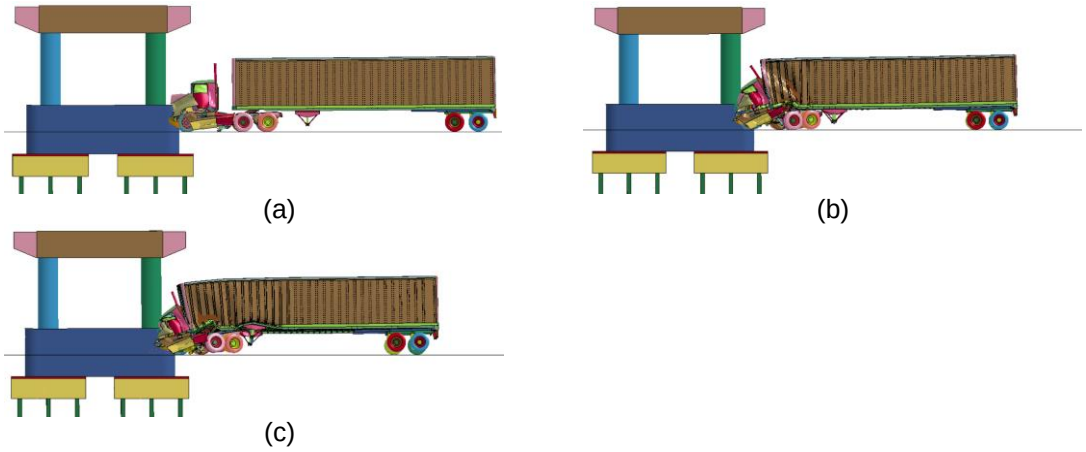

Figure 2.29. Collision simulation of tractor-semitrailer into frame pier with barrier: (a) 50 mph, (b) 70 mph, and (c) 90 mph

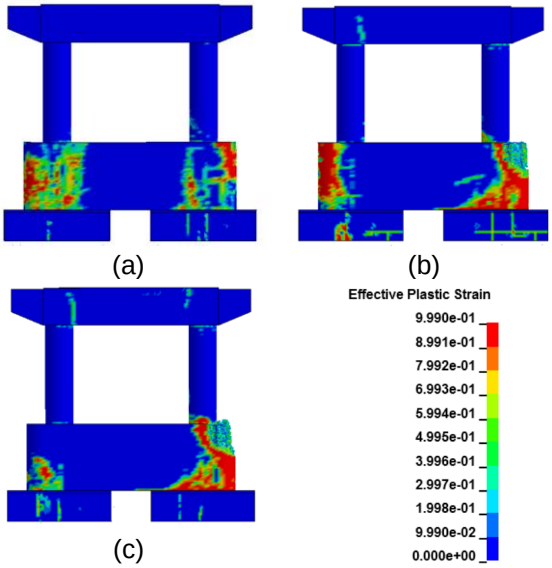

Figure 2.30. Simulation of damage from vehicle collision into the frame pier with a crash wall: (a) 50 mph, (b) 70 mph, and (c) 90 mph

None of the three impact velocities caused the bridge pier to collapse. In addition, Figure 2.31 shows that the various response measures recorded are far less severe than those of the frame pier without the crash wall (Figure 2.25a).

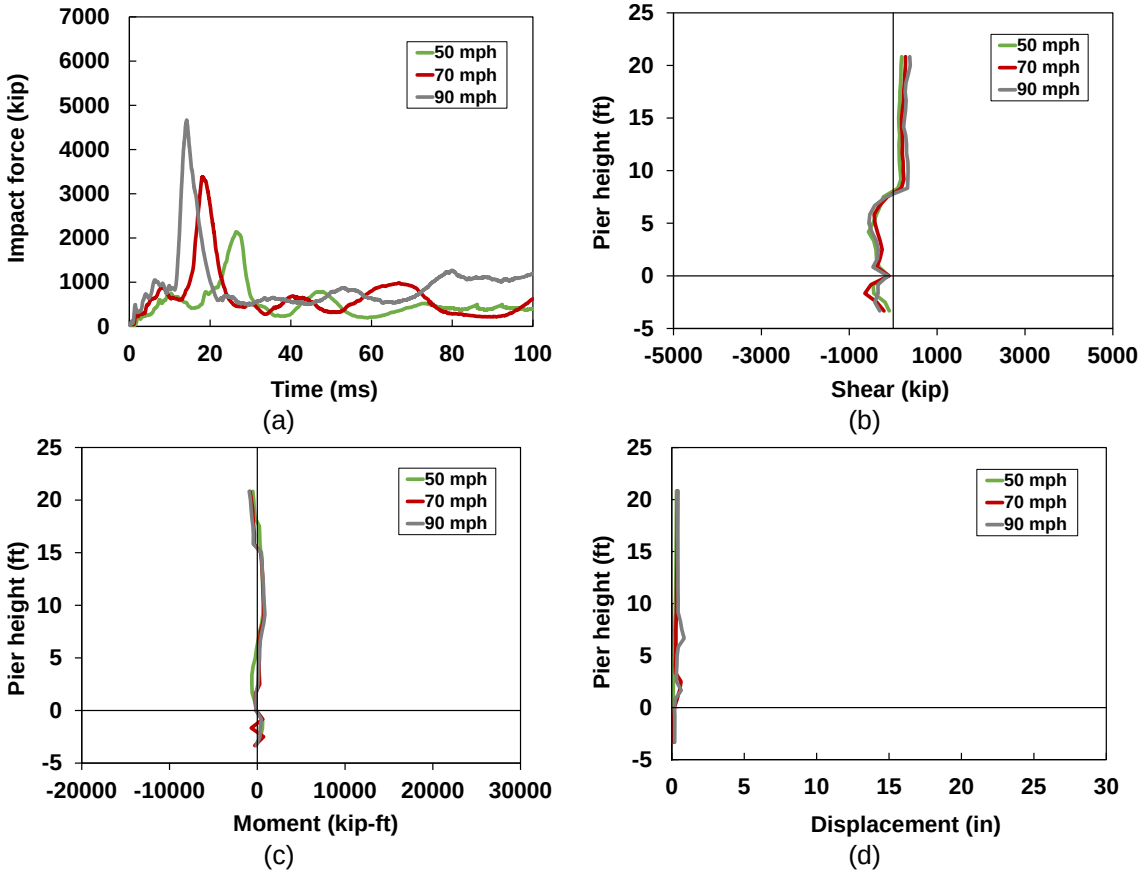

Figure 2.31. Response measures for frame pier with crash wall: (a) impact force, (b) shear force, (c) bending moment, and (d) displacement

These findings indicate that Iowa DOT BDM's current guideline (2020) for a crash wall, with the reinforcement that was included in the modeling, is acceptable.

2.15 Analysis of the Performance of a Crash Barrier Placed Around a Frame Pier

The tractor-semitrailer was allowed to travel toward the frame pier at impact velocities of 50 mph (80.5 km/h), 70 mph (112.7 km/h), and 90 mph (144.8 km/h). The angle of impact was 15°. The simulation results are shown in Figure 2.32 for the termination time of 0.2 s.

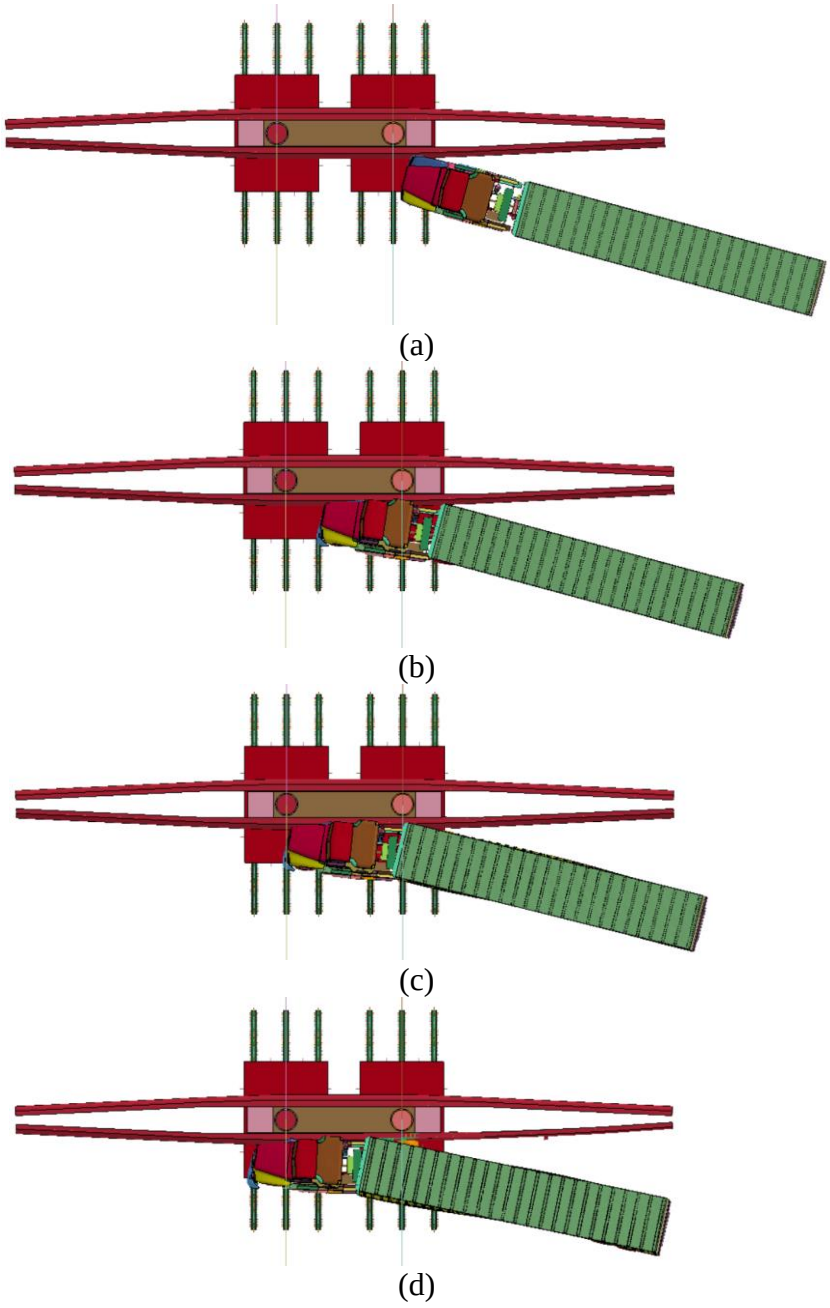

Figure 2.32. Simulation of tractor-semtrailer running into a frame pier with a crash barrier: (a) starting point, (b) 50 mph, (c) 70 mph, and (d) 90 mph

The crash barrier was able to keep the tractor-semitrailer from colliding into the frame pier columns. Even at the highest impact velocity considered, the crash barrier redirected the vehicle away from the pier columns. Therefore, the Iowa DOT's crash barrier that is 54 in. (1.37 m) tall at the location of the columns and tapers to 44 in. (1.12 m) farther from the columns works just fine. The damage in the crash barrier is shown in Figure 2.33, and the figure reveals that the crash barrier undergoes insignificant plastic strains (cracks) at the lowest impact velocity but undergoes significant plastic strains at the two greater impact velocities.

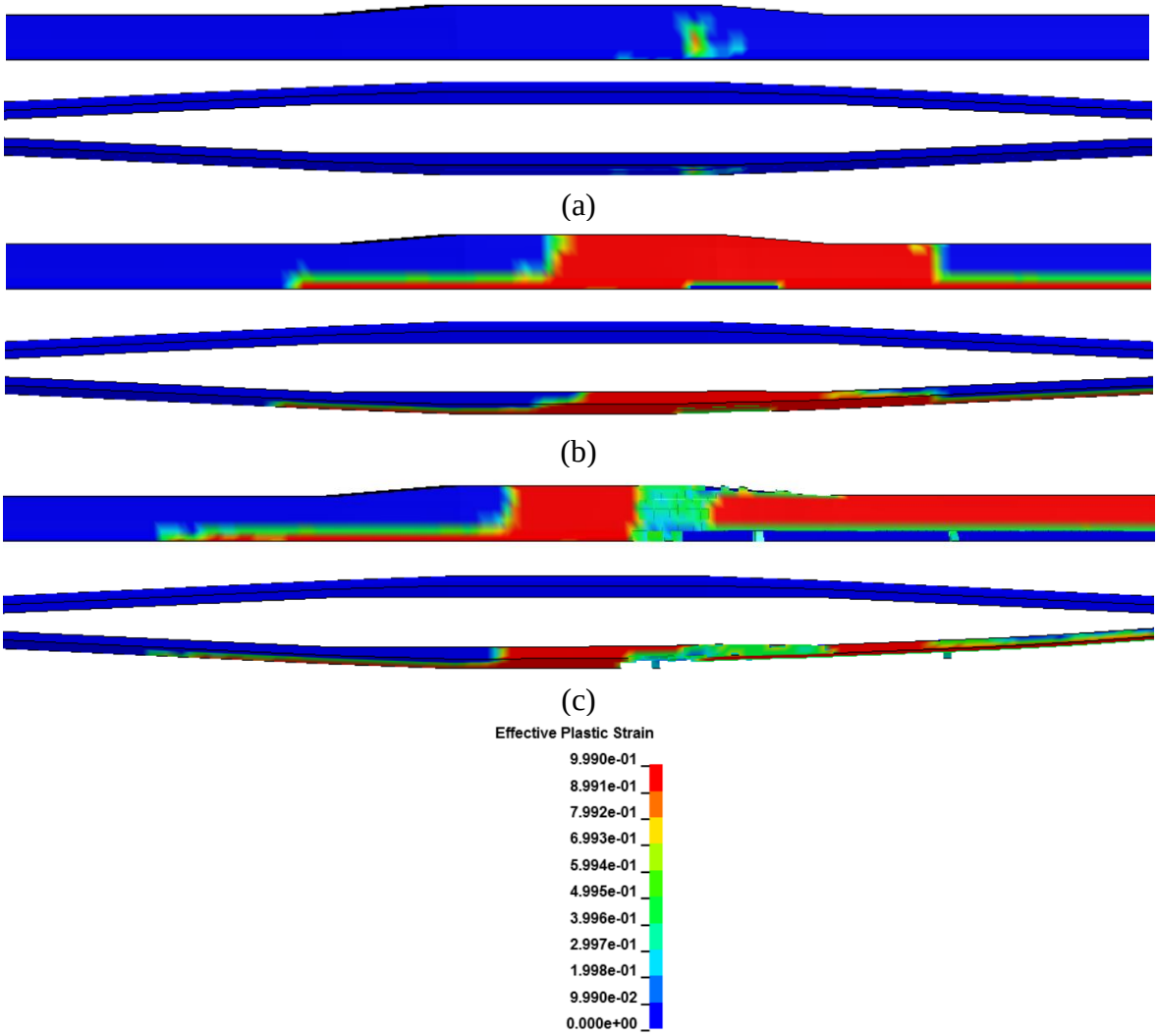

Figure 2.33. Simulation of damage from vehicle collision into the crash barriers around the frame pier (side and top views): (a) 50 mph, (b) 70 mph, and (c) 90 mph

Significant concrete spalling occurs on the barrier due to the highest impact velocity.

3. PARAMETRIC STUDY

3.1 Introduction

This chapter details a parametric study that the researchers performed on the frame pier and T-pier. The investigation evaluated the effect of different frame pier column diameters, the effect of the extension of frame pier spiral reinforcement into the pier cap and pile cap, the effect of different impact angles on the T-pier, and the effect of different tie reinforcement spacing in the T-pier. Various response measures were analyzed, and these included damage pattern (plastic strains), impact force time history, shear force, bending moment, displacement, and internal energy. The damage state description table for the DRI values determined for the T-pier is developed in this chapter.

3.2 Effect of Different Frame Pier Column Diameters

In Chapter 2, the frame pier with a column diameter of 3.5 ft (1.07 m) was investigated. In this chapter, two other column diameters are investigated in addition to the 3.5 ft (1.07 m) diameter: 3 ft (0.91 m) and 4 ft (1.22 m). The two new bridges were modeled the same as the older bridge except for their column diameters and longitudinal reinforcing steel bars. The longitudinal bars in the column were updated so that they were at least 1.0% of the gross concrete section area and the concrete cover was 2 in (50.8 mm). Therefore, the #8 (#25) bar was used for the 3 ft (0.91 m) diameter pier, the #9 (#29) bar was used for the 3.5 ft (1.07 m) diameter pier, and the #10 (#32) bar was used for the 4 ft (1.22 m) diameter pier. The three piers are shown in Figure 3.1.

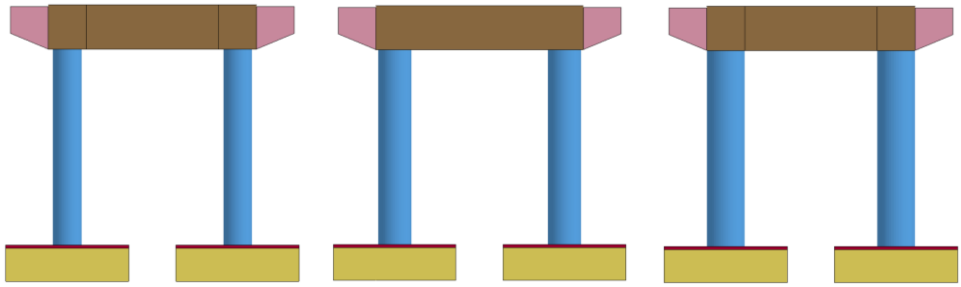

Figure 3.1. Frame pier with different diameters: (a) 3 ft, (b) 3.5 ft, and (c) 4 ft.

The column sizes chosen for this part of the study were based on the typical range of column sizes used for bridge design in the Iowa DOT BDM (2020), i.e., 2.5 ft (0.76 m) to 4 ft (1.22 m). Also, the minimum design requirement of 4 ft (1.22 m) in the stipulations for “no further design required” for vehicular collision design was one of the reasons why the 4 ft (1.22 m) diameter pier was chosen. The “no further design required” condition is based on the premise that the 600 kips (2,669 kN) design force specified for vehicular collision is attained by the pier when some conditions are met. The difference between the 4 ft (1.22 m) frame pier considered in this study and the stipulations for “no further design required” in the Iowa DOT BDM (2020) for vehicular

collision design is that the pier in this study had two columns, while the stipulations require at least three columns.

The stipulations met by the 4 ft (1.22 m) diameter pier investigated in this study were a minimum column diameter of 4 ft (1.22 m), vertical column rebar greater than 1.0% of the gross concrete section of the pier column, and Grade 60 shear reinforcement consisting of a minimum #5 (#16) spiral with a maximum vertical pitch of 4 in (101.2 mm).

The tractor-semitrailer was allowed to collide into the frame piers at impact velocities of 50 mph (80.5 km/h), 70 mph (112.7 km/h), and 90 mph (144.8 km/h). The damage (plastic strains) observed in the piers are shown in Figure 3.2.

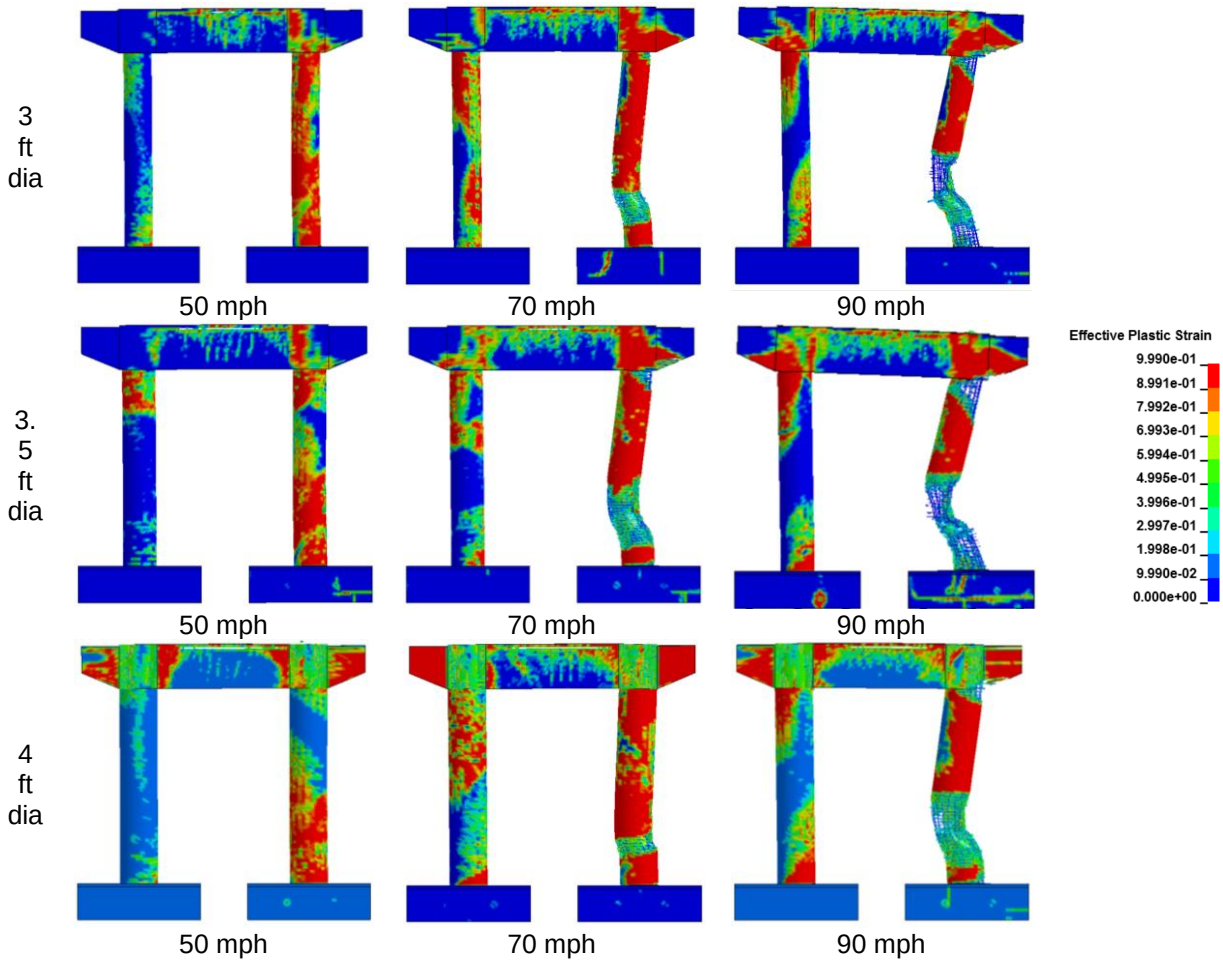

Figure 3.2. Damage in frame pier with different diameters

From visual observation, no plastic hinge developed in the piers when the tractor-semitrailer impact velocity was 50 mph (80.5 km/h). When the vehicle collided into the piers at 70 mph (112.7 km/h), plastic hinges developed at the top of the column and impact location of the 3 ft (0.91 m) and 3.5 ft (1.07 m) diameter piers. For the 4 ft (1.22 m) pier, plastic hinges developed only at the impact location. At an impact velocity of 90 mph (144.8 km/h), plastic hinges

developed at the top of column, impact location, and base of the column for the 3 ft (0.91 m) and 3.5 ft (1.07 m) diameter piers, and only at the top of column and impact location of the 4 ft (1.22 m) pier. From visual inspection of the results, bridge collapse only occurred when the tractor-semitrailer traveling at 90 mph (144.8 km/h) collided into the 3 ft (0.91 m) and 3.5 ft (1.07 m) diameter piers. This is because, when three plastic hinges form in a single column, the column collapses.

The DRI value was determined for each of the nine collision scenarios to investigate how accurately it can predict bridge pier damage. The DRI values are presented in Table 3.1, and they show that seven of the nine collision scenarios are correctly predicted concerning damage.

Table 3.1. Determination of DRI values for frame pier

Velocity (mph)	Tractor Weight (lb)	KE (ft-kip)	ϕV_n (kip)	Pier Dia. (ft)	DRI
50	16,982	1,419	436	3.0	1.08
70	16,982	2,782	436	3.0	2.13
90	16,982	4,599	436	3.0	3.52
50	16,982	1,419	530	3.5	0.76
70	16,982	2,782	530	3.5	1.50
90	16,982	4,599	530	3.5	2.48
50	16,982	1,419	630	4.0	0.56
70	16,982	2,782	630	4.0	1.10
90	16,982	4,599	630	4.0	1.83

The two that were not correctly predicted are the second and eighth scenarios. The DRI for the second scenario was 2.13, which means that the bridge pier is expected to collapse; however, from Figure 3.2, the pier did not collapse and is only in the severe damage state because just two plastic hinges are present. The DRI for the eighth scenario was 1.10, which indicated that the pier was in the moderate damage state; however, from Figure 3.2, the pier was in the severe damage state because it had significant deterioration of the concrete core at the impact location, which led to plastic hinge formation at the impact location. Overall, the DRI values reasonably predict the damage state of frame piers having different diameters that undergo vehicular collision.

Comparing Figure 3.2 and Table 3.1, it is revealed that the stipulations for the “no further design required” condition in the Iowa DOT BDM (2020) prevents frame pier collapse when impacted by a tractor-semitrailer traveling at impact speeds between 50 mph (80.5 km/h) and 90 mph (144.8 km/h).

The response measures of the frame piers for the first 100 ms are shown in Figure 3.3, and they include the impact force, shear force, bending moment, and displacement.

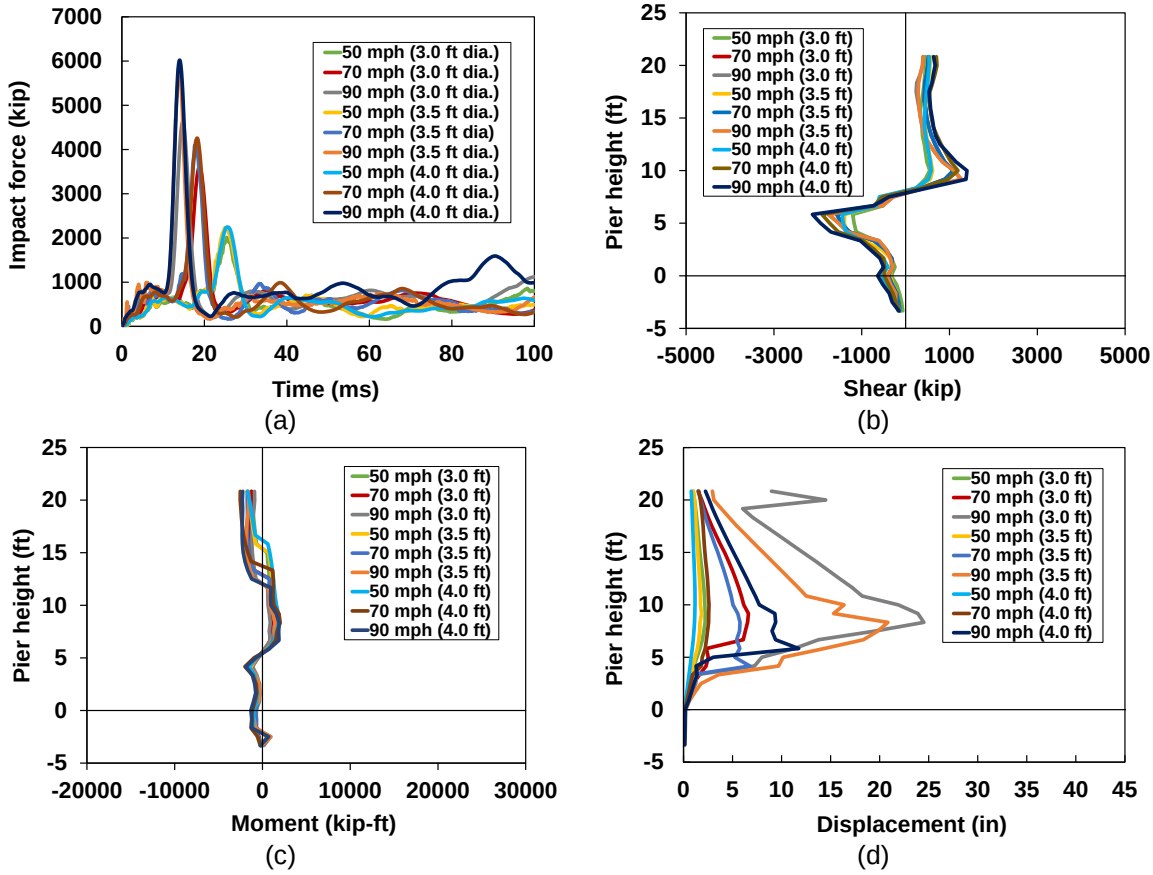

Figure 3.3. Response measures for frame pier with different diameters: (a) impact force time history, (b) shear force, (c) bending moment, and (d) displacement

The impact force plot shows that greater peak impact forces were obtained for greater impact velocities and pier diameters. The mean impact force, covering all three piers, over the first 100 ms of impact for the impact velocities of 50 mph (80.5 km/h), 70 mph (112.7 km/h), and 90 mph (144.8 km/h) were 535 kips (2,379 kN), 650 kips (2,893 kN), and 795 kips (3,538 kN), respectively.

Figure 3.3(b) shows the shear force profiles along the height of the frame pier. The shear force profiles shown were obtained at the time of peak impact force. The peak shear force increased as the impact velocity and pier diameter increased. The base and top of the column were at 0 ft and 21 ft (0 m and 6.40 m), respectively. The pile cap was located in the negative region along the pier. These shear forces are dynamic forces and are due to the peak impact force. The peak shear force was located right below the impact location, and the impact location was where the shear force is 0 kN. At the time of peak impact force, there was little shear force at the top and base of the column compared to that at the impact location.

Figure 3.3(c) shows the bending moment diagram along the pier. The bending moment increased as the impact velocity and column diameter increased. The peak positive bending moment was at

the impact location, and the peak negative bending moments were at the top and base of the column.

The displacement plot at 100 ms during impact is shown in Figure 3.3(d). The displacement was higher for higher impact velocities and smaller column diameters.

3.3 Effect of Extension of Frame Pier Spiral Reinforcement into Pier Cap and Pile Cap

The spiral reinforcement in the three frame piers of different diameters were extended into the pier cap and pile cap to investigate the effect it has on the response of the bridge pier. The frame piers with and without the extended spiral reinforcing steel bar are shown in Figure 3.4.

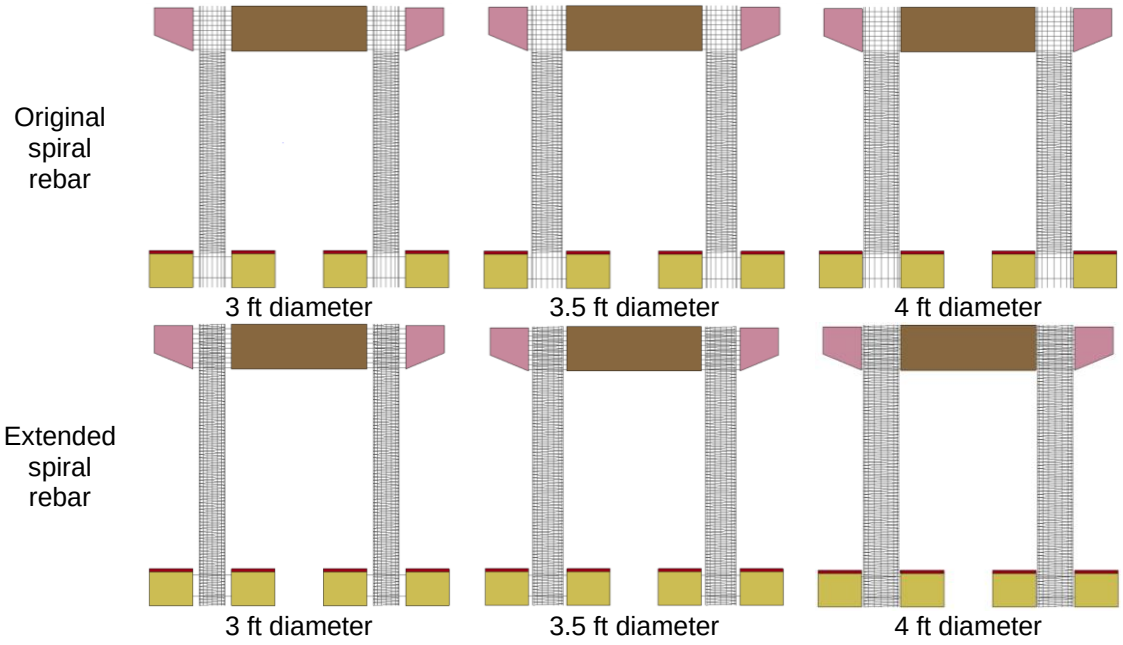

Figure 3.4. Frame pier with and without extended spiral rebar

The tractor-semitrailer was allowed to collide into the bridge piers at impact velocities of 50 mph (80.5 km/h), 70 mph (112.7 km/h), and 90 mph (144.8 km/h). The damage in the frame pier with the extended spiral reinforcing steel bar is shown in Figure 3.5.

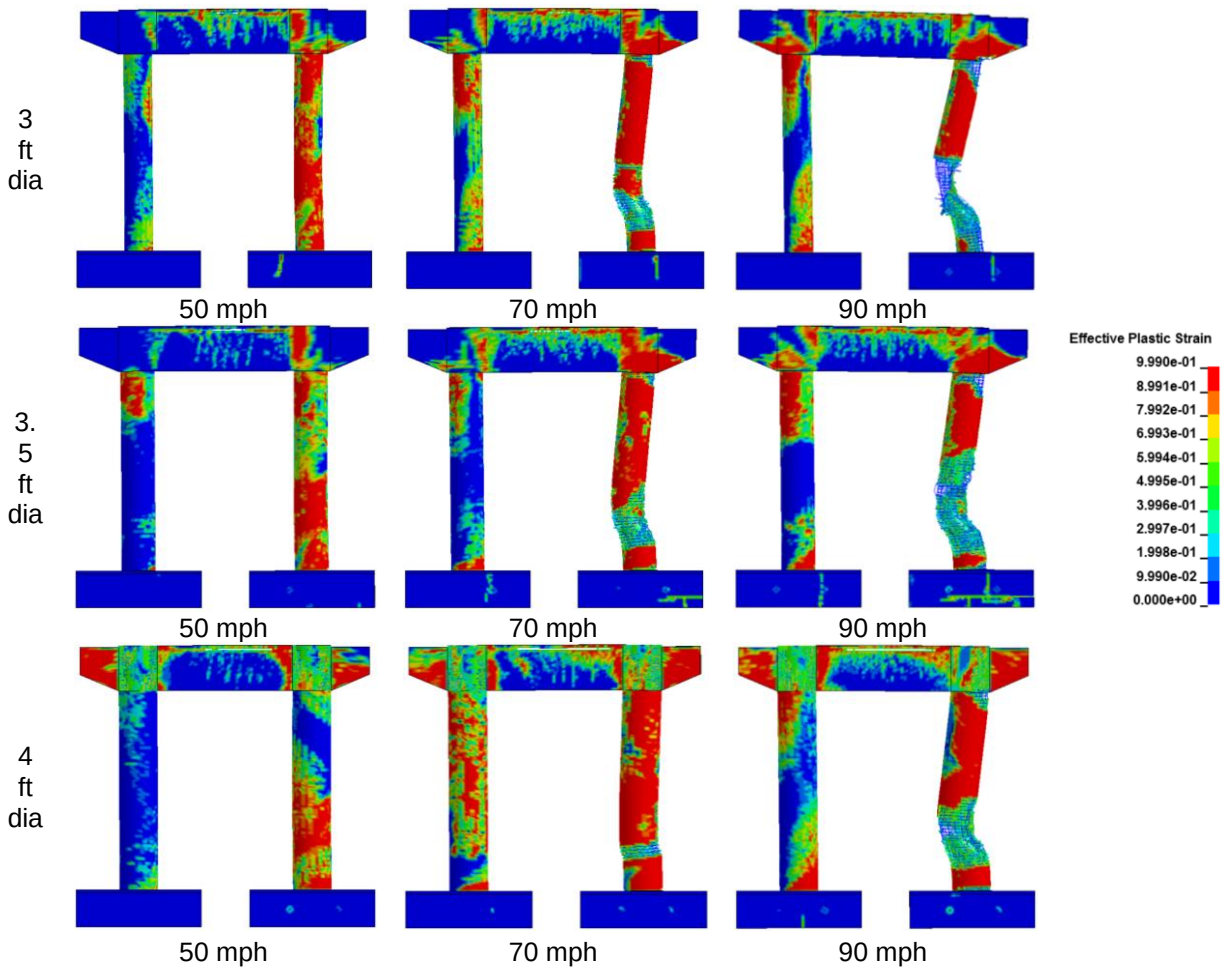

Figure 3.5. Damage in frame pier with extended spiral rebar

Comparing Figure 3.5 to Figure 3.2, no significant difference in damage is apparent based on whether or not the frame pier has extended spirals. Similarly, the impact force time history, shear force, bending moment, and displacement were similar to those shown in Figure 3.3 and, therefore, are not shown in a separate figure. To further investigate the effect of extending the spirals into the pier cap and pile cap, the internal energies of the spiral rebar, longitudinal rebar, concrete column, concrete pier cap, and concrete pile cap were captured at 100 ms during impact. The internal energies are shown in Table 3.2 for the 3 ft (0.91 m) and 4 ft (1.22 m) piers.

Table 3.2. Internal energy of various components of the frame pier

Pier diameter (ft)	Impact velocity (mph)	Spiral Rebar	Concrete Pile Cap (kip-ft)	Concrete Pier Cap (kip-ft)	Concrete Column (kip-ft)	Longitudinal Rebar (kip-ft)	Spiral Rebar (kip-ft)
3	50	Original	2.1	8.6	57.5	49.0	4.0
		Extended	4.1	9.7	61.9	56.3	6.1
	70	Original	5.1	16.2	257.4	151.9	34.6
		Extended	5.6	15.3	345.5	168.8	48.5
	90	Original	7.7	18.6	651.9	358.5	106.0
		Extended	6.7	18.4	634.9	362.8	94.7
4	50	Original	8.2	11.3	34.4	14.2	1.1
		Extended	9.3	11.7	39.3	13.1	1.2
	70	Original	22.6	24.0	183.9	77.1	16.4
		Extended	19.8	19.3	184.6	71.7	15.8
	90	Original	15.0	25.3	624.0	189.4	60.1
		Extended	17.7	22.6	593.7	202.4	64.7

The internal energies show that when impact occurs and the damage state is minor, i.e., localized spalling of concrete cover or tensile cracking of concrete, as in the case of the 50 mph (80.5 km/h) impact velocity, the extended spiral rebar causes various components in the pier to experience greater internal energies. However, when anything aside minor damage occurs, i.e., the moderate, severe, or collapse damage state, the results are not consistent. When the damage state is minor, the pier absorbs more energy because the extended spirals make the pier slightly stiffer, and this leads to an increase in the distribution of energy to other components of the frame pier.

3.4 Effect of Different Impact Angles on T-Pier

Three different impact angles were investigated to evaluate the effect of different vehicular impact angles on a T-pier. The different angles considered were 0°, i.e. along the longitudinal axis of the pier, 45° from the longitudinal axis of the pier, and 90° from the longitudinal axis of the pier. The T-pier and vehicle at the different angles are shown in Figure 3.6.

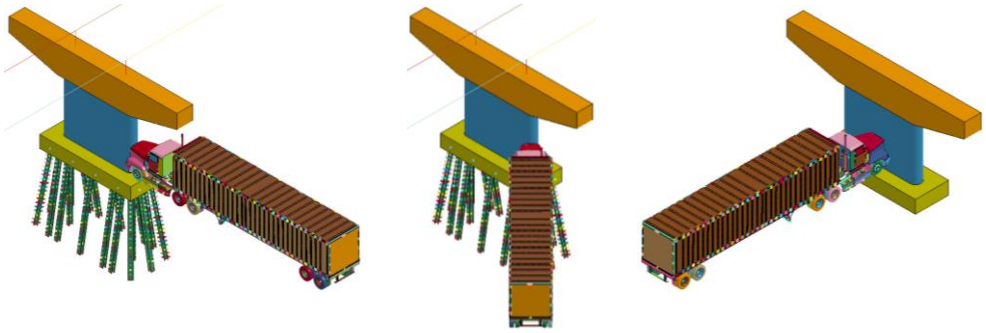

(a) (b) (c)

Figure 3.6. Tractor-semitrailer approaching the T-pier at: (a) 0°, (b) 45°, and (c) 90° from the pier's longitudinal axis

For the 90° impact angle, the superstructure, bearings, piles, and soil were taken out of the model, and boundary conditions were assigned to the top of the pier cap and bottom of the pile cap. This was done because of computation difficulties and an increased length of time to complete simulations when the deleted bridge components were present. The tractor-semitrailer was simulated to collide into the bridge pier at impact velocities of 50 mph (80.5 km/h), 70 mph (112.7 km/h), and 90 mph (144.8 km/h). The damage observed in the piers are shown in Figure 3.7.

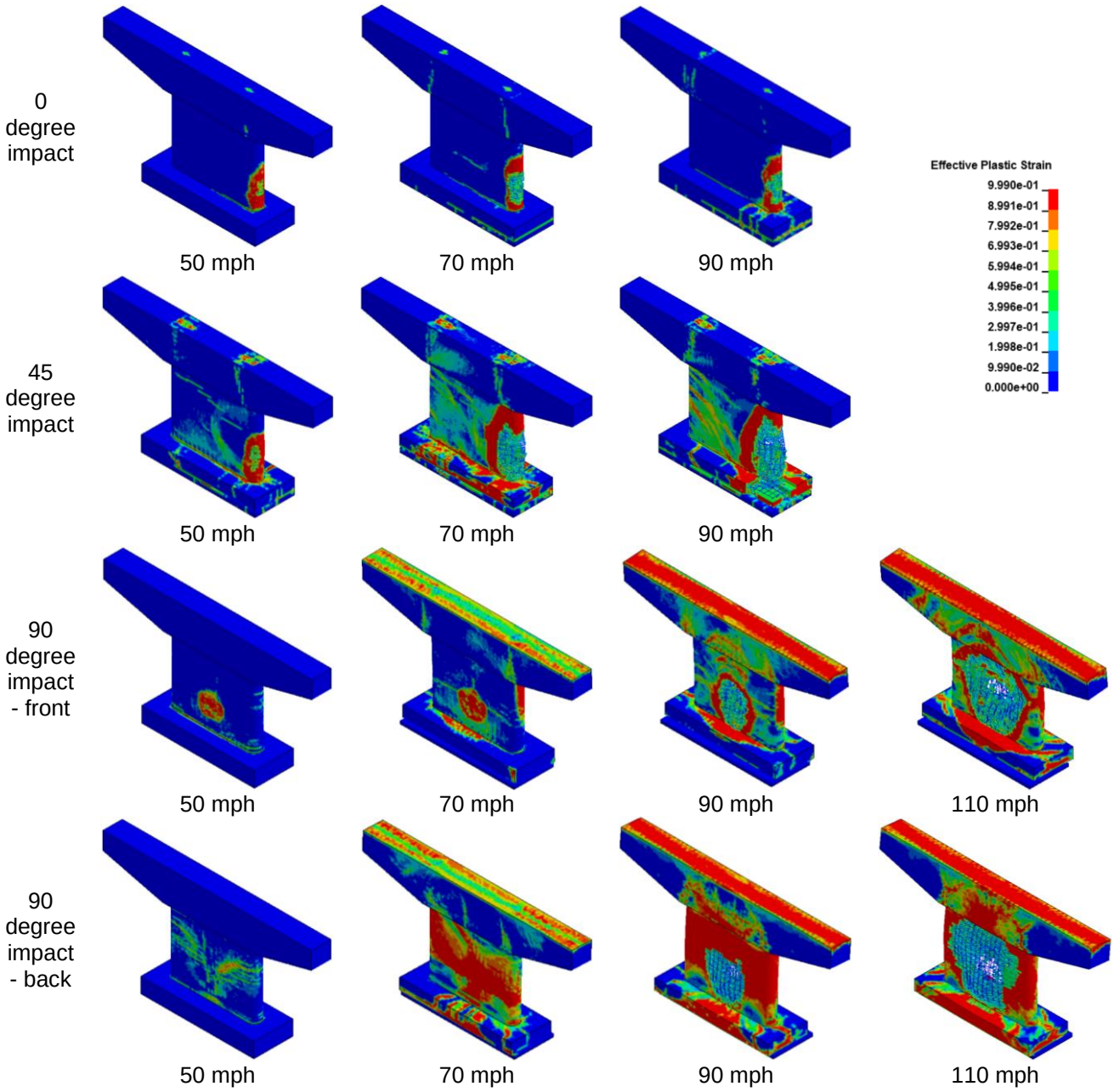

Figure 3.7. Damage in frame pier with different diameters

Figure 3.7 shows greater damage occurs in the T-pier for higher impact velocities and impact angles from the longitudinal axis of the T-pier. Even though significant damage is observed in the T-pier in some of the scenarios, the T-pier does not collapse in any of them. The greatest damage observed is localized deterioration in the column concrete and pile cap concrete and localized yielding of the reinforcing steel bar in the column. The DRI values for the T-pier were determined as shown in Table 3.3.

Table 3.3. Determination of DRI values for T-pier impacted at different angles

Impact Angle (°)	Velocity (mph)	Tractor Weight (lb)	KE (kip-ft)	ϕV_n (kip)	Pier Width (ft)	DRI
0	50	16,982	1,419	1,500	20	0.05
	70	16,982	2,782	1,500	20	0.09
	90	16,982	4,599	1,500	20	0.15
45	50	16,982	1,419	1,305	11.5	0.09
	70	16,982	2,782	1,305	11.5	0.18
	90	16,982	4,599	1,305	11.5	0.30
90	50	16,982	1,419	1,147	3	0.41
	70	16,982	2,782	1,147	3	0.81
	90	16,982	4,599	1,147	3	1.34
	110	16,982	6,869	1,147	3	2.00

For simplicity, the effective shear depth, d_v, was taken as 0.72*h* (AASHTO 2017) for the T-pier, where *h* is the total depth of the section, i.e., 20 ft (6.10 m) for the impact angle of 0° and 3 ft (0.91 m) for the impact angle of 90°. The design shear capacity for the 45° impact angle was taken as the average of the design shear capacities for the 0° and 90° impact angles. The column depth for the 45° impact angle was taken as the average of the column depths for the 0° and 90° impact angles. Pier column collapse was defined as a DRI value of 2.0. To investigate how a DRI value of 2.0 looks in a T-pier, an additional impact velocity of 110 mph (177.0 km/h) was included in the impact scenarios involving the 90° impact angle.

Comparing Figure 3.7 to Table 3.3, significant local damage is caused in the column and pile cap for the 45° impact angle with the 70 mph (112.7 km/h) and 90 mph (144.8 km/h) impact velocities. However, the DRI value was 0.30, which represents minor damage according to the damage state description in Chapter 2. The description of minor damage in Chapter 2 (meant for frame piers), i.e., localized spalling of concrete cover and tensile cracking of concrete, does not fully describe the damage that occurs on the T-pier impacted at the 45° impact angle with 70 mph (112.7 km/h) and 90 mph (144.8 km/h) impact velocities. Therefore, a different set of descriptions is needed for the damage states of the T-pier.

Note that the DRI values below 0.15 in Table 3.3 show the compression cracking and spalling of concrete cover in Figure 3.7. For DRI values between 0.15 and 0.5, any of the following may be present: localized yielding of reinforcement in column, localized deterioration of column concrete core, presence of shear cracking in the pile cap, or localized deterioration of the pile cap. For DRI values between 0.5 and 2.0, there is yielding of column reinforcement, deterioration of concrete core, and possibly significant deterioration of the pile cap. Above 2.0, it is assumed that the pier would have suffered enough damage to lead to possible collapse of it.

For the 90° impact angle, there is significant element deletion below the mat reinforcement in the tension region of the pile cap, and this is because there is no steel (reinforcement or piles) below the mat reinforcement. Even when the piles are present, there is a gap between the piles and

reinforcement in the tension region of the pile cap. Lowering the reinforcement in the tension region of the pile cap fixes the issue. This is illustrated in Figure 3.8.

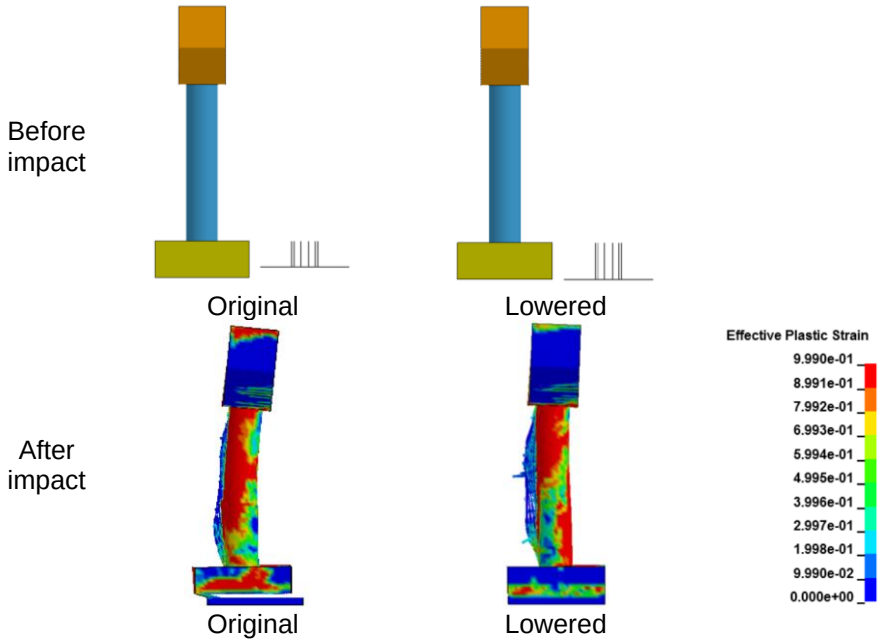

Figure 3.8. Effect of placing the reinforcement in the tension region of the pile cap lower

As a result, the reinforcement in the tension region of the pile cap that meets the steel piles is important to ensure that there is no vertical region in the pile cap without steel reinforcement. This is important when considering vehicular collision for pier design.

The internal energies in the T-pier components are shown in Table 3.4.

Table 3.4. Internal energies in bridge pier components

Impact Angle (°)	Speed (mph)	Concrete Column (kip-ft)	Concrete Pile Cap (kip-ft)	Column Long. Rebar (kip-ft)	Column Ties (kip-ft)	Concrete Pier Cap (kip-ft)
0	50	46.2	0.8	0.4	0.5	1.3
	70	176.5	2.1	5.0	8.9	2.8
	90	436.6	2.2	8.9	22.4	3.4
45	50	58.5	2.9	2.1	1.1	10.5
	70	228.6	5.6	9.0	12.3	13.8
	90	536.9	7.4	20.1	33.6	17.0

These internal energies are captured at 100 ms during the collision. The internal energies presented are those of the column ties, column longitudinal reinforcing steel bar, concrete column, concrete pier cap, and concrete pile cap. The internal energies in the components increase as the impact velocity and impact angle increase. A higher internal energy in a

component means that the component experiences more stresses. The results in Table 3.4 agree with the damage plots in Figure 3.7 and the DRI values in Table 3.3. That is, higher internal energy, damage, and DRI values are observed for higher impact velocities and impact angles. Figure 3.9 shows the impact force time history of the 0° and 45° impact angles along the longitudinal axis of the T-pier.

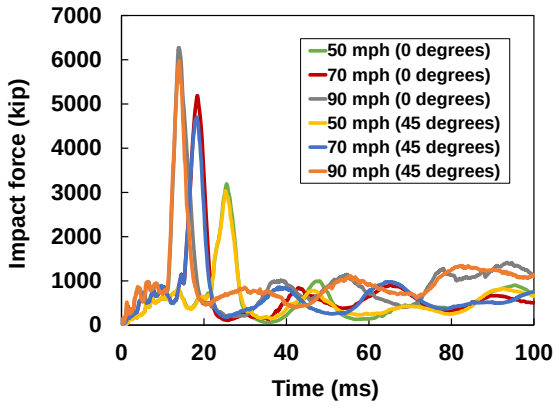

Figure 3.9. Impact force along longitudinal axis of T-pier

The results show that the impact force along the longitudinal axis of the T-pier decreases as the impact angle increases. This decrease in impact force along the longitudinal axis occurs despite the increase in the surface area of collision as the impact angle increases. This is because the pier becomes less stiff to the impacting tractor-semitrailer as the angle of impact increases.

3.5 Effect of Different Spacing of Tie Reinforcement in T-Pier

The researchers also investigated to evaluate the effect of different tie reinforcement spacing in a T-pier column. Gomez and Alipour (2014) investigated the effect of transverse hoop reinforcement spacing in a single circular bridge pier using detailed finite element models. In this study, however, the various conditions considered were a T-pier with no tie rebars, a T-pier with ties spaced at 24 in. (610 mm), and a T-pier with ties spaced at 12 in. (305 mm). Figure 3.10 shows the various conditions of tie reinforcement considered in the T-pier column.

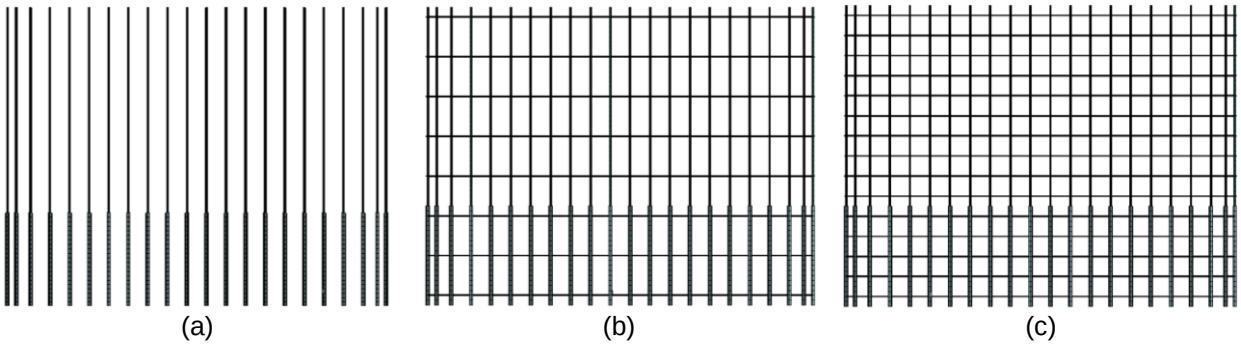

Figure 3.10. Longitudinal reinforcing steel bar and ties in T-pier: (a) no ties, (b) 24-in. tie spacing, and (c) 12-in. tie spacing

The longitudinal reinforcing steel bars were #9 (#29) bars spaced at 12 in. (305 mm) The lower one-third of the column had two #9 (#29) bundled bars as the longitudinal reinforcement. The shear reinforcement was #5 (#16) reinforcing steel bar. The tractor-semitrailer collided into the T-pier at 0° from its longitudinal axis at impact velocities of 50 mph (80.5 km/h), 70 mph (112.7 km/h), and 90 mph (144.8 km/h). The damage in the piers is shown in Figure 3.11, which shows that the bridge pier did not collapse in any of the cases considered. However, by visual inspection, the pier experienced significant damage when no ties were present at a 90 mph (144.8 km/h) impact velocity.

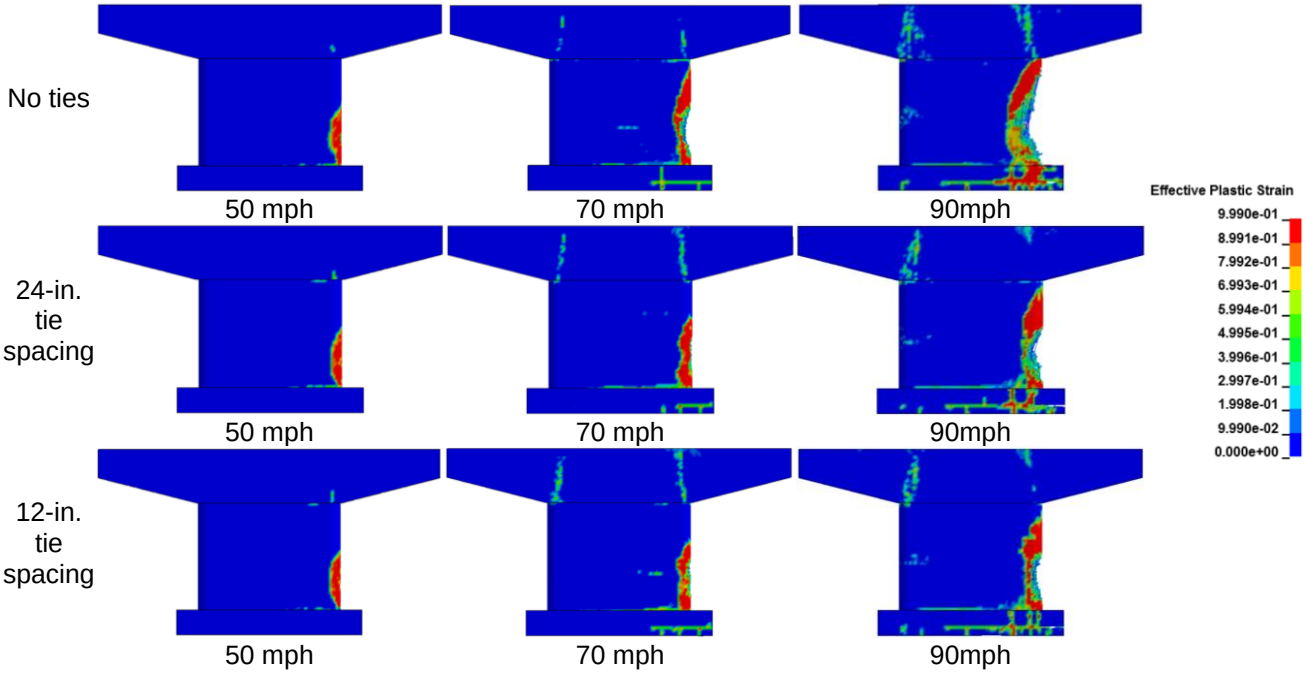

Figure 3.11. Damage in frame pier with different diameters

The DRI values for the T-pier with different tie spacings are presented in Table 3.5.

Table 3.5. Determination of DRI values for T-pier with different tie spacings

Impact Angle (°)	Velocity (mph)	Tractor Weight (lb)	KE (kip-ft)	ϕV_n (kip)	Pier Width (ft)	DRI
No ties	50	16,982	1,419	618	20	0.11
	70	16,982	2,782	618	20	0.23
	90	16,982	4,599	618	20	0.37
24-in. tie spacing	50	16,982	1,419	1,022	20	0.07
	70	16,982	2,782	1,022	20	0.14
	90	16,982	4,599	1,022	20	0.23
12-in. tie spacing	50	16,982	1,419	1,427	20	0.05
	70	16,982	2,782	1,427	20	0.10
	90	16,982	4,599	1,427	20	0.16

The damages observed fall into the category of minor damage according to the description of damage for frame piers. The description of minor damage frame piers is localized spalling of concrete cover and tensile cracking of concrete. This description does not fully describe the damages that occur in all of the collision scenarios involving different tie spacings in the T-pier. Therefore, a different set of descriptions is needed for T-pier vehicle collision damage. Note that the DRI values below 0.15 in Table 3.5 show the compression cracking and spalling of concrete cover in the previous Figure 3.11.

For DRI values between 0.15 and 0.5, any of the following may be present: localized yielding of reinforcement in the column, localized deterioration of the column concrete core, presence of shear cracking in the pile cap, or localized deterioration of the pile cap. These observations agree with Figure 3.7 and Table 3.3. As a result, a damage state description for the T-pier is included as shown in Table 3.6.

Table 3.6. Description of damage state for the DRI values determined for T-piers

Damage State	Description	DRI range
Minor	Compression cracking, Spalling of concrete cover	0.0–0.15
Moderate	Localized yielding of column reinforcement, Localized deterioration of column concrete core, Shear cracking in pile cap, Localized deterioration of pile cap	0.15–0.5
Severe	Yielding of column reinforcement, Deterioration of concrete core, Deterioration of pile cap	0.5–2.0
Collapse	Collapse	> 2.0

Comparing Tables 3.5 and 3.6, for the T-pier to be adequately designed for minor damage in vehicular collision involving impacts as high as 90 mph (144.8 km/h), the ties required would be #5 rebars at a spacing of 12 in (305 mm).

Table 3.7 shows the internal energies in the T-pier components due to different tie spacings.

Table 3.7. Internal energies in bridge components due to different tie spacings

Ties	Speed (mph)	Concrete Column (kip-ft)	Concrete Pile Cap (kip-ft)	Column Long. Rebar (kip-ft)	Column Ties (kip-ft)	Concrete Pier Cap (kip-ft)
No ties	50	46.4	0.8	0.7	0.0	1.2
	70	189.0	1.9	8.4	0.0	2.5
	90	441.1	3.4	84.4	0.0	4.4
24-in. tie spacing	50	39.2	0.7	0.3	0.2	1.1
	70	176.4	1.9	2.6	4.4	2.3
	90	458.7	3.7	73.9	61.5	3.6
12-in. tie spacing	50	41.0	0.7	0.3	0.6	1.2
	70	157.2	2.0	2.1	5.5	2.7
	90	433.6	2.3	40.6	61.8	3.5

The results were captured at 100 ms during collision and show that the column ties gain internal energy as the tie spacing decreases. At the same time, the column longitudinal reinforcement and column concrete lose internal energy as the tie spacing decreases. The concrete pier cap and pile cap did not produce consistent results as the tie spacing decreased, and, therefore, it could not be determined if the tie spacing had an effect on them.

4. COST IMPLICATIONS

Based on the modeling results and the parametric data, few modifications are recommended to bridge piers designed per the Iowa DOT BDM (2020). The one item of potential change would be lowering the bottom mat of reinforcing within frame pier footings to provide connection to the piles for better performance when vehicular impact occurs perpendicular to the long axis of the frame pier.

For a pier to be adequately designed for minor damage in vehicular collision involving impacts as high as 90 mph (144.8 km/h), the ties required would be #5 rebars at a spacing of 12 in. (305 mm).

Other variances previously noted were present when the column or reinforcing was less than recommended in the Iowa DOT BDM. Therefore, the results of this study have no direct impacts on the cost of bridge piers designed per the Iowa DOT BDM.

5. DESIGN RECEOMMNDATIONS

HDR investigated the current Iowa DOT bridge design policies as specified in the Iowa DOT BDM, October 2020 edition, and the three latest AASHTO LRFD Bridge Design Specifications (7th with Interims through 2016, 8th with 2018 Errata, and 9th) with attention given to Articles 5.7, 5.8, 5.10, and 5.11. The focus of this study included spiral and tie reinforcement requirements in Articles 5.7.4.6, 5.8, and 5.10.6 and the seismic requirements in Article 3.10.9.2 and 5.10.11.2. To clearly delineate the three editions, Article references start with the 7th edition with the changes for the 8th and 9th editions stated at the end of each section.

Quoting the Iowa DOT BDM: "In general, the BDM is intended to define Bureau practice for typical Iowa bridges without restricting innovation for unusual site and design conditions. The words 'shall,' 'required,' 'Bureau policy,' and similar terms indicate mandatory specifications that need to be followed unless exceptions are approved by the supervising Unit Leader. Other terms such as 'should,' 'prefer,' and 'recommended' indicate general guidance subject to engineering judgment of the designer."

The Iowa DOT BDM is to be used with other Iowa DOT documents and standards including the latest editions of the Bridges and Structures Bureau Standards, the Construction and Materials Bureau Instructional Memoranda, and Standard Specifications for Highway and Bridge Construction. It also shall be used with the 2017, 8th edition of AASHTO LRFD Bridge Design Specifications except as noted in the preface of the Iowa DOT BDM.

In conclusion, this investigation recommends the following:

- Upon adoption of the AASHTO LRFD Bridge Design Specifications 9th edition, additional attention be given to the changes to Article 5.10.4.3 regarding tie reinforcing in a column.
- Clarification of Iowa DOT guidance on the AASTHO LRFD detailing requirements for plastic hinging when the seismic term SD1 >= 0.1.

Details are listed below for each item.

5.1 Spiral or Tied Determination – AASHTO LRFD 5.7.4.6 (7th Edition)

The BDM states columns and shafts are preferred to be designed as tied, but detailed with spirals with turns spaced at 12 in. on center with an alternate to substitute ties at 12 in. Refer to Iowa DOT BDM Sections 6.3.5 and 6.6.4.1.2.2.

In the 7th edition from AASHTO with the 2016 interims, Article 5.7.4.6 Equation 5.7.4.6-1 specifies a minimum volumetric ratio of spiral reinforcement to be provided for a column or shaft to be considered spirally reinforced. If the area of reinforcing is less than specified, the column is considered "tied." In this case, if spiral reinforcing is used, the reinforcing is considered a "continuously wound tie" instead of a "spiral."

Note that the Iowa DOT BDM Section 6.6.2.6 states: "Frame piers without a crash wall are deemed to meet the 600-kip collision force requirements in AASHTO and no further design of the pier is required with respect to collision when the following stipulations are met:

- Three or more columns connected by a continuous pier cap;
- Minimum column diameters of 4 ft;
- Vertical reinforcement for the columns shall be the greater of what is required by design (not including the Extreme Event II loading) or a minimum of 1.0% of the gross concrete section; and
- Grade 60 shear reinforcement consisting of a minimum #5 tie bar, which is continuously wound (spiral) with a maximum vertical pitch of 4 in. Individual ties shall not be substituted."

A column as described (4 ft diameter, #5 ties, and 2 in. clear cover) has a volumetric ratio of spiral reinforcing equal to 0.007, greater than the 0.006 required for the column to be considered spirally reinforced.

When a column or shaft is considered "tied," i.e., the spiral reinforcement provided does not meet the specifications of Article 5.7.4.6, the factored axial resistance of a compression member is to be calculated by AASHTO LRFD Equation 5.7.4.4-3. If the volumetric ratio of spiral reinforcing of Article 5.7.4.6 is satisfied, the column or shaft would be considered to have "spiral" reinforcement and, thus, Equation 5.7.4.4-2 could be used to calculate the factored axial resistance. The difference between the two equations is the constant as the start of the equation increases from 0.80 to 0.85 when changing from "tied" to "spiral" reinforcement.

Note that AASHTO Article 5.7.4.6 refers to Articles 5.10.6 (Transverse Reinforcement for Compression Members) and 5.10.11 (Provisions for Seismic Design) for additional spiral and tie reinforcement criteria. These articles are addressed below.

- The 8th edition added the definition of the volumetric ratio of spiral reinforcing term in the equation and all of the articles in Chapter 5 were renumbered. The new article number is 5.6.4.6.
- The 9th edition did not change from the 8th Edition.

5.2 Minimum Longitudinal Reinforcement – AASHTO LRFD Article 5.7.4.2 (7th Edition)

The Iowa DOT BDM Section 6.6.4.1.2.1 specifies columns for frame piers to have minimum longitudinal reinforcement per AASHTO Equation 5.7.4.2-3 without reduction in the column cross-section. The minimum longitudinal reinforcement for columns for T-piers is allowed to be further reduced based on reducing the column to a minimum of 50% of the actual cross-section area. However, if using this reduced area, the following two design cases must be evaluated:

- Checking the actual column cross-section with actual longitudinal reinforcement for all AASHTO LRFD load combinations.

- Checking the effective column cross-section with the actual longitudinal reinforcement provided for all AASHTO LRFD load combinations. The effective column cross-section is the actual column cross-section uniformly reduced, resulting in the ratio of actual area of longitudinal reinforcement provided to the effective column area satisfying AASHTO LRFD Equation 5.7.4.2-3.

The 8th edition of the AASHTO LRFD renumbered all of the articles in Chapter 5. The new article number is 5.6.4.2.

The 9th edition of AASHTO LRFD did not change from the 8th edition.

5.3 Minimum Transverse Reinforcement – AASHTO LRFD Article 5.8.2.5 (7th Edition)

The Iowa DOT BDM Section 6.6.4.1.2.1 specifies for columns with a large lateral load, the designer shall check column shear capacity. The column will need sufficient transverse reinforcement to meet both shear stirrup requirements and column tie requirements. In the 7th edition of the AASHTO LRFD, Articles 5.8.2.4 through 5.8.2.9 define the shear resistance and minimum transverse steel requirements.

The 8th edition of the AASHTO LRFD renumbered all of the articles in Chapter 5. The new article numbers are 5.7.2.3 through 5.7.2.8.

The 9th edition of the AASHTO LRFD did not change from the 8th edition.

5.4 Transverse Reinforcement for Compression Members – AASHTO LRFD Article 5.10.6 (7th Edition)

The Iowa DOT BDM Sections 6.3.5 and 6.6.4.1.2.2 specify columns and shafts are preferred to be designed as tied, but detailed with spirals with turns spaced at 12 in. on center with an alternate to substitute ties at 12 in. The tie design must satisfy AASHTO LRFD Article 5.10.6.3. This article contains additional guidelines regarding the size and number of ties required.

There is guidance for a further reduction for columns designed for plastic hinging due to seismic loading at the end of the article. Note, this is a fundamentally different type of plastic hinging compared to the plastic hinging caused by vehicular impact and does not apply for vehicular impact. These seismic loading requirements may potentially apply to bridges built in Iowa as noted below.

- The 8th edition of AASHTO LRFD tie requirements are the same as the 7th edition.
- The 8th and 9th editions of the AASHTO LRFD renumbered all of the articles in Chapter 5. The new article number is 5.10.4.
- The 9th edition of the AASHTO LRFD changed the tie requirements, reducing the effective spacing of the ties from 48 in. to 24 in. The previous language in the AASHTO LRFD 8th

edition stated: “No longitudinal bar or bundle shall be more than 24.0 in., measured along the tie, from a restrained bar or bundle.” In the 9th edition, it now reads: “the spacing of laterally restrained longitudinal bars or bundles shall not exceed 24 in. measured along the perimeter tie.” Note that the 9th edition commentary figures for acceptable tie arrangements were also changed to be consistent with the revised tie spacing.

5.5 Provisions for Seismic Design – AASHTO LRFD Article 5.10.11 (7th Edition)

The Iowa DOT BDM is silent on this section, defaulting to the AASHTO LRFD.

The 7th edition of the AASHTO LRFD Article 5.10.11.2 – Seismic Zone 1 divides the zone into two regions. In the less seismically active region, SD1 < 0.10, no additional detailing requirements for transverse reinforcement are required, except the connection between the superstructure and the substructure shall be as specified in Article 3.10.9.2. Article 3.10.9.2 states for bridges in Seismic Zone 1 with an *As* less than 0.05, the horizontal design connection force shall not be less than 0.15 times the vertical reaction due to the tributary permanent load and tributary live loads assumed to exist during an earthquake. For all other sites in Seismic Zone 1, the horizontal design connection force shall be not less than 0.25 times the vertical reaction due to the tributary permanent load and tributary live loads assumed to exist during an earthquake.

For more seismically active regions in Seismic Zone 1 with $0.10 \leq SD1 < 0.15$, the detailing requirements for the transverse reinforcement at the top and bottom of a column shall be as specified in Articles 5.10.11.4.1d and e in addition to the requirements of Article 3.10.9.2.

Article 5.10.11.4.1d lists the requirements for hoops and ties. This includes both the required volumetric ratio and the details necessary to be considered a hoop or tie. These requirements greatly increase the amount of transverse steel located in the potential hinge regions of a pier over what is typically seen in piers designed for bridges in Iowa.

Article 5.10.11.4.1e lists the spacing requirements for hoops and ties. The following apply specifically to standard Iowa DOT columns and shafts:

- Ties are to be provided at the top and bottom of the column over a length not less than the greatest of the maximum cross-section column dimension, one sixth of the clear height of the column or 18 in.
- Extended into the top and bottom connections as specified in Article 5.10.11.4.3 (not less than one-half the maximum column dimension or 15 in. from the faces of the column connection into the adjoining member)
- Provided at the top of pile in pile bents over the same length as specified for columns
- Spacing not to exceed one-quarter of the minimum member dimension or 4 in. center to center

In reference to columns in Iowa, these requirements are potentially applicable in the south and eastern parts of the state. If the Site Class is determined to be E or F, SD1 will be greater or equal to 0.10. It should be noted, a Site Class of E or F should not be assumed and only used per the direction of the owner or as established by geotechnical data per AASHTO 3.10.3.1.

The 8th edition of the AASHTO LRFD added a note stating lap splices were allowed in Seismic Zone 1 and all of the articles in Chapter 5 were renumbered. The new article numbers are 5.11.2 and 5.11.4.1.4.

The 9th edition of the AASHTO LRFD did not change from the 8th edition.

6. SUMMARY AND CONCLUSIONS

This study investigated the differences between the AREMA (2014), AASHTO (2017). and Iowa DOT BDM (2020) concerning vehicular collisions. The researchers evaluated the performance of common Iowa bridges and their components when a 80 kip (36.287 metric ton) tractor-semitrailer collides into them at three different velocities. The researchers also performed a parametric study on a frame pier and T-pier that experience vehicular collision. The findings were as follows:

- There are a few differences between the three design manuals investigated in this study concerning pier protection for vehicular collisions and pier column detail requirements. However, for the most part, the requirements in all three are similar.

- The frame pier with column diameters of 3.5 ft (1.07 m) commonly used in Iowa, with a spiral of #5 (#16) rebar and a 4 in. (101.6 mm) pitch, experiences minor damage when impacted by a tractor-semitrailer at an impact velocity of 50 mph (80.5 km/h). The design shear capacity of such a pier is 530 kips (2,359 kN). Therefore, the vehicular collision design force of 600 kips (2,669 kN) specified by AASHTO (2017) is adequate for the impact velocity of 50 mph (80.5 km/h), which was the impact velocity used to develop the design force. There is, however, severe damage and failure for the impact velocities of 70 mph (112.7 km/h) and 90 mph (144.8 km/h), respectively.

- The DRI values and damage description for the frame pier accurately predicted the damage observed in the frame pier due to vehicular collision.

- The T-pier commonly used in Iowa did not collapse under any of the three impact velocities considered when it was impacted along its longitudinal axis.

- The minimum requirements for a crash wall specified in the Iowa DOT BDM (2020) were able to keep the frame pier from failure when it was struck by a tractor-semitrailer traveling at the three impact velocities considered. This is true when reinforcement spaced at 12 in. (0.30 m) in both the longitudinal and transverse directions are included in the crash wall. The Iowa DOT BDM (2020) does not specify minimum reinforcement for the crash wall. The minimum required crash wall height specified is less than that specified by AREMA (2014). Therefore, AREMA (2014) requirements are expected to be adequate if the reinforcement considered in this study is implemented.

- The standard 54 in. (1.37 m) tall concrete barrier utilized by the Iowa DOT successfully redirects a tractor-semitrailer and therefore prevents it from hitting the frame pier it is set up to protect. This is true when the tractor-semitrailer impacts the concrete barrier at an angle of 15°.

- The average vehicular impact force over the first 100 ms of impact for the impact velocities of 50 mph (80.5 km/h), 70 mph (112.7 km/h), and 90 mph (144.8 km/h) are 535 kips (2,379

kN), 650 kips (2,893 kN), and 795 kips (3,538 kN), respectively. These averages cover three frame pier column diameters: 3 ft (0.91 m), 3.5 ft (1.07 m), and 4 ft (1.22 m).

- The 4 ft (1.22 m) diameter column frame pier with at least 1.0% longitudinal reinforcement, #5 (#16) spiral rebar at a 4 in. (101.6 mm) pitch made of Grade 60 steel, does not collapse for any of the three impact velocities considered.

- Extending the spiral reinforcement in the column of the frame pier to the pier cap and pile cap only slightly increases the stiffness of the pier and does not significantly increase the pier's resistance to vehicular collision loads.

- Greater impact angles on a pier from its longitudinal axis causes the pier to experience greater damage. It is important that there is no vertical region in the pile cap without steel reinforcement when considering vehicular collision design for impact velocities of 70 mph (112.7 km/h) and greater.

- The T-pier without tie reinforcing experiences minor damage when impacted at the 50 mph (80.5 km/h) impact velocity. #5 (#16) ties spaced at 24 in. (0.61 m) are required for minor damage at 70 mph (112.7 km/h). For the T-pier to be adequately designed for minor damage in vehicular collision involving impacts as high as 90 mph (144.8 km/h), the ties required would be #5 rebars at a spacing of 12 in (305 mm).

- The DRI damage state description for the frame pier does not accurately describe the damage for the T-pier. Therefore, a DRI damage state description table was developed for the T-pier.

REFERENCES

AASHTO. 2014. *Standard Specifications for Highway Bridges*. American Association of State Highway and Transportation Officials, Washington, DC.

——. 2017. *AASHTO Load and Resistance Factor Design (LRFD) Bridge Design Specifications*. 8th edition. American Association of State Highway and Transportation Officials, Washington, DC.

API. 2002. *API Recommended Practice 2A-WSD: Planning, Designing, and Constructing Fixed Offshore Platforms—Working Stress Design*. 21st edition. American Petroleum Institute, Washington, DC.

AREMA. 2014. *AREMA Manual for Railway Engineering: Volume 2–Structures*. American Railway Engineering and Maintenance-of-Way Association, Lanham, MD.

Auyeung, S. and A. Alipour. 2016. Evaluation of AASHTO Suggested Design Values for Reinforced Concrete Bridge Piers Under Vehicle Collisions. *Transportation Research Record: Journal of the Transportation Research Board*, No. 2592, pp. 1–8.

Auyeung, S., A. Alipour, and D. Saini. 2019. Performance-Based Design of Bridge Piers under Vehicle Collision. *Engineering Structures*, Vol. 191, pp. 752–765.

Bowles, J. E. 1988. *Foundation Analysis and Design*. 4th edition. McGraw Hill Book Company, New York, NY.

Buth, C. E., W. F. Williams, M. S. Brackin, D. Lord, S. R. Geedipally, and A. Y. Abu-Odeh. 2010. *Analysis of Large Truck Collisions with Bridge Piers: Phase 1. Report of Guidelines for Designing Bridge Piers and Abutments for Vehicle Collisions*. Texas Transportation Institute, Texas A&M University System, College Station, TX.

El-Hacha, R., H. Elagroudy, and S. Rizkalla. 2004. Bond Characteristics of Micro-Composite Multi-Structural Formable Steel Reinforcement. *5th Structural Specialty Conference of the Canadian Society for Civil Engineering*, Vol. 263, pp. 1–10.

El-Tawil, S., E. Severino, and P. Fonseca. 2005. Vehicle Collision with Bridge Piers. *Journal of Bridge Engineering*, Vol. 10, No. 3, pp. 345–353.

Fujikake, K., B. Li, and S. Soeun. 2009. Impact Response of Reinforced Concrete Beam and Its Analytical Evaluation. *Journal of Structural Engineering*, Vol. 135, No. 8, pp. 938–950.

Gomez, N. L. and A. Alipour. 2014. Study of Circular Reinforced Concrete Bridge Piers Subjected to Vehicular Collisions. Structures Congress, April 3–5, Boston, MA.

Gomez, N., S. Auyeung, and A. Alipour. 2015. Performance Assessment of Bridges with Different Bent Configurations under Vehicle Collision. Transportation Research Board 94th Annual Meeting, January 11–15, Washington, DC.

Iowa DOT. 2020. *LRFD Bridge Design Manual*. Iowa Department of Transportation, Ames, IA.

Klinga, J. V. and A. Alipour. 2015. Assessment of Structural Integrity of Bridges under Extreme Scour Conditions. *Engineering Structures*, Vol. 82, pp. 55–71.

Lindeburg, M. R. 2018. *PE Civil Reference Manual for the NCEES PE Civil Exam*. 16th edition. Professional Publications, Inc. (PPI), A Kaplan Company, Belmont, CA.

LSTC. 2016. *LS-DYNA Theory Manual*. Livermore Software Technology Corporation, Livermore, CA.

Malvar, L. J. and J. E. Crawford. 1998. Dynamic Increase Factors for Steel Reinforcing Bars. 28th Department of Defense Explosives Safety Board Seminar, August 18–20, Orlando, FL.

Matlock, H. 1970. Correlations for Design of Laterally Loaded Piles in Soft Clay. *Proceedings of the 2nd Offshore Technology Conference*, Houston, TX, Vol. 1, pp. 577–594.

NAVFAC. 1986. *Foundations and Earth Structures Design Manual 7.02*. Naval Facilities Engineering Command, Alexandria, VA.

NTRC. 2018. *FEM Models for Semitrailer Trucks*. National Transportation Research Center, Knoxville, TN.

Oppong, K., D. S. Saini, and B. Shafei. 2020. Vulnerability Assessment of Bridge Piers Damaged in Barge Collision to Subsequent Hurricane Events. *Journal of Bridge Engineering*, Vol. 25, No. 8, pp. 1–14.

Reese, L. C., W. R. Cox, and R. D. Koop. 1975. Field Testing and Analysis of Laterally Loaded Piles in Stiff Clay. *Proceedings of the 7th Offshore Technology Conference*, Houston, TX, Vol. 2, pp. 473–483.

Saini, D. S. and B. Shafei. 2017. Calibration of Barge Models for the Reliable Prediction of Impact Force on Bridge Piers. Structures Congress April 6–8, Denver, CO.

Tachibana, S., H. Masuya, and S. Nakamura. 2010. Performance Based Design of Reinforced Concrete Beams under Impact. *Natural Hazards and Earth Systems Sciences*, Vol. 10, pp. 1069–1078

Xu, L., X. Lu, H. Guan, and Y. Zhang. 2013. Finite-Element and Simplified Models for Collision Simulation between Over-Height Trucks and Bridge Superstructures. *Journal of Bridge Engineering*, Vol. 18, No. 11, pp. 1140–1151.

THE INSTITUTE FOR TRANSPORTATION IS THE FOCAL POINT FOR TRANSPORTATION AT IOWA STATE UNIVERSITY.

InTrans centers and programs perform transportation research and provide technology transfer services for government agencies and private companies;

InTrans contributes to Iowa State University and the College of Engineering's educational programs for transportation students and provides K–12 outreach; and

InTrans conducts local, regional, and national transportation services and continuing education programs.

IOWA STATE UNIVERSITY

Visit **InTrans.iastate.edu** for color pdfs of this and other research reports.